

# Avances en el diagnóstico ecocardiográfico de la hipertensión pulmonar en la dirofilariosis cardiopulmonar canina

Jorge I. Matos Rivero

Doctorado de Investigación en Biomedicina  
Tesis Doctoral con Mención Internacional  
Diciembre del 2023



ULPGC  
Universidad de  
Las Palmas de  
Gran Canaria

Escuela de  
Doctorado



**PROGRAMA DE DOCTORADO DE  
INVESTIGACIÓN EN BIOMEDICINA**

**TESIS DOCTORAL**

**AVANCES EN EL DIAGNÓSTICO  
ECOCARDIOGRAFICO DE LA HIPERTENSIÓN  
PULMONAR EN LA DIROFILARIOSIS  
CARDIOPULMONAR CANINA**

**ADVANCES IN THE ECHOCARDIOGRAPHIC  
DIAGNOSIS OF PULMONARY HYPERTENSION IN  
CANINE CARDIOPULMONARY DIROFILARIOSIS**

**DOCTORANDO:  
JORGE ISIDORO MATOS RIVERO**

**DIRECTORES:  
JOSÉ ALBERTO MONTOYA ALONSO  
ELENA CARRETÓN GÓMEZ**

**TESIS DOCTORAL CON MENCIÓN INTERNACIONAL**

**ESCUELA DE DOCTORADO-UNIVERSIDAD DE LAS  
PALMAS DE GRAN CANARIA**

**LAS PALMAS DE GRAN CANARIA,  
DICIEMBRE DE 2023**

Código: 00107/2023

Reunida a 03/01/2024 la Comisión Académica del Programa de Doctorado en Investigación en Biomedicina por la Universidad de Las Palmas de Gran Canaria ha evaluado la solicitud de autorización para presentar la tesis doctoral de:


Apellidos: <b>MATOS RIVERO</b>	Nombre: <b>JORGE ISIDORO</b>
DNI/NIE/Pasaporte:	Email: <b>jorge.matos@ulpgc.es</b>
Tutor: <b>MONTOYA ALONSO, JOSÉ ALBERTO</b>	
Directores: <b>MONTOYA ALONSO, JOSÉ ALBERTO</b> <b>CARRETÓN GÓMEZ, ELENA</b>	
Programa de Doctorado: <b>Programa de Doctorado en Investigación en Biomedicina por la Universidad de Las Palmas de Gran Canaria</b>	
Línea de Investigación: <b>Clínica Veterinaria</b>	
Título definitivo de la tesis:  <b>AVANCES EN EL DIAGNÓSTICO ECOCARDIOGRAFICO DE LA HIPERTENSIÓN PULMONAR EN LA DIROFILARIOSIS CARDIOPULMONAR CANINA</b>	
Códigos de la UNESCO:	
Campo <b>31 - CIENCIAS AGRARIAS</b>	Disciplina <b>3109 - CIENCIAS VETERINARIAS (VER 2401)</b>
	Subdisciplina <b>310804 - MEDICINA INTERNA (VER 3205)</b>

Miembros de la Comisión Académica presentes en la firma del acta

- MONTOYA ALONSO, JOSÉ ALBERTO
- SERRANO SÁNCHEZ, JOSÉ ANTONIO
- MARCHENA GÓMEZ, JOAQUÍN
- WÄGNER, ANNA MARIA CLAUDIA

La Comisión Académica ha tomado el siguiente acuerdo:

<b>PRESENTACIÓN DE LA TESIS DOCTORAL</b>
Solicitud de autorización de presentación de tesis <b>favorable</b>


Universidad de Las Palmas de Gran Canaria		
Página 1 / 2	ID Documento 3QswFUOhA.8daGawsNaJBQ\$\$	
Este documento ha sido firmado electrónicamente por	Fecha de firma	
JOSÉ ALBERTO MONTOYA ALONSO	03/01/2024 18:35:29	

Documento firmado digitalmente. Para verificar la validez de la firma copie el ID del documento y acceda a / Digitally signed document. To verify the validity of the signature copy the document ID and access to <https://sede.ulpgc.es/VerificadorFirmas/ulpgc/VerificacionAction.action>

<b>COMPENDIO DE PUBLICACIONES</b>
Solicitud de autorización de presentación de tesis <b>favorable</b>

<b>OPTAR A LA MENCIÓN INTERNACIONAL EN EL TÍTULO DE DOCTOR</b>
Solicitud de autorización de presentación de tesis <b>favorable</b>

En Las Palmas de Gran Canaria a fecha de la firma digital

Universidad de Las Palmas de Gran Canaria		
Página 2 / 2	ID Documento 3QswFUOhA.8daGawsNaJBQSS	
Este documento ha sido firmado electrónicamente por	Fecha de firma	
JOSÉ ALBERTO MONTOYA ALONSO	03/01/2024 18:35:29	

Documento firmado digitalmente. Para verificar la validez de la firma copie el ID del documento y acceda a / Digitally signed document. To verify the validity of the signature copy the document ID and access to <https://sede.ulpgc.es/VerificadorFirmas/ulpgc/VerificacionAction.action>

## INFORME EXPERTO EXTERNO EXTERNAL REFEREE REPORT

<b>Nombre del experto:</b> <i>Name of the referee:</i>	Ana Cristina Silvestre Ferreira
<b>Categoría:</b> <i>Position:</i>	Professor Auxiliar
<b>Departamento, Universidad, Organismo de adscripción:</b> <i>Department, University or Organism of adscription:</i>	Departamento de Ciências Veterinárias da Universidade de Trás-os-Montes e Alto Douro
<b>Doctor por la Universidad de:</b> <i>Doctor by the University of:</i>	Las Palmas de Gran Canaria
<b>Año de defensa de la tesis doctoral:</b> <i>Year of the Doctoral Thesis Defense:</i>	2005

<b>Título de la tesis:</b>	Avances en el diagnóstico ecocardiografico de la hipertensión pulmonar em la dirofilariosis cardiopulmonar canina
<i>Title of the thesis:</i>	Advances in the echocardiographic diagnosis of pulmonary hypertension in canine cardiopulmonary dirofilariosis
<b>Nombre del doctorando/a que presenta la tesis:</b> <i>Name of the PhD student:</i>	Jorge Isidoro Matos Rivero

**1. Especificar los motivos que avalan la calidad de la tesis mencionada para su defensa pública en relación a los siguientes aspectos: / Specify reasons endorsing the quality of the above-mentioned thesis for its public reading with respect to:**

**1.1 Objetivos / Objectives:**

Los objetivos propuestos son claros y bien definidos.

**1.2 Originalidad del trabajo / Originality of the work:**

El desarrollo de nuevas técnicas ecocardiográficas que permiten la detección de la hipertensión pulmonar así como la distinción entre perros sin hipertensión (sanos o infectados) y perros infectados com hipertensión, hace deste un trabajo innovador y de gran utilidad clínica.

**1.3 Metodología / Methodology:**

La presentación del diseño del estudio y sus resultados es excelente y la discusión bien estructurada.

**1.4 Antecedentes y bibliografía / Background and references:**

El trabajo está apoyado en una bibliografía amplia y actualizada.

**2. Valoración absoluta y/o ponderada de la tesis presentada en comparación con otros trabajos de investigación en su campo / *Absolute and/or relative assessment of the thesis in comparison with other research works in the same field:***

La tesis está bien presentada, con una buena organización y una metodología apropiada para cumplir con los objetivos propuestos, encontrándose apoyada en una amplia y actualizada bibliografía. Consta de 3 artículos publicados en revista revisada por pares científicos con buen factor de impacto, un programa de investigación que demuestra muy buen nivel y que certifica la calidad del trabajo científico hecho por el candidato, así como su reconocimiento por parte de la comunidad científica. En mi opinión, los resultados presentados en este trabajo estimularán más investigaciones y generarán más interés en el estudio de este tema.

**3. ¿Considera que la tesis anteriormente mencionada es apta para su lectura y defensa pública? / *Considering all the above, is the thesis judged to be suitable for public presentation?***

**Sí/Yes X      No**

**INFORME EXPERTO EXTERNO**  
**EXTERNAL REFEREE REPORT**

<b>Nombre del experto:</b> <i>Name of the referee:</i>	<b>María Montserrat Díaz Espineira</b>
<b>Categoría:</b> <i>Position:</i>	<b>UHD (Universitaire Hoofddocent) Associate Professor DVM, PhD, Diplo.EVCIM-CA</b>
<b>Departamento, Universidad, Organismo de adscripción:</b> <i>Department, University or Organism of adscription:</i>	<b>Department of Clinical Sciences Division: Internal Medicine Companion Animals Faculty of Veterinary Medicine. Utrecht University The Netherlands</b>
<b>Doctor por la Universidad de:</b> <i>Doctor by the University of:</i>	<b>Universidad Complutense de Madrid (febrero 1994) Utrecht University, The Netherlands (december 2008)</b>
<b>Año de defensa de la tesis doctoral:</b> <i>Year of the Doctoral Thesis Defense:</i>	<b>Febrero 1994 December 2008</b>

<b>Título de la tesis:</b>	<b>Avances en el diagnóstico ecocardiográfico de la hipertensión pulmonar en la dirofilariosis cardiopulmonar canina</b>
<i>Title of the thesis:</i>	<b>Advances in the echocardiographic diagnosis of pulmonary hypertension in canine cardiopulmonary dirofilariosis</b>
<b>Nombre del doctorando/a que presenta la tesis:</b> <i>Name of the PhD student:</i>	<b>Jorge Isidoro Matos Rivero</b>

**1. Especificar los motivos que avalan la calidad de la tesis mencionada para su defensa pública en relación a los siguientes aspectos: / Specify reasons endorsing the quality of the above-mentioned thesis for its public reading with respect to:**

This scientific study provides valuable information to assist and improve the diagnose and clinical evaluation of dogs with cardiopulmonary dirofilariosis. Successful treatment of this disease requires an accurate assessment of its severity in each patient in order to make the right therapeutic decisions, establish prognosis and prevent severe and life threatening side effects and complications.

Noninvasive diagnostic techniques for pulmonary hypertension (PH) are essential in veterinary medicine for different reasons (financial, anesthesia risks, time, availability of sophisticated invasive techniques).

The research work in this thesis has been accurately performed, its background is thoroughly described and the results have valuable clinical relevance.

The thesis has a very pleasant reading. Figures, graphics and tables support and illustrate the text. The thesis layout has been done with care.

**1.1 Objetivos / Objectives:**

The objectives of this thesis are tight described and are clear. Their background and the way to accomplish these objectives are presented.



## **1.2 Originalidad del trabajo / *Originality of the work:***

This thesis applies different specific echocardiographic studies explicitly in dogs with cardiopulmonary dirofilariasis. The results and conclusions of this research provides valuable information (PV:PA ratio, TDI, GS, FWS, TMAD) to be used as a complementary diagnostic tool to identify and estimate the severity of PH in heartworm-infected dogs.

## **1.3 Metodología / *Methodology:***

The methodology in this thesis is accurately described. In the introduction or state of the art of the theme, a broad and thorough overview on all the aspects of the disease (aetiology, epidemiology, clinical signs, diagnostic methods, treatment, prophylaxis, prognosis, pathophysiology) and echocardiography (in the diagnosis of pulmonary hypertension in canine cardiopulmonary dirofilariasis) is displayed. In each scientific publication, material and methods (study animals, echocardiography, statistical analysis), results, discussion and conclusions are accurately presented. Limitations of the studies are also critically addressed.

## **1.4 Antecedentes y bibliografía / *Background and references:***

The literature and references to other scientific works are present through all the thesis. In the different sections, results from other researches are exposed and compared with the results and data of this study. Literature from veterinary medicine but also human medicine have been included.

## **2. Valoración absoluta y/o ponderada de la tesis presentada en comparación con otros trabajos de investigación en su campo / *Absolute and/or relative assessment of the thesis in comparison with other research works in the same field:***

The results and conclusions of this thesis provide valuable information with clinical and practical relevance. This thesis gives veterinary professionals worthwhile evidence on the possibility to use adjunct diagnostic tools for identifying and evaluating PH in dogs with heartworm disease.

## **3. ¿Considera que la tesis anteriormente mencionada es apta para su lectura y defensa pública? / *Considering all the above, is the thesis judged to be suitable for public presentation?***

**Sí/Yes**

**Firma y fecha**  
**Signature and date.**

**Dr. M.M.Diaz Espineira**

**DVM, PhD, Diplo.ECVIM-CA**

**Department of Clinical Sciences**  
**Division: Internal Medicine Companion Animals**  
**Faculty of Veterinary Medicine**  
**Utrecht University**  
**The Netherlands**

**December 19<sup>th</sup> 2023**



# Agradecimientos

A mi familia, los que tanto se han preocupado por mi felicidad. Los primeros que han celebrado mis éxitos y me han apoyado en mis derrotas. Sin ellos mis propósitos hubieran sido inalcanzables. En particular, mis padres me regalaron la más bonita de las infancias y siempre me apoyaron para convertirme en lo que soy hoy en día. Nunca podré devolver tanto amor.

A José Alberto Montoya Alonso y Elena Carretón Gómez, por la confianza, la cercanía, el cariño, la paciencia y las enseñanzas recibidas. Personas brillantes y maravillosas por partes iguales. Dignos ejemplos a seguir, con rigor científico y calidad humana.

A la totalidad de mi grupo de investigación, compañeros de faena que he tenido la suerte de conocer y me han dado la oportunidad de crecer personal y profesionalmente. Ellos, al igual que yo, somos afortunados de compartir pasión y colaborar en los desafíos que se nos plantean.

A los tutores que he tenido la suerte de disfrutar en mis estancias. Patricia, Laura, Luis, Laín, Claudia, Rui, Rodrigo, Susana y Alicia, personas magníficas que me han abierto sus puertas para aprender y vivir experiencias inolvidables.

A mis amigos, a los que han estado siempre y a los que se han incorporado recientemente. Los que son auténticos por dentro y por fuera. Los que no piden nada a cambio y son fuentes inagotables de risas, alegrías y energía rehabilitadora.

A Sara por ser mi apoyo inquebrantable, amiga, confidente y compañera de vida. Gracias por regalarme tu generosidad, dulzura, ternura y amor. Imprescindible en mi camino, iluminándome incluso en los momentos de más oscuridad, permitiendo que cada día salga el sol.

A todos los pacientes y sus propietarios que han puesto su confianza en mí para que hoy pueda estar escribiendo estas palabras.

En especial a mi negrito, eternamente mi compañero peludo.



# TABLE OF CONTENTS

Page

<b>1</b>	<b>1. ABBREVIATIONS</b>
<b>5</b>	<b>2. STATE OF THE ART</b>
7	2.1. Canine Cardiopulmonary Dirofilariosis
18	2.2. Pathophysiology of Canine Cardiopulmonary Dirofilariosis
22	2.3. Echocardiographic Diagnosis of Pulmonary Hypertension in Canine Cardiopulmonary Dirofilariosis
<b>41</b>	<b>3. OBJECTIVES</b>
<b>47</b>	<b>4. SCIENTIFIC PUBLICATIONS</b>
49	4.1. Echocardiographic Assessment Of The Pulmonary Vein To Pulmonary Artery Ratio In Canine Heartworm Disease
61	4.2. Usefulness Of Tissue Doppler Imaging For The Evaluation Of Pulmonary Hypertension In Canine Heartworm Disease
73	4.3. Right Ventricle Strain Assessed by 2-Dimensional Speckle Tracking Echocardiography (2D-STE) to Evaluate Pulmonary Hypertension in Dogs with <i>Dirofilaria immitis</i>
<b>87</b>	<b>5. CONCLUSIONS</b>
<b>95</b>	<b>6. EXTENDED SUMMARY</b>
<b>99</b>	<b>7. SIMPLE SUMMARY</b>
<b>115</b>	<b>8. REFERENCE LIST</b>
<b>127</b>	<b>9. SCIENTIFIC CONTRIBUTIONS</b>





**1.**  
**ABBREVIATIONS**





100x: visualization increased by 100  
 2D: Bidimensional  
 2D-mode: Bidimensional mode  
 2D-STE: Bidimensional speckle tracking echocardiography  
 A': E': Tissue Doppler peak A' to peak E' ratio  
 A': Tissue Doppler end diastolic peak  
 ACVIM: American college of veterinary internal medicine  
 AHWS: American society of heartworm disease  
 ANOVA: Analysis of Variance  
 Ao: Aorta  
 AT: Acceleration time  
 CI 95%: Confidence interval of 95%  
 CO<sub>2</sub>: Carbon dioxide  
 CHF: Congestive heart failure  
 CT: Computed axial tomography  
*D. immitis*: *Dirofilaria immitis*  
 DNA: Deoxyribonucleic acid  
 E: Early diastolic transmitral doppler peak  
 ECG: Electrocardiogram  
 E': Tissue Doppler early diastolic peak  
 ESDA: European society of dirofilariasis and angiostrongilosis  
 ET: Ejection time  
 FWS: Free wall strain  
 Global-TDI: Global TDI index of myocardial function  
 GS: Global strain  
 HRI: Heart rate indexed  
 HR: Heart rate  
 IVCT: Isovolumetric contraction time  
 IVRT: Isovolumetric relaxation time  
 Kg: Kilograms  
 LA: Left atrium  
 L1: Larvae phase 1  
 L3: Larvae phase 3  
 LV: Left ventricle  
 MHz: Megahertz  
 MDR1: P-glycoprotein coding gene  
 m: Meters  
 mm: Millimeters  
 mmHg: Millimeters of mercury  
 ml: Milliliters  
 PA: Pulmonary artery  
 PAm<sub>ax</sub>: Maximum diameter of pulmonary artery  
 PAm<sub>in</sub>: Minimum diameter of pulmonary artery  
 PCR: Polymerase chain reaction  
 PCG: Phonogram  
 PH: Pulmonary hypertension  
 PRPG: Pulmonary regurgitation pressure gradient  
 PT: Pulmonary trunk  
 PVC: Peak ventricular contraction  
 PV: Pulmonary vein  
 PV<sub>max</sub>: Maximum diameter of pulmonary vein  
 PV<sub>min</sub>: Minimum diameter of pulmonary vein  
 RA: Right atrium  
 ROC: Receiver operating characteristic  
 RPADi: Right pulmonary artery distensibility index  
 R-CHF: Right congestive heart failure  
 R-TEI: Right myocardial performance index  
 RV: Right ventricle  
 RV AFI: Right ventricle automatic functional imaging  
 s: Seconds  
 S: Tissue Doppler systolic peak  
 S1: First cardiac sound  
 S2: Second cardiac sound  
 SC: Circumferential strain  
 Sen: Sensibility  
 SL: Longitudinal strain  
 Sp: Specificity  
 SR: Radial strain  
 TAPSE: Tricuspid annular plane systolic excursion  
 TDI: Tissue Doppler imaging  
 TMAD: Tissue motion annular displacement  
 TRPG: Tricuspid regurgitation pressure gradient  
 TRV: Tricuspid regurgitation velocity  
 x-axis: Abscissa or horizontal axis  
 y-axis: Ordinate or vertical axis



The background features a light beige, textured paper surface. It is decorated with wavy, overlapping lines in a muted green color that create a sense of depth and movement. Three solid gold circles are scattered across the page: one large circle on the left side, one smaller circle in the upper right corner, and another large circle at the bottom center.

# 2.

## STATE OF THE ART

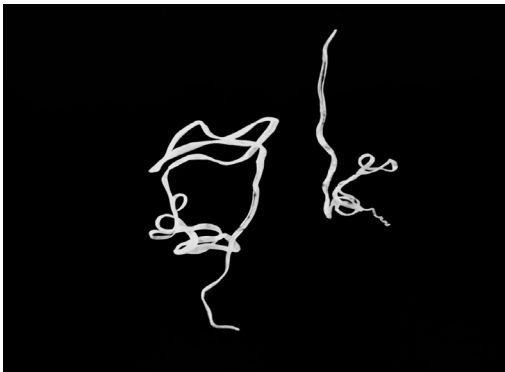


# 2.1.

## Canine Cardiopulmonary Dirofilariosis

### A. Etiology

*Dirofilaria immitis* (Leidy, 1856) is a parasite belonging to the phylum *Nematoda*, class *Secernentea*, order *Spirurida*, suborder *Spirurina*, superfamily *Filaroidea*, family *Onchocercidae* (Bowman & Atkins, 2009). The *Dirofilaria* genus consists of thin and elongated parasites, whitish in color. *D. immitis* is the largest species among the filarids of medical and veterinary importance. Females are 250 to 310 mm long and 1.0 to 1.3 mm wide. Males are 120 to 200 mm long and 0.7 to 0.9 mm wide. The anterior end is rounded and blunt, with a rudimentary buccal capsule without lips, but with small cephalic papillae and an esophagus that is differentiated into a muscular and glandular region (McCall *et al.*, 2008). The caudal ends of males are conical and spirally coiled, and they also have five pairs of preanal papillae and six pairs of postanal papillae. While females have rounded caudal ends with the vulvar opening located behind the junction of the esophagus and intestine, about 2.7 mm from the anterior end. In all *Dirofilaria* species the spicules are of unequal length and are often used as diagnostic characters. They do not have a gubernaculum (Simón *et al.*, 2009) (Figure 1).



\*Figure 1. Macroscopic visualization of two adult *Dirofilaria immitis* parasites, a female individual on the left and a male individual on the right. Parasites obtained from the necropsy of an infected dog.

This nematode is responsible for cardiopulmonary heartworm disease, a process colloquially known as “heartworm disease”, the definitive hosts being mammals, mainly carnivores. Its presence has been confirmed in domestic canids, as well as wild species (wolves, foxes, coyotes, dingoes, etc.), domestic and wild felines, mustelids, sea lions, rodents, ungulates, even non-human primates and humans (Strickland, 1998; Sasai, 2000; Simón *et al.*, 2005; Liesner *et al.*, 2016; Smith *et al.*, 2022). However, dogs and other canids are the natural hosts in which the parasite load found has been greater, and they act as the main reservoir (Hidaka *et al.*, 2003).

Members of the genus *Dirofilaria* require an arthropod intermediate host to complete their life cycle. *D. immitis* is transmitted by mosquitoes of the Family *Culicidae*. Several authors have pointed out the genera *Aedes*, *Culex*, *Culiseta*, *Anopheles*, *Mansonia*, *Coquillettidia* and *Psorophora* as competent intermediate hosts capable of developing the different larval stages until the infective phase (Simón *et al.*, 2012). The biological cycle of the parasite begins when the adult parasite reproduces and releases *microfilariae* (L1) into the bloodstream of the definitive host. To mature, it needs the intermediate host to feed on the definitive host and ingest the L1. In the mosquito, two maturations develop until the third larval stage (L3) in the Malpighian tubules of the mosquitoes. Subsequently, when the mosquito feeds on a new host, L3 infects it and reaches sexual maturity in the next 6 months (Montoya & Carretón, 2012).

Cardiopulmonary dirofilariosis involves the symbiosis between *D. immitis* and the bacteria *Wolbachia pipientis* (Manoj *et al.*, 2021). This is a gram-negative bacteria, belonging to the group of intercellular *Rickettsiae*. It is present in all stages of the nematode life cycle, supplying the parasite with essential metabolites during evolution and embryonic development, and *D. immitis* in turn guarantees the survival and transmission of the bacteria (Santhakumari *et al.*, 2021).

## **B. Epidemiology**

Cardiopulmonary heartworm disease is a cosmopolitan disease with worldwide distribution (Anvari *et al.*, 2020). The highest prevalences are found in areas where temperature and humidity remain high for at least part of the year, so these environmental conditions favor the development and maintenance of mosquito vector populations (Chikwetoa *et al.*, 2014; Borthakur *et al.*, 2015). Therefore, in warmer areas transmission occurs throughout the year, while in colder areas the transmission period is reduced to a few months per year (Evanson *et al.*, 2019). Its presence and transmission requires, in addition to intermediate hosts, climatic factors that maintain adequate temperature and humidity for mosquitoes to develop, and so that the ingested *microfilariae* can complete their larval phase until they become the infecting form (Davood *et al.*, 2020). In summary, the prevalence is very different in the regions of the world, depending on various epidemiological factors such as the distribution of transmitting mosquitoes, their fertility and population density, the living conditions and behavior of the hosts, and environmental temperature, among others (Cancrini & Kramer, 2001).

Due to the increase in global temperature and the consequent increase in vectors, the disease is in a process of global expansion, with a significant percentage of dogs affected in the world: 10.91% (Wang *et al.*, 2016; Levy *et al.*, 2017; Wang *et al.*, 2018; Anvari *et al.*, 2020; Silva *et al.*, 2020; Genchi & Kramer, 2020). In Europe there is a global prevalence of 10.45%, the highest prevalence is found mainly in mediterranean and southern countries (Portugal, Spain, France, Italy and Greece), where the disease is endemic (Morchón *et al.*, 2012; Maia *et al.*, 2015; Piantedosi *et al.*, 2017; Figueredo *et al.*, 2017; Pérez *et al.*, 2021; Morchón *et al.*, 2022). In addition, heartworm is known to be spreading to non-endemic areas of northern and northeastern Europe. Most cases involve dogs that have traveled to endemic areas, but there are cases, such as in England, Switzerland, Austria, Poland, the Netherlands and Denmark, where indigenous cases of heartworm disease have been reported (Pekacz *et al.*, 2022; Alvarez *et al.*, 2023; Wright *et al.*, 2023).

In Spain the prevalence is 6.25%, the highest prevalence is found in the Canary Islands, the south of the Iberian Peninsula, in regions near the mediterranean sea, and in irrigated areas and near large rivers (such as the banks of the Tormes River or the Ebro Delta) (Montoya *et al.*, 2015; Montoya *et al.*, 2017; Montoya *et al.*, 2020; Villanueva *et al.*, 2021; Montoya *et al.*, 2022). Furthermore, prevalence data have recently been reported in the north of the Iberian Peninsula, which confirms the expansion of the disease throughout the Spanish territory (Diosdado *et al.*, 2017; Diaz *et al.*, 2020; Montoya *et al.*, 2022; Villanueva *et al.*, 2022).

In the Canary Islands the prevalence is 9.97%, but it is not uniform, being higher in Tenerife with 22.5%, followed by Gran Canaria with 20.7%. There are also high prevalence on islands such as La Palma with 15.7% and La Gomera with 16.3%. The incidence is much lower in Fuerteventura with 1.8% in dogs and is absent in El Hierro and Lanzarote (Carretón *et al.*, 2016; Montoya *et al.*, 2016). The prevalence is also not uniform within each island, due to the great variety of climates and demographic factors; it is higher in steppe and temperate climates where humidity is provided by trade winds, rain or the presence of water reservoirs. It is also high in coastal areas, which provide an ideal climate for the parasite and are often home to the islands' largest cities. The prevalence is much lower in areas with dry and desert climates (Montoya *et al.*, 2016; Morchón *et al.*, 2023).



## C. Clinical signs

Clinical signs are mainly the result of vascular lesions, alterations in cardiac and pulmonary blood flow, and increased pulmonary arterial pressure (Carretón *et al.*, 2020). *D. immitis* has a usually chronic presentation, with most dogs showing no symptoms for months or years. This depends, to a large extent, on the parasite load, the immune reaction of each individual and the physical exercise performed (Digangi *et al.*, 2017). The symptoms are rooted in the extent of the lung disease and the specific effects of cardiovascular damage; these lesions include an increase in the afterload of the right ventricle (RV) due to progressive damage to the pulmonary artery (PA) and the lung parenchyma. Mild cases present with few or no associated clinical signs and are diagnosed incidentally. The first symptoms include mild cough and exercise intolerance, hyporexia may also occur (Romano *et al.*, 2020).

Moderate cases present with chronic cough, weight loss and poor body condition. The mucous membranes may appear pale due to poor peripheral perfusion due to low cardiac output and concomitant anemia associated with metabolic stress and hemolysis caused by an increase in erythrocyte fragility. Mucosal paleness may increase after physical activity, due to low pulmonary arterial perfusion capacity. An increase in intensity in the first heart sound (S1) may be reported during cardiac auscultation in the right hemithorax of the animal and the presence of a mild holosystolic murmur (tricuspid valve regurgitation). Lung auscultation is generally normal, although slight crackles, wheezing, and bronchial snoring may be detected (Spasojevic-Kosic & Lalosevic, 2020).

Severe cases usually manifest with tachypnea and tachycardia, the animal being intolerant to physical activity, sometimes presenting syncope even with mild exercise. Dyspnea during exercise is evident and the presence of a restrictive respiratory pattern with rapid and shallow respirations is a reflection of the extent of pulmonary arterial damage. The mucous membranes appear pale, cold and dry to the touch, caused by decreased peripheral blood perfusion and anemia. Cardiac arrhythmias are rare, occurring in only less than 10% of patients reported with chronic disease. Pulmonary auscultation normally reveals crepitations over the caudal lobes, and at cardiac level an obvious murmur can be heard in the projection area of the pulmonary and tricuspid valve, with frequent splitting of second heart sound (S2). When right congestive heart failure (CHF) is established, ascites and limb edema can be seen (Yoon *et al.*, 2013; Ames & Atkins, 2020).

Cardiorespiratory shock may be reported due to the presence of pleural or pericardial effusion, in addition to the phenomenon of cardiac tamponade, anorexia, weight loss and dehydration. Sudden death is rare and usually occurs after respiratory failure or atrial fibrillation (Arita *et al.*, 2003).

## D. Diagnostic methods

Heartworm infection can be diagnosed by assessing the presence of circulating antigens in the blood, serum, or plasma. Enzyme-linked immunosorbent assay serological tests/technique and commercial immunochromatography kits are considered the “gold standard” techniques for diagnosing the disease. These are very specific and sensitive tests to detect parasitization in dogs (98-100%). Circulating antigens are detectable around 6 to 7 months after infection, so there will be no reason to test in puppies younger than 6 months or when a canine has received preventative treatment on a regular basis (Bolio-Gonzalez *et al.*, 2007; DiGangi *et al.*, 2017; Constantinoiu *et al.*, 2023; Das *et al.*, 2023).

The presence of *D. immitis* adults can also be diagnosed by microscopically examining the blood for the presence of *microfilariae*. Tests for the determination of the presence of microfilaremia validate the serological results, diagnose cases without antigens detected in the antigen tests due to antigen-antibody complexes, also identify reservoir patients of the infection and alert the veterinarian of a high burden of *microfilariae* (Adebayo *et al.*, 2020). There are various techniques, among which the “Thick drop” or blood smear visualization stands out. It is a simple test that consists of spreading a drop of blood on a slide and observing it under the microscope without resorting to the use of staining or concentration of the sample. Detects approximately 75% of positive cases that are microfilaremic. In this technique it is possible to visualize the movement of the *larvae*, but it is not an effective technique to morphologically differentiate between the *microfilariae* of the different genera of *Filaridae* that affect the dog (Kitagawa *et al.*, 1997; Hidaya *et al.*, 2003).

The Knott technique has the advantage that in addition to being more reliable for detecting positive cases, it is the preferred technique to morphologically identify *larvae* and differentiate *D. immitis* from other filarids. It consists of generating the lysis of blood cells by adding formalin, then centrifuging the sample and staining



\*Figure 2. Microscopic visualization of a *microfilariae* (larval phase 1) by performing the Knott technique. Blood sample from a parasitized dog in the island of Gran Canaria.

transferred to a slide and stained with methylene blue. A cover is placed and observed microscopically at 100x magnification (Venco *et al.*, 2001; Lane *et al.*, 2021).

Animals can be amicrofilaremic due to: prior administration of preventive drugs (macrocytic lactones), single-sex infections, prepatent infections, and also immune-mediated destruction of *microfilariae*. Up to 20% of dogs infected with adult worms can be amicrofilaremic, so a negative *microfilariae* test is not enough to rule out an infection; these tests must be accompanied by an antigen test. If using any of the tests described above, *microfilariae* are identified, and according to their morphology correspond to *D. immitis*, it is considered a definitive diagnosis of infection, since the specificity (Sp) is 100%. It should be noted that the intensity of microfilaremia does not correlate with the load of adult parasites, so it cannot be related to the severity of the disease (Montoya & Carretón, 2012; Simón *et al.*, 2012).

When the identification of *microfilariae* does not provide a precise diagnosis, they can be defined by histochemical staining of anatomical regions with the alkaline phosphatase technique (*D. immitis microfilariae* present two zones of phosphatase activity near the anal and excretory pores) and by amplification of *microfilariae* DNA by PCR (McCall *et al.*, 2008; Pekacz *et al.*, 2022; Constantinoiu *et al.*, 2023).

it with methylene blue. Finally, a drop of the preparation is placed between a slide and a coverslip to view under the microscope at 100x magnification (Figure 2). Similarly, the filter technique is also an available technique, the effectiveness of which is similar to the Knott test. This technique consists of passing a solution of 1 ml of blood with anticoagulant, with 10 ml of a lysing solution, through a membrane with pores 5 microns in diameter. Because the diameter of the *microfilariae* ranges between 6 and 7 microns, they do not pass through the pores, being retained in the filter membrane. This membrane together with the retained content is

The echocardiographic examination constitutes an alternative tool in the diagnosis of cardiopulmonary heartworm disease. Through ultrasound observation of cardiovascular structures, the presence of findings compatible with the presence of adult worms can be determined. The areas of inspection are the right and left PA, the main PA, and the right heart chambers. The presence of adult parasites is reported with the persistence of two parallel hyperechoic lines (constituting an “equal sign”) (Cavaliere *et al.*, 2017). Multiple views and echocardiographic modalities can be used to determine parasitization, constituting an essential tool in the case of obtaining a doubtful or suspicious result in the determination of antigens or microfilaremia (Maerz, 2020). However, echocardiography has important drawbacks in its use as a diagnostic method; It presents a high degree of specialization, it is a test highly dependent on the operator’s experience, and it is also a technique that entails high economic costs compared to other more routine diagnostic methods (Chetboul & Tissier, 2012; Keene *et al.*, 2019; Kim *et al.*, 2020; Greet *et al.*, 2021).

There are also different auxiliary tests that the patient can undergo, such as physical examination, thoracic radiography, electrocardiogram, blood count, biochemical profile and urinalysis. None of these tests provide specific and definitive signs for the diagnosis of cardiopulmonary heartworm disease in the canine species. The main objective of ancillary diagnostic tests is to determine the state of the disease and the patient’s suitability to undergo adulticidal treatment (Hayward *et al.*, 2004; Hwang *et al.*, 2013; Tudor *et al.*, 2014; Tae-Rim *et al.*, 2020; Grosso *et al.*, 2022; Rodríguez-Bendas *et al.*, 2022; Vetter *et al.*, 2023). The objective should also be to start treatment as soon as possible to stop the progression of the disease and prevent the transmission of the infection.

## **E. Treatment**

Treatment for cardiovascular heartworm disease varies depending on the severity of the disease. The parasite load, extension and severity of the lesions produced must be taken into account before starting therapy. The goal of therapy is to improve the patient’s clinical condition and eliminate all life stages of the parasite with as few complications as possible. Adult worms are the greatest risk; the longer they remain in the animal, the greater the damage to the cardiopulmonary system, and consequently the worse signs of illness and death (Antinoff, 2002; Bové *et al.*, 2010; Bradbury *et al.*, 2010; Alho *et al.*, 2016).

The destruction of a high number of parasites in the blood leads to the appearance of considerable side effects, which is why the treatment is complex and can bring serious risks after it has started. Prior to therapy, dogs infected with *D. immitis* should be evaluated and classified for risk of thromboembolism following administration of the adulticidal drug. Factors to consider include number of adult parasites possibly present based on echocardiographic examination, size and age of the patient, concurrent health factors, severity of lung disease, and the degree to which physical exercise can be restricted during the treatment period (Cottrell *et al.*, 2004; Carretón *et al.*, 2019). Restriction of physical activity is of utmost importance since, together with all the factors previously mentioned, it represents a high risk of thromboembolism due to vasoconstriction of the pulmonary vasculature during physical activity (Pariaut *et al.*, 2020).

The information obtained in diagnostic tests will help make treatment decisions. On some occasions, an auxiliary treatment regimen must be chosen prior to adulticidal treatment to improve the patient's hemodynamic and respiratory status. Treatment is generally accompanied by supportive medication as well as non-steroidal anti-inflammatory drugs, glucocorticoids, antiplatelet agents, analgesics and fluid therapy (Pajas *et al.*, 2018; Tjostheim *et al.*, 2019). While in cases with signs of right CHF, patients are usually stabilized prior to adulticidal treatment through the use of diuretics, vasodilators and positive inotropic agents. On the other hand, in cases of caval syndrome, with the presence of worms in the right heart cavities and vena cava, severe signs of disease must be stabilized and it is usually decided to remove the parasites surgically (Lee *et al.*, 2008; Iizuka *et al.*, 2009; Yoon *et al.*, 2011; Lee *et al.*, 2022).

In the 1990s, melarsomine dihydrochloride replaced thiacetarsamide sodium because it is easier to administer and provides greater safety and efficacy. Melarsomine dihydrochloride is the only adulticidal drug currently authorized. Its form of administration is by deep intramuscular injection into the epiaxial lumbar muscles, in the L3 – L5 region. In approximately one third of patients, a local reaction may occur at the injection site. Melarsomine dihydrochloride is effective against worms older than 4 months (Ciuca *et al.*, 2022; Vercelli *et al.*, 2022; Voros *et al.*, 2022).

The currently standard treatment protocol recommended by the European and American societies for the prevention of cardiopulmonary dirofilariosis, ESDA and AHWS respectively, consists of a double adulticidal and microfilaricidal action. The protocol includes the administration on the first day of treatment of a macrocyclic

lactone (the AHWS recommends the use of ivermectin or moxidectin) in order to eliminate *microfilariae*. In this way, administered prior to the adulticidal treatment, they control possible new infections, eliminate existing susceptible *larvae* and allow others to mature before the administration of melarsomine to the point where they are susceptible to the treatment. The administration of macrocyclic lactone will be repeated periodically every 30 days until the treatment protocol is completed. Subsequently, a course of doxycycline is administered at a dose of 10 mg/kg every 12 hours for 28 days. It is considered essential in the treatment of heartworm disease due to its action against *Wolbachia pipientis*. Finally, a first injection of melarsomine (2.5 mg/kg) in the day 60 of treatment, a second injection in the day 90, and a third injection 24 hours (day 91) after the second injection are administered to complete the protocol (Moorhead *et al.*, 2023; Ward *et al.*, 2023).

Recent research has demonstrated the usefulness in reducing the dose of doxycycline to 5 mg/kg every 12 hours, and its effectiveness has also been proven in reducing the waiting period until the first dose of melarsomine, reducing the standard protocol of 91 days to 61. Restriction of the patient's physical exercise is essential during the application of the treatment and in the following 4 to 6 weeks after completion, in order to reduce thromboembolic effects (Carretón *et al.*, 2019; Carretón *et al.*, 2020). The success of the treatment is confirmed with the determination of the absence of antigen carried out 6 months after the last dose of melarsomine. Corticosteroids can be used during the protocol to minimize possible adverse reactions to parasite death after administration of melarsomine and macrocyclic lactones in high risk patients. Prednisone used at a dose of 0.5 mg/kg can be used if pulmonary inflammation and thromboembolic phenomena are suspected (Dantas-Torres *et al.*, 2023).

This protocol is recommended, since it minimizes the risk of thromboembolism caused by the death of the parasites, and allows the patient to eliminate embolic fragments more safely, with fewer pulmonary complications. The protocol eliminates around 98% of adult nematodes. These efficacy rates refer to the percentage of dead nematodes in each dog and not the percentage of dogs with elimination of all parasites. Other studies have shown that patients treated with this protocol have increased seroconversion to an antigen-negative state. The combination of doxycycline, ivermectin and melarsomine significantly reduces the severity of arterial lesions and thrombi (Romito *et al.*, 2023).

## F. Prophylaxis

*D. immitis* infection can be prevented despite the high susceptibility of the canine species. Chemoprophylaxis, when applied appropriately, is undoubtedly the most effective method of prevention in areas of endemic presentation. It is possible for an animal to become infected by missing or delaying the administration of a single preventive dose. These areas are the ones that tend to have warm temperatures almost all year round, an abundance of stagnant water and mosquito populations. Chemoprophylaxis should begin one month before the transmission period and end one month after it; however, in endemic areas, or in regions where the climate allows transmission throughout the year, the administration of chemoprophylactics throughout the whole year is recommended. Puppies should start it as soon as possible, between 6 to 8 weeks of age (Simón *et al.*, 2005; Bowman & Atkins, 2008; McCall *et al.*, 2008). Before starting a preventive regimen in older canines with no medical history, antigen and *microfilariae* testing should be performed. They are also indicated at the beginning and end of each transmission season in those animals that receive scheduled chemoprophylaxis, and in those that receive continuous chemoprophylaxis it is recommended that they be evaluated once a year. It is carried out to exclude the possibility of infection due to poor compliance by the tutor during the previous season, and to verify that there was no pre-existing infection, or to detect failures in the product (Levy *et al.*, 2017; Ames & Atkins, 2020).

The treatment of choice is based on monthly oral or topical administration of a macrocyclic lactone, or injection every 6 months of a slow-release formulation of moxidectin. The macrocyclic lactones currently on the market are ivermectin (6 to 12 µg/kg), milbemycin (0.5 to 0.99 mg/kg), moxidectin (2.5 – 6.8 mg/kg) and selamectin (6 to 12 mg/kg). These drugs are highly effective and are among the safest medications used in veterinary medicine, even in Collies, which are more sensitive breeds (mutation of the MDR1 glycoprotein related to the metabolization of macrocyclic lactones) (Simón *et al.*, 2012). Macrocyclic lactones do not prevent larval inoculation, but they do prevent larval development and kill third and fourth stage larvae within weeks or months of infection, which is why they provide a therapeutic window of long efficacy and prophylaxis at times in which there is a lapse in the administration of preventive treatment by the owner (Spasojevic-Kosic & Lalosevic, 2020; Vercelli *et al.*, 2022).

## G. Prognosis

It is considered that any infected animal that presents an asymptomatic clinical picture has a generally favorable prognosis. Those cases of infections with severe symptoms, although they have a reserved prognosis, a large percentage can be treated effectively. It is important to classify patients prior to starting adulticidal treatment based on clinical findings and diagnostic tests. Its severity should also be evaluated, as well as the possibility of thromboembolism during adulticidal treatment. On certain occasions the standard treatment protocol cannot be carried out and modifications must be used when the animal's clinical condition is not capable of tolerating the therapy, there is even the option of refusing to carry out the treatment (Montoya & Carretón, 2012; Romano *et al.*, 2021) (Figure 3).



\*Figure 3. Hospitalized patient for adulticidal treatment through the administration of intramuscular melarsomine. High-risk patient due to the presence of a high parasite load and signs of severe cardiorespiratory alterations.

All those animals with chronic and severe parasitosis, for which adulticidal and microfilaricidal therapy was successful, will receive therapy to control the possible consequences of the disease. The most notable lesions are disseminated intravascular coagulation, multiple pulmonary thromboembolisms, right CHF, eosinophilic pneumonia, pulmonary fibrosis and pulmonary arterial hypertension. Most of the disorders mentioned above are considered permanent and irreversible once established, so correct management by the veterinarian and the owner is essential, in order to achieve an improvement in the symptoms and quality of life of the patient treated for cardiopulmonary dirofilariosis (Tudor *et al.*, 2014; Falcón-Cordón *et al.*, 2019).



## 2.2.

# Pathophysiology Of Canine Cardiopulmonary Dirofilariosis

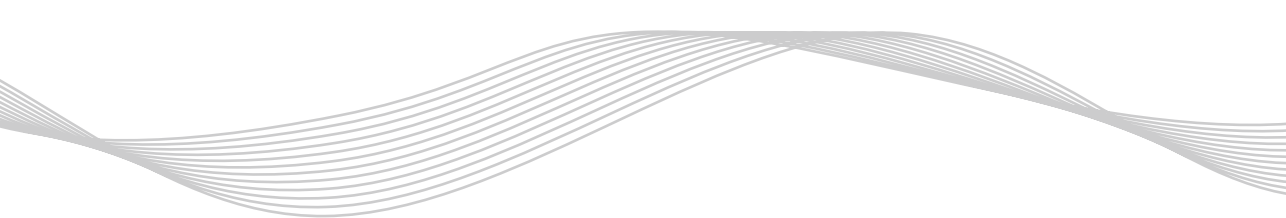
*D. immitis* parasitosis is characterized by the combination of the host's acute and chronic immune response. Heartworm disease causes a multisystem disorder with the lungs, heart, liver and kidneys being the organs most affected. The severity of the lesions will depend on the relative number of nematodes, the duration of the infection and the host's immune reaction (Bové *et al.*, 2010; Carretón *et al.*, 2020). The adult forms are normally found in the pulmonary vascular surface, on many occasions being able to migrate to the main PA, right heart and even the vena cava, in cases of severe infections (Cancrini & Kramer, 2001) (Figure 4).

The pulmonary arterial system is the main site associated with the pathology caused by *D. immitis*, and as the disease progresses, the effects are seen as both functional and pathological alterations, not only in the vascular surface but also in the underlying interstitial lung tissue. The greatest effect at the level of the PA is produced by the immunological response of the host, as well as to toxic substances and physical trauma, which, as a consequence, give rise to villous proliferation of the intimal layer of the vascular endothelium, local inflammation, pulmonary hypertension, disruption of vascular integrity and fibrosis. All of this can be aggravated by arterial and venous obstruction caused by live worms or together to thromboembolism with dead parasites (Pajas *et al.*, 2018; Maerz, 2020).



\*Figure 4. Massive *Dirofilaria immitis* infection, obstructing pulmonary circulation, observed through necropsy analysis in a male Cocker Spaniel dog, 15 kg in weight and 7 years old.

Pulmonary vascular lesions begin to develop within days of the arrival of *D. immitis* to the pulmonary arterial system, which can be as early as 3 months post infection. Endothelial damage with detachment and villous proliferation is usually observed, histologically termed proliferative pulmonary endarteritis. Leukocyte and platelet activation and chemotaxis occur; the arrival of these cells



and the release of trophic factors induce inflammation and a proliferation of smooth muscle with collagen accumulation and fibrosis (Tjostheim *et al.*, 2019; Tae-Rim *et al.*, 2020).

The villi produced by this mechanism are pathognomonic for the disease; they are formed by smooth muscle cells, collagen, and an endothelial-type coverage. The extension is directly related to the parasite load and the duration of parasitosis (Venco *et al.*, 2001; Romano *et al.*, 2021). The inflammatory reaction seems to be aggravated by the action of *Wolbachia pipientis*, being related to arterial lesions, peri-vascular inflammation, endothelial proliferation and a greater probability of the presence of thrombi (Manoj *et al.*, 2021; Santhakumari *et al.*, 2021).

Pulmonary hypertension caused by *D. immitis* parasitosis can be defined by two different, closely associated mechanisms. Pulmonary arterial hypertension associated with endothelial damage caused by the presence of parasites and pulmonary hypertension due to the formation of pulmonary emboli or thromboembolism. Thickening of the vascular endothelium and narrowing of the lumen of the peripheral branches of the PA are the main factor in blood flow obstruction and pulmonary hypertension. In the same way, there is a loss of distension capacity of the damaged pulmonary arteries during cardiac systole and diastole. Pulmonary capacity to maintain low and stable pressures becomes difficult (Venco *et al.*, 2001; Spasojevic-Kosic & Lalosevic, 2020; Yuchi *et al.*, 2023). Distally, smaller caliber vessels may be partially or totally occluded by parasitic emboli or thromboemboli, as well as by an endovascular reaction. These are believed to be the main factors attributable to PA dilation observed by imaging techniques in advanced cases of the disease (Roldán-Alzate *et al.*, 2014).

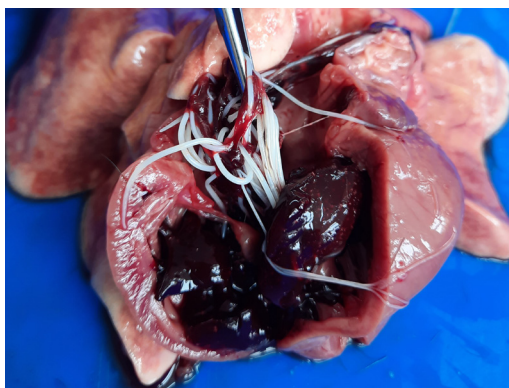
Macroscopically, the lesions show a thickening of the vascular walls and a rough texture of the vascular surface of the large blood vessels, but blood flow is not obstructed due to a decrease in the arterial lumen. The large arteries dilate as pulmonary hypertension becomes more severe. Blood flow is mainly affected by the decreased lumen of the peripheral arterial branches and the loss of compliance during the cardiac cycle and the inability to balance blood pressures during systole and diastole (Chikwetoa *et al.*, 2014; Venco *et al.*, 2014).

The decrease in compliance of the large blood vessels increases cardiac work significantly. In the first stage, pulmonary blood pressure remains stable and increases slightly during physical exercise. As pulmonary hypertension develops, the afterload (resistance to blood outflow) of the RV increases, and in response there is initially right ventricular concentric hypertrophy characterized by diastolic dysfunction (Nagueh *et al.*, 2009). In an advanced stage, systolic dysfunction is caused, associated with a noticeable increase in cardiac size caused by dilation and eccentric hypertrophy of the RV and atrium (RA), added to the increase in size of the PA. Right heart dilation occurs in response to the increase in end-systolic volume (Serrano-Parreño *et al.*, 2017; Falcón-Cordón *et al.*, 2019).

The greater the severity of the disease and the patient's activity, the greater the compensatory cardiac work. In advanced cases, the inability to generate and maintain the perfusion pressures necessary to circulate blood through the pulmonary circuit develops (Tudor *et al.*, 2014). As a result of volume overload in the right cardiac chambers, normally associated with the presence of tricuspid regurgitation and low contractility, a decrease in cardiac output and a retrograde increase in venous pressure is generated. Finally, signs of right CHF appear, such as ascites, pleural effusion, pericardial effusion, and subcutaneous edema. Generally, right CHF occurs gradually and chronically. However, acute cases may occur due to thromboembolism phenomena after adulticidal treatment or due to the natural death of a large number of nematodes (Hidaya *et al.*, 2003; Lee *et al.*, 2008).

Another cause of the acute presentation may be the retrograde migration of adult worms from the PA to the RV, RA and/or vena cava. This phenomenon is called caval syndrome associated with cardiopulmonary heartworm disease and is a relatively rare but severe complication of the disease caused by *D. immitis* (Small *et al.*, 2008; Lee *et al.*, 2022). The reason for this aberrant distribution is not fully understood, but it may be due to the presence of a relatively high nematode load and retrograde migration of adult forms due to hemodynamic changes, such as an acute episode of increased pulmonary hypertension, or reduction in cardiac output. The function of the tricuspid valve is severely altered due to the presence of worms in the right heart chambers and regurgitation is superimposed on chronic pulmonary hypertension. Right ventricular filling can be compromised by arrhythmias and obstruction by the nematodes. There is a decrease in ventricular preload and subsequent worsening of CHF (Figure 5). The prognosis is unfavorable, and emergency surgery is usually required to remove

the parasites through surgical procedures. However, even in animals undergoing surgical treatment, mortality is around 40% or higher due to the usual presence of cardiogenic shock complicated by anemia, metabolic acidosis, and disseminated intravascular coagulation (Yoon *et al.*, 2011; Pariaut *et al.*, 2020).



\*Figure 5. Representative image of performing a necropsy on a dog suffering from heartworm caval syndrome. Multiple adult worms can be observed in the right atrium and ventricle, producing severe cardiovascular disorders.

Other pathological alterations associated with parasitization by *D. immitis* in dogs include damage to the lung parenchyma, normally due to a hypersensitivity reaction against the parasites with the presence of immune-mediated destruction of *microfilariae* in the pulmonary circulation, producing an inflammatory response called eosinophilic pneumonia. On the other hand, once right CHF develops, passive chronic venous congestion can be observed at the liver level. Hepatomegaly of variable degree is commonly present, a darker tone due to venous congestion, the capsular surface may present a

lobular or granular pattern and central lobular necrosis may be observed due to congestion and dilation of the central veins and hepatic sinusoids (Antinoff, 2002; Hwang *et al.*, 2013; Maerz, 2020). Most dogs with chronic parasites have renal glomerulonephritis, which can be severe. The lesions present include inflammation and fragmentation of the basement membranes, with loss of endothelial cells, fragmentation and atrophy. The severity of kidney lesions has been linked to the degree of microfilaremia, the formation of immune complexes and reaction to the presence of *Wolbachia pipientis* surface proteins (Carretón *et al.*, 2020; Rodríguez-Bendas *et al.*, 2022; Vetter *et al.*, 2023). Cases of aberrant migrations of larvae and adult parasites have also been reported, with alterations found in the central nervous system, reproductive system, ocular disorders and skeletal muscles (McCall *et al.*, 2008; Montoya & Carretón, 2012; Pajas *et al.*, 2018; Adebayo, 2020).



## 2.3.

# Echocardiographic Diagnosis Of Pulmonary Hypertension in canine cardiopulmonary dirofilariosis

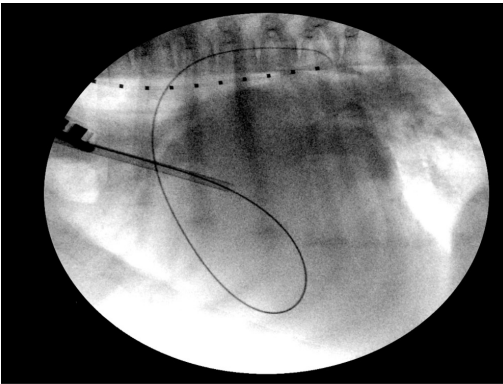
The pulmonary circulation's objectives are blood gas exchange, being a reservoir of intravascular volume and acting as a filter against thromboembolisms and infections from the respiratory system. It is a low pressure circuit, with average systolic pressure values of 20 mmHg, diastolic pressure of 8 mmHg and mean pressure of 14 mmHg (Cavaino *et al.*, 2018b; Braz *et al.*, 2021). In systole, right ventricular contraction causes the ejection of blood with high concentrations of CO<sub>2</sub> from the RA and the vena cava towards the PA, whose main trunk branches into right and left PA and, through the vascular tree, reaches the functional unit, the alveolocapillary membrane, where gas diffusion and oxygen uptake occur. The oxygenated blood is collected by the pulmonary veins (PV) and conducted to the left heart, to be ejected through the left ventricle (LV) towards the Aorta (Ao) and thus perfuse the body (Lyssens *et al.*, 2022).

The general characteristics of the pulmonary circulation are that the PA carry unoxygenated blood and the PV return oxygenated blood, it has high vascular compliance, has greater capacitance than the systemic circulation and less resistance to blood flow. Pulmonary circulation is regulated by local control through hypoxic vasoconstriction and elevation of venous pressure, hormonal control through vasoconstrictor substances (catecholamines, endothelin, antithrombin I, thromboxane) and vasodilators (cholinergic factor, isoproterenol, prostaglandins) and through parasympathetic nervous control through acetylcholine as a neurotransmitter and sympathetically through norepinephrine (Naeije, 2013; Visser, 2017).

Pulmonary hypertension is a complex syndrome of multifactorial etiology that consists of a progressive and sustained increase in pulmonary vascular resistance that results in persistent elevation of pulmonary arterial pressure (Chan *et al.*, 2019). The sustained increase in pulmonary pressure over time causes an imbalance in the endothelial release of vasoconstrictor and vasodilator substances, which leads to hypertrophy of the arterial *tunica media*, thickening and fibrosis of the *media* and *adventitia* layers, and necrotic arteritis (Boissiere *et al.*, 2008). The pathophysiology is variable depending on the etiological classification. In the case of canine cardiopulmonary dirofilariosis, the classification of the American

College of Veterinary Internal Medicine (ACVIM) has stated that it belongs to group 5, being causes of precapillary pulmonary hypertension of parasitic origin along with *Angiostrongylus vasorum* infection (Reinero *et al.*, 2020).

In human medicine, the criterion standard method for the diagnosis of pulmonary hypertension is direct assessment of pulmonary arterial pressure by right heart catheterization, and in humans, pulmonary hypertension has been defined as a systolic pulmonary arterial pressure  $\geq 25$  mmHg, or when the mean pulmonary pressure rises above 20 mmHg at rest (Lang *et al.*, 2015). However, estimation through invasive catheterization in veterinary practice is not routinely feasible for various reasons such as economic cost, possible anesthetic complications in patients with cardiac pathologies, the time invested in the procedure, etc. Additionally, previous research has shown that in humans, the risk of PA catheterization is exacerbated when humans have pulmonary hypertension (Kellihan & Stepien, 2012; Gentile-Solomon *et al.*, 2016). Therefore, cardiac catheterization is an invasive procedure that requires general anesthesia and is not routinely performed on dogs in a clinical setting (Figure 6).



\*Figure 6. Representative image of performing right heart catheterization using fluoroscopic guidance to measure intracavitary pressures and determine pulmonary arterial pressures in a canine patient infected with *Dirofilaria immitis*.

The main factors that favor the development of pulmonary hypertension in dogs are: increase in blood flow, increase in vascular resistance, and/or increase in venous pressures. Based on this, hypertension can be classified as precapillary or postcapillary (Reinero *et al.*, 2020). The causes that generate the appearance of pulmonary hypertension of postcapillary origin are the increase in blood flow, which may be due to the increase in cardiac output and left-to-right shunts (Heejin *et al.*, 2014; Greet *et al.*, 2021). On the other hand, postcapillary pulmonary hypertension can be secondary to left-sided heart

disease that causes increased filling pressure of the left atrium (LA) or LV (called pulmonary arterial wedge pressure). It develops because increased pressure in the LA increases the load on the RV and indirectly requires the development of higher right ventricular systolic pressures (Huang & Tai, 2013; Lee & Choi, 2022).

Increased pulmonary arterial pressure can also be caused by an increase in pulmonary vascular resistance due to structural changes of the PA associated with a wide variety of causes, mostly produced in the lung parenchyma. Increased pulmonary arterial pressure associated with increased pulmonary vascular resistance in the absence of increased LA pressure defines precapillary pulmonary hypertension (Morita *et al.*, 2019; Roels *et al.*, 2019).

Postcapillary pulmonary hypertension resulting from chronic and progressive left-sided heart disease can cause vasoconstriction of the PA and pulmonary vascular disease, which consequently increases pulmonary vascular resistance. Therefore, postcapillary pulmonary hypertension can occur in isolation, or it can occur together with increased pulmonary vascular resistance, generating combined postcapillary and precapillary pulmonary hypertension (Tidholm *et al.*, 2009; Toaldo *et al.*, 2016; Tuleski *et al.*, 2022).

Imaging diagnostic techniques play a fundamental role in the estimation of canine pulmonary hypertension, since they represent a quick and, in most cases, accurate solution, to be able to estimate pulmonary pressures and other useful parameters in the presentation of different cardiorespiratory pathologies. Advanced techniques such as high-field magnetic resonance imaging, computed axial tomography (CT) or angiography are used to diagnose pulmonary hypertension (Cannon *et al.*, 2009; Granger *et al.*, 2016; Sutherland-Smith *et al.*, 2018). Echocardiography currently provides the most accurate, non-invasive, available and cost-effective estimation of pulmonary pressure in dogs. Echocardiography should be viewed as an essential clinical tool to help assess the likelihood that a dog has pulmonary hypertension. However, it should not be considered as a definitive diagnostic test for confirmation of the presence of pulmonary hypertension. The definitive diagnosis of pulmonary hypertension always requires evaluation by catheterization of the RV (Nijhawan *et al.*, 2019; Morita *et al.*, 2022).

Generally, echocardiographic evaluation of pulmonary hypertension relies heavily on the characteristic morphological cardiac changes that occur as a consequence of pulmonary hypertension and on the estimation of PA pressure from spectral Doppler tracings. As described above, because right ventricular catheterization is rarely used for the definitive diagnosis of pulmonary hypertension in dogs, veterinarians have traditionally relied on echocardiography for the diagnosis, classification, and treatment of dogs with pulmonary hypertension. Echocardiographic determinations are intended to avoid misdiagnosis and

inappropriate treatment of pulmonary hypertension that could have a lasting impact on the dog and its owner (Schober *et al.*, 2006; Paradies *et al.*, 2014).

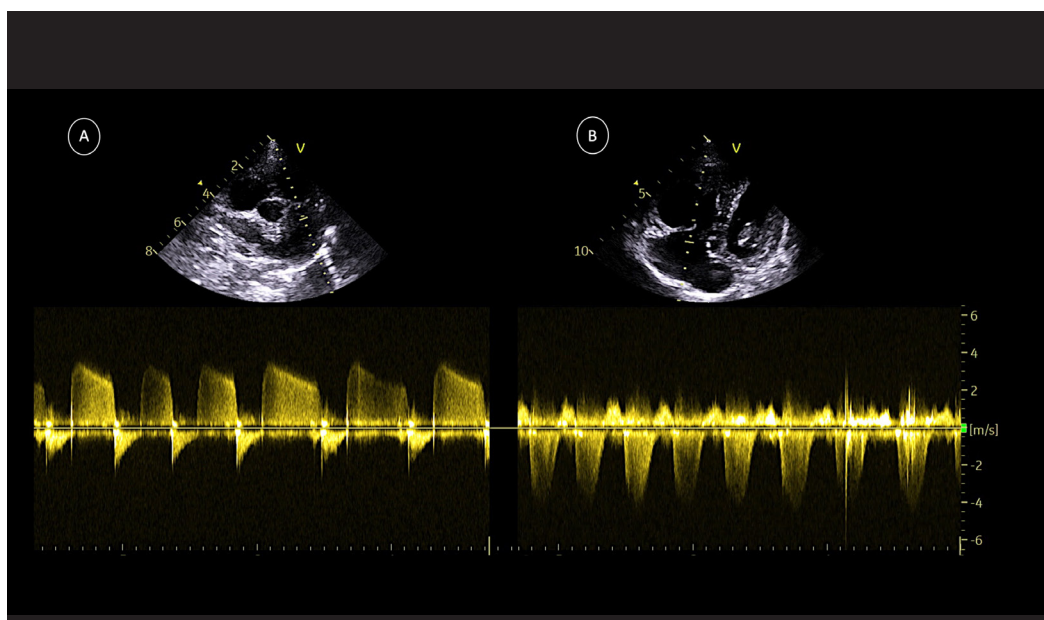
However, the use of echocardiography as a technique for estimating pulmonary arterial pressure has serious limitations. Ultrasonographic examination presents a high degree of inaccuracy, variability and imprecision, particularly in the Doppler mode. The factor of the skill or experience of the operator, the variability of equipment and software for analyzing ultrasound images and the individual particularities of canine patients represent serious difficulties in estimating pulmonary arterial pressure in veterinary medicine (Teshima *et al.*, 2006; Oleynikov & Yi, 2022).

Echocardiographic evaluation of pulmonary hypertension is only one aspect, although an important one, in the overall clinical evaluation of a dog with suspected pulmonary hypertension. Echocardiographic findings should always be interpreted within the context of other clinical findings, especially the presence or absence of clinical signs suggestive of pulmonary hypertension and right CHF status, as well as the results of alternative diagnostic tests (Vezzosi *et al.*, 2018a, Visser *et al.*, 2020). In the case of cardiopulmonary dirofilariosis, the use of echocardiography should be considered to evaluate the presence of pulmonary hypertension in dogs that reside in endemic areas for the infection or that have had the disease in the past. Ultrasonographic examination is especially essential if the heartworm patient presents clinical signs such as cough, dyspnea, syncope or exercise intolerance or thoracic radiological abnormalities are observed such as increased silhouette of the right heart, dilation of the pulmonary trunk, dilated and tortuous PA or broncho-infiltrates (Venco *et al.*, 2014; Serrano-Parreño *et al.*, 2017a; Serrano-Parreño *et al.*, 2017b; Pajas *et al.*, 2018).

Traditionally in veterinary medicine, the degree or severity of pulmonary hypertension has been classified as mild, moderate or severe, regardless of its origin. These categories are based on the pressure gradient derived from echocardiographic assessment of tricuspid regurgitation velocity or systolic PA pressure estimated by other less accurate methods (Serres *et al.*, 2007; Vezzosi *et al.*, 2018; Visser *et al.*, 2020). Recently, the international consensus on pulmonary hypertension developed by the ACVIM recommends taking into consideration the clinical impact of pulmonary hypertension, and not diagnosing it solely and exclusively with echocardiographic estimation (Reinero *et al.*, 2020). It has been proposed that the limits used for the classification



of pulmonary hypertension (mild 30-49 mmHg, moderate 50-79 mmHg and severe >80 mmHg) are arbitrary and the categories are potentially misleading or defective, especially when attempting to differentiate between the presence of mild and moderate pulmonary hypertension or the absence of pulmonary hypertension. Likewise, the etiological origin and the cardiovascular and respiratory pathophysiology (pre-capillary, post-capillary or combination) have a resounding impact on the severity of the patient's clinical picture, regardless of the echocardiographic estimate reported. Therefore, it is not recommended to standardize the study of pulmonary hypertension in a general way in all patients, and specific methods and protocols should be sought for each pathological condition (Sampedrano *et al.*, 2006; Wess *et al.*, 2017; Cavaino *et al.*, 2018a; Roels *et al.*, 2021; Lee *et al.*, 2022). However, it has generally been proposed that the clinical definition of pulmonary hypertension should include dogs with an intermediate or high probability of pulmonary hypertension and, specifically, a tricuspid regurgitation pressure gradient limit >46 mmHg (TRV >3.4 m/s) (Figure 7).



\*Figure 7. Representative image of the echocardiographic determination of the maximum speed of pulmonary valve regurgitation (A: 3.84 m/s; 58.98 mmHg), and tricuspid maximum speed regurgitation (B: 4.63 m/s; 85.75 mmHg), using continuous spectral Doppler in an animal parasitized by *Dirofilaria immitis* and suffers from pulmonary hypertension.

This is roughly equivalent to what has conventionally been called at least moderate pulmonary hypertension (Kellihan & Stepien, 2012; Visser *et al.*, 2016; Vezzosi *et al.*, 2018a). Previous research focused on canine pulmonary hypertension reports the clinical usefulness of assessing tricuspid regurgitation velocities greater than 3.4 m/s or the presence of pulmonary valve insufficiency above 2.2 m/s (Schober *et al.*, 2006; Paradies *et al.*, 2014; Sutherland-Smith *et al.*, 2018; Roels *et al.*, 2019). However, regurgitation jets are not always present, or are difficult to analyze, so the measurement depends on the cardiovascular composition and the skill of the operator, and difficulty in obtaining reliable maximum speeds is common. Through ultrasonography, findings and data can be obtained in various methods that estimate pulmonary pressure and support the diagnosis of pulmonary hypertension in a non-invasive way (Toaldo *et al.*, 2016; Morita *et al.*, 2019; Wolf *et al.*, 2021). However, new reliable, repeatable, with high sensitivity (Sen), Sp and acceptable diagnostic accuracy in relation to right heart catheterization methods for the determination of pulmonary hypertension should be investigated in veterinary medicine.

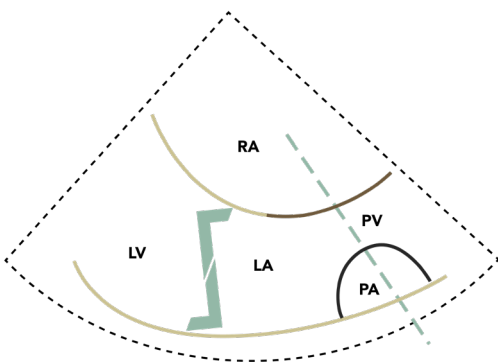
### **2.3.1. Structural Changes in Pulmonary Vasculature**

The PV and PA are dynamic structures that physically change their diameter during the cardiac cycle. Vessel size depends on the volume of flow through the vessel, intravascular hydrostatic pressure, and vascular compliance. PV are more expandable than PA and generally increase in size with increases in left ventricular end-diastolic pressure or increased pulmonary blood flow. PA enlarge with increased pulmonary blood flow, pulmonary hypertension, idiopathic dilation of the PA, or due to valvular or subvalvular pulmonary stenosis (poststenotic dilation) (Biretoni *et al.*, 2016).

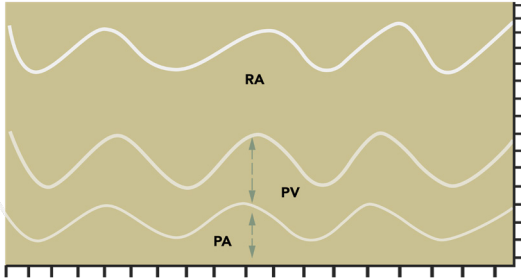
In this sense, veterinarians have traditionally evaluated these vascular structures to obtain valuable information about the hemodynamic status of canine patients. In this way, the evaluation of the relative size of the PV and PA on radiographs comparing them with each other and with respect to the size of the ribs is routinely performed (Heejin *et al.*, 2014; Tudor *et al.*, 2014). Furthermore, the PV and PA associated with the same bronchus are approximately the same size in normal dogs (Hayward *et al.*, 2004; Adams *et al.*, 2017; Lee *et al.*, 2022). In

recent years, the use of CT in the study of cardiorespiratory diseases in veterinary medicine has increased. The use of CT angiography and the measurement of the relationship between vascular structures at the thoracic level has offered optimal results in the evaluation of the presence of pulmonary hypertension in animals that suffer from pathologies different than heartworm (Cannon *et al.*, 2009; Granger *et al.*, 2016; Sutherland-Smith *et al.*, 2018). In this sense, the diameters of PV and PA have recently been studied and the relationship between the PA and its adjacent PV taken in a cross-sectional image using in the canine species has been evaluated (Soliveres *et al.*, 2021). As in human medicine, the assessment of these structures through the ratio between the PV and the PA has proven to be a powerful predictive value in estimating pulmonary hypertension when the value is  $<1.0$  (Ascha *et al.*, 2017).

As a result of the comparison between the pulmonary vessels, recently, multiple investigations have evaluated the diameter of the PV and the diameter of the PA in dogs and cats as a valuable echocardiographic index (Biretoni *et al.*, 2016; Patata *et al.*, 2019; Roels *et al.*, 2021). Diameters of PV and PA can be easily and conveniently imaged by transthoracic echocardiography in dogs and cats using a slightly modified right parasternal 4-chamber view, and a short-axis right parasternal view at the level of the bifurcation of the pulmonary trunk, to obtain M-mode imaging or 2D imaging (Merveille *et al.*, 2015). It can be observed the confluence of both vascular structures (right PV and PA) and is relatively easy to see their dynamic changes from the cardiac cycle and cardiorespiratory pathologies. The relationship between PV and PA is maintained in both systole and diastole, and the anatomical landmarks are easily detectable by echocardiography (Figure 8 & 9).



\*Figure 8. Representation of the determination of the relationship between the right pulmonary artery and vein (PV:PA) by echocardiographic method in two-dimensional mode using a right parasternal long axis 4-chamber view. RA: right atrium, LV: left ventricle, LA: left atrium, PV: pulmonary vein, PA: pulmonary artery.



\*Figure 9. Representation of the determination of the relationship between the right pulmonary artery and vein (PV:PA) by echocardiographic method in monodimensional mode using a right parasternal long axis 4-chamber view. RA: right atrium, PV: pulmonary vein, PA: pulmonary artery.

Biretoni *et al.*, (2011) first described the use of PV to PA ratio (PV:PA) measured by echocardiography in dogs at the XXI European congress of veterinary internal medicine (ECVIM Congress, Seville, Spain). The right PA and the right PV and their variations in indices were analyzed in dogs with myxomatous mitral valve disease at different stages. With the aim of knowing if these measurements could be helpful to early distinguish dogs in CHF (increased in PV diameters). The right ostium of the PV and the right PA were measured using the M-mode from modified right parasternal long-axis

views at the maximal and minimal diameters, and at the peak of the QRS and end of the T-waves. An optimal cut-off of 1.8 was showed to PV:PA at the end of the T-waves value with 85% Sen and 62% Sp for detecting CHF. The conclusion was that echocardiographic indices could be useful in discriminating subclinical and CHF in dogs with similar degrees of cardiac enlargement.

Subsequently, a study developed by the same authors reported reference intervals in healthy dogs from M-mode and 2D images using modified right parasternal long and short axis views. Measurements of the right ostium of the PV and the right PA were timed with electrical events (peak of the QRS complex and end of the T wave) or mechanical events (PV and PA vessels at their respective maximum and minimum diameters). In all cases, to measure the diameter of the PV and PA, the inner-edge-to-inner-edge method was used drawing a line perpendicular to the medial PV and passing through the center of the adjacent right PA at the site of the maximum vascular diameter. In normal dogs, regardless of echocardiographic view or cardiac cycle time, the PV:PA ratio approached 1.0 with good intra- and interobserver reproducibility. ECG-timed fractional changes in PV and PA diameter were at least 50% smaller than mechanically timed changes, regardless of the echocardiographic view used. Physiologically the echocardiography derived relationship between PV and PA in healthy dogs approaches 1.0, similar to what has been documented radiographically (Biretoni *et al.*, 2016).

PV:PA ratio measured by echocardiography has recently been used to predict CHF in dogs suffering from myxomatous degenerative valvular disease. The ratio was measured in 2D and M-mode using a right parasternal long axis 4-chamber view optimized to simultaneously visualize a longitudinal section of the medial PV and the right PA in cross-section. The dimensions were obtained by tracing a line perpendicular to the medial PV and passing through the center of the adjacent right PA. For both measurements, were used the inner edge-to-inner edge method at the end of the T wave. The PV:PA in healthy dogs was approximately 1.0. The presence of CHF could be best predicted by measuring PV:PA in 2D echocardiography (cut-off, 1.7; AUC, 0.98; CI, 0.97–0.98; P <0.001) with a Sen of 96% and Sp of 91% (Merveille *et al.*, 2015).

The PV:PA ratio has been proposed as an index that can help discriminate cats suffering from CHF. A previous study determined reference intervals for various PV and PA variables in healthy cats and cats with clinical and subclinical cardiomyopathy with the objective of determining their diagnostic usefulness to identify CHF. PV and PA were measured at the minimal and maximal diameters using M-mode images obtained from a modified right parasternal long axis view. The results showed that the median PVmin/P Amin value in healthy cats was approximately 0.51 and the PVmax/P Amax value was 0.67. Cats with CHF had higher PVmin/P Amin and PVmax/P Amax values compared to subclinical and healthy cats. When evaluating the diagnostic performance of these variables in cardiomyopathic cats, PVmin/P Amin values had higher accuracy compared to the LA:Ao value when identifying cats with CHF (Patata *et al.*, 2019).

These studies have shown that the PV:PA ratio, obtained from a modified view of the right parasternal long axis and using the inner-edge-to-inner-edge method, discriminated dogs and cats with CHF from healthy animals and patients with subclinical heart disease. Furthermore, certain variables PV and PA performed better than other measures in discriminating cardiomyopathic cats with and without CHF (Biretoni *et al.*, 2011; Merveille *et al.*, 2015; Patata *et al.*, 2019).

Recent studies apply the PV:PA ratio in the identification of pulmonary hypertension in dogs. Firstly, a retrospective study analyzed the PV:PA measured by both 2D and M-mode in dogs suffering from pulmonary hypertension of precapillary origin excluding cardiopulmonary heartworm disease. A right parasternal long axis four-chamber view was optimized to simultaneously visualize the right ostium of the PV in the longitudinal section and the right PA in the cross section. For both measurements, the inner edge-to-inner edge method

was used with measurements timed to the end of the T wave. Results of the study identified the 2D PV:PA as the strongest predictor for the presence for moderate pulmonary hypertension (TRPG >50 mmHg) using a cutoff value of <0.70 (Sen: 96%,Sp: 82%) (Roels *et al.*, 2019). On the other hand, the same authors later used the measurement of PV:PA ratio following the same protocol to assess survival in West Highland White Terriers with canine idiopathic pulmonary fibrosis. The cut-off value of <0.7 was used as a measure to determine the presence of pulmonary hypertension in the patients analyzed (Roels *et al.*, 2021). These investigations highlight the potential usefulness of echocardiographically derived PV:PA as a complementary, non-invasive tool for the diagnosis of at least moderate, precapillary pulmonary hypertension determination in dogs.

In large animals, various studies have also been carried out on this ratio, highlighting the one carried out by Caivano *et al.*, (2019) in which a total of 70 healthy horses were used, and obtained reference intervals in the diameter of both vessels and their relationship. Using a right parasternal long axis view, the maximum and minimum diameters of right PV and right PA were measured using M-mode. Median of the minimum and maximum PV:PA was 0.51 and 0.60, respectively. No relationships between either bodyweight or heart rate and any of the vein or artery variables were identified. Inter- and intra-observer variability measurement was very good for all PV and PA measurements. Measuring of PV and PA diameters using M-mode transthoracic echocardiography is feasible in equine cardiology (Cavaino *et al.*, 2019; Ferraro *et al.*, 2023).

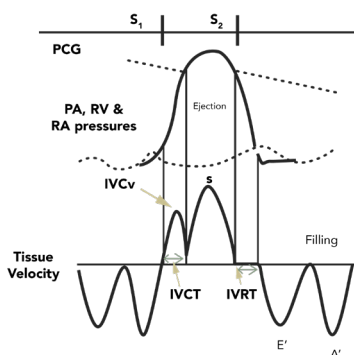
### **2. 3. 2. Tissue Doppler imaging**

Tissue Doppler imaging (TDI) for echocardiographic evaluation of myocardial function was first described in 1989 in human medicine, and was a true revolution in the quantitative evaluation of myocardial function. Doppler ultrasound is based on the detection of a change in frequency of ultrasound signals reflected by moving objects. In the heart, both blood flow and myocardial contraction cause changes in velocity. Blood flow causes high-frequency, low-amplitude signals that are obtained using traditional spectral Doppler. TDI images are designed to characterize low-velocity, high-amplitude signals of myocardial motion, and are obtained by reversing the low-pass filter used in traditional Doppler into a high-pass filter (Sampedrano *et al.*, 2006).

The myocardium comprises subendocardial and epicardial layers, with the subendocardium characterized by longitudinally arranged myofibers. Throughout ventricular contraction, these layers exert varying tension, causing the endocardium to move over greater distances. TDI specifically assesses the longitudinal component of myocardial contraction across the entire cardiac cycle (Morita *et al.*, 2021).

TDI is obtained using pulsed-wave tissue Doppler or color tissue Doppler. Pulsed-wave TDI measures the longitudinal myocardial velocity peak of a single segment, and is performed instantaneously without further processing. Color tissue Doppler images require post-processing after echocardiographic imaging and can interrogate velocities from multiple sites simultaneously. However, color tissue Doppler represents the mean maximum velocity and is 25% lower than Pulsed-wave TDI. Therefore, the two methods are not interchangeable with each other (Koenig *et al.*, 2017).

During a cardiac cycle, the TDI representation shows three peaks: one positive systolic peak and two negative diastolic peaks. The positive systolic wave (S velocity) reflects myocardial contraction, while the negative waves indicate early diastolic myocardial relaxation (E' velocity), and active atrial contraction in late diastole (A' velocity). Additionally, periods of isovolumetric contraction (IVCT) and relaxation (IVRT) can be identified (Figure 10). Pulsed-wave TDI velocity measurements are obtained by placing the sample volume at the level of the mitral or tricuspid annulus or within the basal myocardial segment of the LV or RV. Although TDI velocities can be measured from the septal or lateral annulus, the current recommendation is to express velocity as the average of the septal and lateral measurements (Fontes-Sousa *et al.*, 2009; Mandour *et al.*, 2020).



\*Figure 10. Diagram illustrating the correlation between tissue Doppler imaging tracings and invasive hemodynamic variables: PCG, phonocardiogram; ECG, electrocardiogram; S, peak systolic myocardial velocity; E', peak early diastolic myocardial velocity; A', peak late atrial myocardial velocity; IVCT, isovolumic contraction time; IVRT, isovolumic relaxation time; S1, first heart sound; S2, second heart sound; PA, pulmonary artery; RV, right ventricle; RA, right atrium.

TDI measurements have been used in various cardiac conditions, validated as markers of left and right ventricular systolic dysfunction, left and right ventricular diastolic dysfunction, left and right ventricular dyssynchrony, and auricular function (Chetboul *et al.*, 2005; Koffas *et al.*, 2006; Serres *et al.*, 2007; Toaldo *et al.*, 2016; Morita *et al.*, 2019). Its usefulness extends to the evaluation of specific cardiac diseases in small animals, such as degenerative mitral valve disease in dogs, dilated cardiomyopathy in dogs, and hypertrophic cardiomyopathy in cats, among others, with prognostic implications (Sampedrano *et al.*, 2006; Chetboul *et al.*, 2007; Toaldo *et al.*, 2016). Tissue Doppler measurements are more sensitive than conventional echocardiography in detecting early myocardial alterations in primary (hypertrophic and dilated cardiomyopathies) and secondary disorders (e.g., ischemia), making TDI useful in screening and detection of subclinical myocardial dysfunction, as well as to evaluate the effectiveness of therapeutic interventions (Yuchi *et al.*, 2023). Echocardiographic assessment of right ventricular function is often underreported due to the difficulty in achieving accurate assessment, given its retrosternal position, which presents additional challenges in imaging. Similar to the LV, pulsed TDI velocities in the RV exhibit a gradient from the base to the apex, with velocities on the laterals of the RV being greater than those on the laterals of the LV (Tidholm *et al.*, 2009).

The S velocity measures longitudinal contraction of the ventricle and serves as a surrogate for ventricular systolic function. Nonetheless, TDI has limitations as it is unable to fully distinguish active myocardial contraction from the tethering effects of adjacent myocardium, lacking Sp in terms of site differentiation. The TDI E' velocity is measures of ventricular relaxation in early diastole and are relatively independent of volume load. E' velocity can be measured from the septal or lateral annulus in the apical four-chamber view, although regional variation exists (Morita *et al.*, 2016). In normal subjects, transmitral velocity E is greater than velocity A; however, in early diastolic dysfunction, this pattern is reversed, and E velocity is reduced, making it difficult to use the mitral inflow pattern to assess diastolic dysfunction. However, the E' velocity proves useful when relating it to the transmitral E velocity in the analysis of left ventricular diastolic function (E:E'). The TDI late diastolic velocity, A', is useful in evaluating atrial function. A' velocity serves as a marker of global atrial function and normally increases with age in human medicine, without significant regional variations. This velocity correlates with other measures of atrial function, such as peak transmitral velocity A, atrial fraction, and atrial ejection force. High-speed color TDI allows evaluation of segmental atrial function (Yuchi *et al.*, 2023).



IVRT refers to the early stages of ventricular diastole, when both the atrioventricular and semilunar leaflets are closed. During this phase, there is no change in the amount of blood in the ventricle, but there is a precipitous drop in intraventricular pressure. When the ventricle begins to contract, the pressure exceeds that of the corresponding atrium, resulting in the closure of the atrioventricular leaflets. At the same time, the pressure is not enough to open the semilunar valves. However, the ventricles are in the IVCT state, since there is no change in the total volume of the ventricle. The IVRT is defined in TDI as the time interval between S and the start of E', and the IVCT is defined as the time interval between the end of A' and the start of S. The duration of IVRT and IVCT of the RV are intimately determined by the RA pressure, the PA systolic pressure and the heart rate (Chetboul *et al.*, 2005; Serres *et al.*, 2007).

The S wave derived from pulsed-wave and color TDI has been studied in healthy dogs, demonstrating reproducibility and repeatability. In addition, reference intervals for each parameter (S, E' and A') have been also established in dogs. Pulsed-wave TDI derived S shows a robust correlation with invasively assessed right ventricular function in healthy dogs. In 2005, a study demonstrated the usefulness of TDI for the estimation of pulmonary hypertension causing right ventricular dysfunction (Boissiere *et al.*, 2005). Clinically, color TDI-derived S proves diagnostically valuable in dogs with pulmonary hypertension and may offer early predictive value for dilated cardiomyopathy in dogs (Chetboul *et al.*, 2007). Therefore, indices of RV function using TDI, such as S, E':A', and G-TDI (global TDI index defined as  $S * E':A'$ ), have been outlined in dogs with pulmonary hypertension. A G-TDI value below 11.8 cm/s predicted pulmonary hypertension with 89% Sen and 93% Sp. Additionally, an E':A' value below 1.12 predicted pulmonary hypertension with 89% Sen and 90% Sp (Serres *et al.*, 2007).

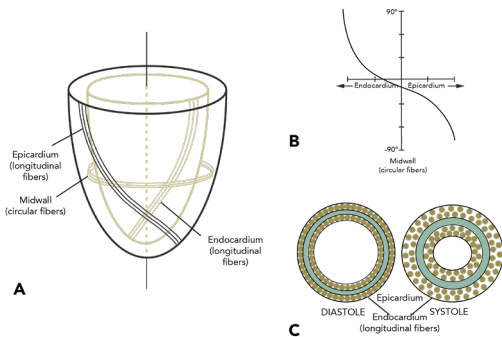
Currently, the diagnostic value of the optimized measures in TDI mode for the assessment of precapillary and postcapillary pulmonary hypertension in small animals has been reinforced and is considered a fundamental echocardiographic mode for the analysis of cardiac ventricular function (Toaldo *et al.*, 2016; Morita *et al.*, 2019; Silva *et al.*, 2020). However, the use of TDI in heartworm disease has not been previously reported through a large study with different races, ages, sexes, and degrees of parasite burden. The hemodynamic changes reported through TDI in the right heart chambers derived from the presence of adult parasites can be a useful tool for the evaluation of pulmonary hypertension findings and be considered a predictive factor for the presence of signs of right CHF. It is

important to note that detailed TDI interrogation of the RV can be challenging in patients with significant respiratory effort, and TDI assessment of the RV is considered supportive of pulmonary hypertension rather than diagnostic (Morita *et al.*, 2019).

Despite the relative robustness of TDI measurements, there is a learning curve associated with acquiring and analyzing TDI data. Commercially available machines may employ various algorithms, which may result in different TDI rates. The precise location in the spectral trace of the pulsed Doppler envelope where tissue velocity should be measured is unclear; a recent study suggests measurement in the middle portion of the spectral trace. The main disadvantage of the TDI is that the quality of analysis depends on the interrogation angle, and if this angle exceeds 20 degrees, the velocity could be underestimated. Accurate TDI imaging also requires high frame rates (>40 frames per second) to acquire images with excellent temporal resolution. Although TDI signals are robust, it is common to observe some variation in signal amplitude and timing due to minor alterations in the position of the sample volume. This aspect is particularly crucial in desynchrony studies, since cursor position can affect synchronization. Interpretation of pulsed TDI traces can sometimes be difficult, especially at high heart rates where multiple peaks may overlap (Sampedrano *et al.*, 2006; Koffas *et al.*, 2006; Toaldo *et al.*, 2016).

### **2. 3. 3. Two-dimensional speckle tracking**

Echocardiography serves as the predominant diagnostic tool for cardiovascular assessment in both veterinary and human medicine. However, accurately assessing cardiac mechanics proves challenging due to the intricate geometry of the myocardium and the interplay of determinants influencing cardiac function. Within the subendocardial region, fibers align longitudinally along the heart's axis with a right-handed helix, transitioning to circumferentially oriented fibers in the midwall, and reverting to longitudinal orientation with a left-handed helix in the subepicardial region (Chetboul *et al.*, 2007). This double helical structure is vital for efficient cardiac function, enabling simultaneous shortening in longitudinal and circumferential directions, resulting in a twisting motion that enhances energy efficiency and facilitates effective blood pumping (Figure 11).



\*Figure 11. A: Illustration depicting the longitudinal endocardial and epicardial fibers, as well as the circular midwall fibers in the left ventricle. B: The orientation of cardiac fibers varies along the cardiac short axis, transitioning from the endocardium to the epicardium. C: The presence of variable fiber angles facilitates a contraction and twisting action during systole, followed by a relaxation and untwisting motion during diastole. Wall thickening is characterized by the thickening and inward movement of cardiac fibers.

In conventional echocardiography, a dysfunctional myocardial segment may still exhibit movement due to the tethering effect from adjacent segments. Deformation analysis represents an approach aimed at minimizing the limitations inherent in conventional techniques (Chetboul *et al.*, 2018).

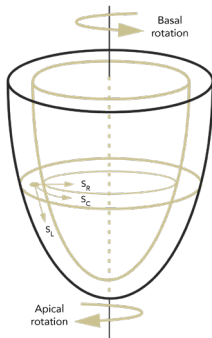
Speckle tracking echocardiography represents a non-Doppler technique that employs computer software analysis of images generated by conventional 2D ultrasound mode. In this method, the Doppler ultrasound signal produces artifacts known as speckles, which are random reflections (Cavaino *et al.*, 2020). These speckles remain stable throughout the cardiac cycle, serving as natural acoustic markers. The speckle tracking software can identify and track a cluster of speckles from frame to frame, enabling the calculation of motion parameters (displacement and velocity) and deformation parameters (strain and strain rate) (Morita *et al.*, 2017).

Strain calculated using speckle tracking is the percentage of change from the original length, with negative values indicating narrowing or shortening, and

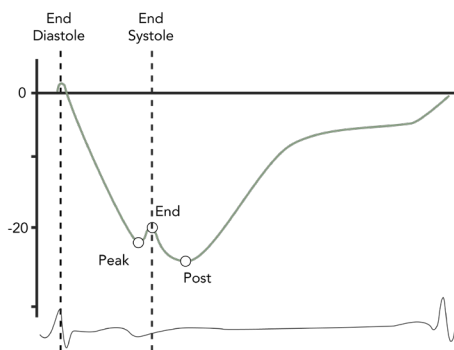
Ventricular motion encompasses a combination of narrowing, shortening, lengthening, widening, and twisting. As the myocardium moves and changes position, it undergoes deformation and alters shape, as different segments do not move at the same velocity. Since myocardial fibers lack compressibility, any shortening in one direction leads to expansion in other directions (Feldhutter *et al.*, 2022).

Conventional echocardiography techniques struggle to capture certain aspects of cardiac mechanics. The twisting motion and overall wall thickening throughout the entire ventricle are challenging to depict accurately. Moreover, measurements of wall motion cannot differentiate between active and passive movement of a myocardial segment.

positive values indicating lengthening or thickening. Strain rate represents the average change in strain per unit of time and is expressed as 1/s. Both motion and deformation occur in three dimensions and are described along the three cardiac axes. The nomenclature includes longitudinal for base-to-apex, circumferential for rotational, and radial or transverse for inward motion and deformation (Visser *et al.*, 2015b) (Figure 12).



\*Figure 12. Illustration depicting the right ventricle with emphasis on the longitudinal (SL), circumferential (SC), and radial (SR) axes, as well as basal and apical rotation.



\*Figure 13. Graphical representation displaying cardiac time and the electrocardiographic trace on the x-axis, while strain is depicted on the y-axis. End diastole is identified using the R wave of the ECG. In this illustration, end systole is specifically indicated to highlight distinctions among peak systolic strain, end systolic strain, and postsystolic strain.

In the field of cardiology, speckle tracking echocardiography typically standardizes the assessment of mechanical events to determine parameters of movement and strain. Consequently, end diastole is commonly identified at the commencement of the cardiac cycle. This is established in the 2D echocardiography image as the frame preceding the complete closure of the mitral valve, or through surrogate indicators such as the R peak of the electrocardiogram, or the maximum volume of the RV or LV. End systole serves as the customary endpoint and aligns with aortic valve closure. This is determined from apical long axis views or by employing surrogates like the end of the T wave on the electrocardiogram, the termination of the negative spike post-ejection on the speckle tracking derived velocity trace, or the minimum volume of the ventricle (Hamabe *et al.*, 2021) (Figure 13).

The majority of conducted studies focused on reporting either peak systolic strain (the initial peak strain value identified) or maximum systolic strain (the highest strain value identified). Due to the diverse layers of fibers in the heart oriented in different directions, the motion and deformation

can exhibit variability based on the location within the myocardial wall. As a result, speckle tracking software typically provides reports on endocardial deformation. Generally, software packages divide the ventricular wall into six equidistant segments, labeled as basal, mid, and apical segments. The data can be presented in various ways: globally (encompassing all segments across all views), per ventricular wall (comprising three segments of either the ventricular free wall or the septum), or individually for each specific segment (Visser *et al.*, 2015a; Chetboul *et al.*, 2018; Hamabe *et al.*, 2021).

The speckle tracking determinations of global and right ventricular free wall longitudinal strain are typically obtained from the left apical 4-chamber slice optimized for the RV. Likewise, the longitudinal displacement of specific segments of the fibers of the tricuspid valve annuli towards the ventricular apex can also be analyzed, obtaining percentage of strain or centimeters of displacement (tissue motion annular displacement) (Wolf *et al.*, 2018; Visser *et al.*, 2018; Silva *et al.*, 2020). These determinations are at the level of the longitudinal subendocardial layer, since it is better visualized and the assessment is more precise and, in addition, it is the layer that contributes 80% to the contraction of the RV. Longitudinal endocardial strain provide additional information on myocardial function independently of myocardial velocity (Locatelli *et al.*, 2016; Feldhutter *et al.*, 2022)

Speckle tracking echocardiography has been recently implemented in veterinary cardiology, longitudinal strain determinations of both the LV and RV in healthy dogs have been reported (Visser *et al.*, 2015; Morita *et al.*, 2017; Feldhutter *et al.*, 2022). Likewise, circumferential fiber strain has also been assessed to a lesser extent (Chetboul *et al.*, 2007; Cavaino *et al.*, 2020; Hamabe *et al.*, 2021). Previous research has focused on the clinical application of early detection of LV dysfunction in dogs. However, speckle tracking imaging is a promising functional imaging modality that appears to be more sensitive for the detection of RV dysfunction compared to conventional indices in veterinary medicine (Locatelli *et al.*, 2016; Chetboul *et al.*, 2018). Previous speckle tracking echocardiography studies carried out in dogs with pulmonary hypertension caused by causes other than heartworm disease reported values comparable to those published on pulmonary hypertension in people, highlighting the usefulness of longitudinal strain measurements to assess the alterations caused by pulmonary hypertension in the functionality of the RV (Visser *et al.*, 2015; Morita *et al.*, 2019; Cavaino *et al.*, 2020; Feldhutter *et al.*, 2022). To date, speckle tracking technology has not

been applied to canine cardiopulmonary dirofilariosis, so the usefulness of strain determinations in the hemodynamic changes caused by precapillary pulmonary hypertension originating in many cases of disease is unknown.

Obtaining a high-quality image stream makes the speckle tracking process relatively straightforward and reproducible, with postprocessing times kept within acceptable limits due to continuous advancements in computer processing. The computerized nature of the process reduces some of the subjective human elements in analysis. Speckle tracking can derive the majority of parameters of interest (motion, deformation, volume) from a select few views, with strain being the echocardiographic parameter closest to measuring actual contractility. Therefore, speckle tracking offers added value in evaluating cardiac mechanics and function. The advantages also include the capacity for both global and regional functional evaluation and, unlike TDI determinations, speckle tracking images are independent of the acquisition angle (Cavaino *et al.*, 2020; Hamabe *et al.*, 2021; Feldhutter *et al.*, 2022).

Nevertheless, the widespread clinical utility of strain is currently a subject of scrutiny. The software may generate curves and output, occasionally disregarding fundamental image concerns like foreshortening or Doppler artifacts, leaving it to the operator's expertise to assess the validity of the output. Consequently, measurements are unlikely to be routinely conducted in standard cases until technological enhancements are made. The application of these indices is impeded by the requisite and time-intensive post-processing analysis, compounded by the diverse array of analysis software that yields variations in clinical outcomes. Additionally, strain necessitates excellent 2D image quality (> 40 frames per second) with distinct visualization of myocardial borders (Chetboul *et al.*, 2007; Locatelli *et al.*, 2016; Chetboul *et al.*, 2018).



The background features a textured, light beige surface with faint, wavy green lines that create a sense of movement and depth. Three solid gold circles are scattered across the page: one in the upper left, one in the upper right, and one in the lower right.

# **3.** **OBJECTIVES**





3.1. Structural changes in the pulmonary vasculature reflect cardiorespiratory hemodynamic alterations. Assessment of pulmonary vein and pulmonary artery diameter in dogs and cats has previously been shown to be a valuable echocardiographic index. It was proposed to evaluate the relationship between the vein and the pulmonary artery (PV:PA) in dogs affected by cardiopulmonary dirofilariosis with the hypothesis that there must be a direct association with the presence or absence of pulmonary hypertension. Likewise, the investigation between the echocardiographic methods of determination, two-dimensional and one-dimensional mode, was analyzed to determine the degree of correlation between both measurements.

*3.1. Los cambios estructurales en la vasculatura pulmonar reflejan alteraciones hemodinámicas cardiopulmonares. La evaluación del diámetro de la vena y la arteria pulmonar en perros y gatos se ha mostrado previamente como un índice ecocardiográfico valioso. Se propuso evaluar la relación entre la vena y la arteria pulmonar (PV:PA) en perros afectados por dirofilariosis cardiopulmonar, con la hipótesis de que debe haber una asociación directa con la presencia o ausencia de hipertensión pulmonar. De igual manera, se analizó la correlación entre los métodos ecocardiográficos de determinación, modo bidimensional y monodimensional, para determinar el grado de correlación entre ambas mediciones.*



3.2. Tissue Doppler imaging (TDI) has been widely used in veterinary medicine to evaluate cardiac functionality. It was proposed to evaluate the hemodynamic changes that could be detected by TDI in the right heart chambers of dogs affected by cardiopulmonary dirofilariosis with the hypothesis that the determinations could be a useful tool for the evaluation of the presence of pulmonary hypertension in the animals analyzed. Thus, the objective of this study was to evaluate the usefulness of the measurements obtained by echocardiographic examination in TDI mode (E', A', S, E':A', Global TDI, HRI-IVCT, HRI-IVRT, R-TEI ), to detect the presence of pulmonary hypertension in dogs infected by *Dirofilaria immitis*.

3.2. La imagen de Doppler tisular se ha utilizado ampliamente en medicina veterinaria para evaluar la funcionalidad cardíaca. Se propuso evaluar los cambios hemodinámicos que podrían detectarse mediante TDI en las cavidades cardíacas derechas de perros afectados por dirofilariosis cardiopulmonar con la hipótesis de que las determinaciones podrían ser una herramienta útil para la evaluación de la presencia de hipertensión pulmonar en los animales analizados. Así, el objetivo de este estudio fue evaluar la utilidad de las mediciones obtenidas mediante examen ecocardiográfico en modo TDI (E', A', S, E':A', Global TDI, HRI-IVCT, HRI-IVRT, R- TEI ), para detectar la presencia de hipertensión pulmonar en perros infectados por *Dirofilaria immitis*.



3.3. Two-dimensional speckle tracking echocardiography has improved the assessment of cardiac functionality by being able to analyze specific segments of the ventricular myocardium influenced by diverse phenomena such as pulmonary hypertension. Therefore, due to the high percentage of canine patients who suffer from canine cardiopulmonary dirofilariosis and generate pulmonary hypertension, it is essential to know the diagnostic value of the longitudinal strain of the right ventricle (GS and FWS) and the measurements of the annular displacement of the tricuspid movement (TMAD) using two-dimensional speckle tracking echocardiography. The objective was to evaluate the usefulness of GS, FWS and TMAD measurements in a group of dogs infected with heartworm to determine the cut-off values to estimate the presence of pulmonary hypertension.

3.3. La ecocardiografía speckle tracking bidimensional ha mejorado la evaluación de la funcionalidad cardíaca al poder analizar segmentos específicos del miocardio ventricular influenciados por diversos fenómenos como la hipertensión pulmonar. Por lo tanto, debido al alto porcentaje de pacientes caninos que padecen dirofilariosis cardiopulmonar canina y generan hipertensión pulmonar, es fundamental conocer el valor diagnóstico de la tensión longitudinal del ventrículo derecho (GS y FWS) y las mediciones del desplazamiento anular del movimiento tricúspide (TMAD) mediante la ecocardiografía speckle tracking bidimensional. El objetivo fue evaluar la utilidad de las mediciones de GS, FWS y TMAD en un grupo de perros infectados con dirofilariosis para determinar los valores de corte que permitan estimar la presencia de hipertensión pulmonar.





The background features a textured, light beige surface. On the left side, there are several sets of thin, wavy lines in shades of green and grey that curve across the page. Four large, solid olive-green circles are scattered across the page: one in the upper left, one in the upper right, one in the lower left, and one in the lower right.

# 4. SCIENTIFIC PUBLICATIONS





## 4.1.

# Echocardiographic Assessment Of The Pulmonary Vein To Pulmonary Artery Ratio In Canine Heartworm Disease


**Matos, J.I.;** Caro-Vadillo, A.; Falcón-Cordón, Y.; García-Rodríguez, S.N.; Costa-Rodríguez, N.; Carretón, E.; Montoya-Alonso, J.A. Echocardiographic Assessment of the Pulmonary Vein to Pulmonary Artery Ratio in Canine Heartworm Disease. *Animals* 2023, 13, 703. [https:// doi.org/10.3390/ani13040703](https://doi.org/10.3390/ani13040703)

JOURNAL CITATION REPORTS:  
JCR-Q1 (VETERINARY SCIENCES)  
CiteScore-Q1 (GENERAL VETERINARY)  
Impact Factor: 3.231  
SCImago Journal Rank: 0.684



## Article

# Echocardiographic Assessment of the Pulmonary Vein to Pulmonary Artery Ratio in Canine Heartworm Disease

Jorge Isidoro Matos <sup>1</sup>, Alicia Caro-Vadillo <sup>1,2</sup>, Yaiza Falcón-Cordón <sup>1</sup>, Sara Nieves García-Rodríguez <sup>1</sup>, Noelia Costa-Rodríguez <sup>1</sup>, Elena Carretón <sup>1,\*</sup> and José Alberto Montoya-Alonso <sup>1</sup>

<sup>1</sup> Internal Medicine, Veterinary Medicine and Therapeutic Research Group, Faculty of Veterinary Medicine, Research Institute of Biomedical and Health Sciences (IUIBS), Universidad de Las Palmas de Gran Canaria (ULPGC), 35016 Las Palmas de Gran Canaria, Spain

<sup>2</sup> Hospital Clínico Veterinario, Faculty of Veterinary Medicine, Universidad Complutense de Madrid (UCM), 28040 Madrid, Spain

\* Correspondence: elena.carreton@ulpgc.es

**Simple Summary:** Pulmonary hypertension (PH) is a phenomenon frequently seen in dogs with heartworms. Given the seriousness of this condition, numerous studies have focused on determining its presence. In this study, the pulmonary vein to pulmonary artery ratio (PV:PA ratio), determined by echocardiography, is evaluated in 151 dogs to determine its usefulness in the detection of PH in heartworm. The results showed that the PV:PA ratio could be useful as a complementary diagnostic method to estimate the presence of moderate or severe PH in these patients.

**Abstract:** **Background:** *Dirofilaria immitis* produces proliferative pulmonary endarteritis and pulmonary thromboembolism in infected dogs. The pulmonary vascular lesions lead to irreversible and persistent structural damage and, as a consequence, sustained precapillary pulmonary hypertension (PH). The purpose of this study was to assess the diagnostic value of the pulmonary vein to pulmonary artery ratio (PV:PA ratio) to determine moderate or severe PH (>50 mmHg) in dogs with heartworm disease. **Methods:** A total of 151 naturally heartworm-infected and 66 healthy dogs were included in the study. The presence/absence of PH was based on the right pulmonary artery distensibility index (RPAD index < 29.5%), and the PV:PA ratio was echocardiographically measured by the time–motion mode (M mode) and two-dimensional mode (2D mode). Other echocardiographic parameters were also assessed (pulmonary trunk to aorta ratio, tricuspid regurgitation pressure gradient, and AT:ET ratio). **Results:** The results of the PV:PA ratio showed a highly positive correlation between the M and 2D modes ( $r = 0.928$ ). The PV:PA ratio obtained by the M mode was identified as the strongest predictor for RPAD index ( $R^2 0.628$ ,  $p < 0.0001$ ) with a good diagnostic accuracy (AUC = 0.99). The results of PV/PA by the 2D mode showed a similar prediction for the RPAD index ( $R^2 0.606$ ,  $p < 0.0001$ ) with a good diagnostic accuracy (AUC = 0.98). Both of the 2D and M modes' PV:PA ratios decreased significantly with the presence of PH. A cut-off value of  $\leq 0.845$  showed high sensitivity and specificity for the M mode (97% and 94%, respectively) and the 2D mode (96% and 93%, respectively). **Conclusions:** The PV:PA ratio may be useful as a complementary diagnostic method for the estimation of moderate or severe PH in dogs with heartworm.

**Keywords:** *Dirofilaria immitis*; heartworm disease; pulmonary vein; pulmonary artery; PV:PA ratio; RPAD index; pulmonary hypertension; animal diseases



**Citation:** Matos, J.I.; Caro-Vadillo, A.; Falcón-Cordón, Y.; García-Rodríguez, S.N.; Costa-Rodríguez, N.; Carretón, E.; Montoya-Alonso, J.A.

Echocardiographic Assessment of the Pulmonary Vein to Pulmonary Artery Ratio in Canine Heartworm Disease. *Animals* **2023**, *13*, 703. <https://doi.org/10.3390/ani13040703>

Academic Editor: Christian Matthias Bauer

Received: 12 December 2022

Revised: 10 February 2023

Accepted: 11 February 2023

Published: 17 February 2023



**Copyright:** © 2023 by the authors. Licensee MDPI, Basel, Switzerland. This article is an open access article distributed under the terms and conditions of the Creative Commons Attribution (CC BY) license (<https://creativecommons.org/licenses/by/4.0/>).

## 1. Introduction

Canine heartworm is a serious disease caused by *Dirofilaria immitis*, which is transmitted through the bite of vector mosquitoes and mainly affects canids and felines, both domestic and wild. Direct contact of *D. immitis* adults with the intimal layer of pulmonary arterial vessels causes irreversible proliferative pulmonary endarteritis, with a reduction in

the vascular lumen and a loss of elasticity of the pulmonary arteries [1]. In addition, there is an obstruction to blood flow due to the presence of parasites in the pulmonary arteries and the consequent formation of thrombi and emboli [2]. These events chronically lead to increased resistance to blood flow, which in turn increases pressure in the pulmonary arteries, as is defined as precapillary pulmonary hypertension (PH) [3]. PH in dogs with heartworm is a common, serious, and life-threatening condition, and many of the clinical signs seen in infected dogs are due to the presence of PH [4].

Currently, echocardiography provides the most accurate, non-invasive, available, and cost-effective estimate of pulmonary arterial pressure in dogs. The right pulmonary artery distensibility Index (RPAD index) was previously validated as a valuable and useful method to estimate the presence of PH in dogs infected with heartworm disease [2,5] and has also been shown as an effective method for the diagnosis of PH due to other causes, especially when it is not possible to assess tricuspid or pulmonary regurgitation flows [6]. However, new effective and useful echocardiographic parameters should be implemented to estimate the severity of PH due to the high presentation of this phenomenon in dogs infected by *D. immitis* [4].

The structural changes observed in the pulmonary vasculature are a reflection of cardiorespiratory hemodynamic alterations. Evaluation of pulmonary vein (PV) diameter and pulmonary artery (PA) diameter in dogs and cats has been shown to be a valuable echocardiographic index. The PV:PA ratio has been useful in the diagnosis of pulmonary venous congestion in the feline and canine species derived from left heart failure [7]. In addition, the application of the PV:PA ratio in the identification of PH has been validated in dogs suffering from idiopathic pulmonary fibrosis in the West Highland terrier breed [8], and in other pathologies that produce precapillary PH due to pulmonary or thromboembolic pathologies [9]. Therefore, the aim of this study was to determine if PH in dogs with heartworm can be assessed using the PV:PA ratio, and to evaluate its accuracy compared to other indices to estimate PH.

## 2. Methods

### 2.1. Study Animals

In the present prospective study, 217 client-owned dogs presented to the Veterinary Teaching Hospital of the University of Las Palmas de Gran Canaria (Canary Islands, Spain), between September 2020 and July 2022, were included. The dogs lived in a hyperendemic area of *D. immitis* [10]. A complete record was kept for each animal, including identification (age, sex, breed, and weight), clinical history, and demographic data. Of them, 69.6% (151/217) were diagnosed with heartworm infection using a commercial immunochromatographic test kit (Urano test *Dirofilaria*<sup>®</sup>, Urano Vet SL, Barcelona, Spain), while 30.4% (66/217) were considered healthy based on the absence of clinical signs according to history, physical examination, cardiovascular assessment, echocardiographic evaluation, and the negative results of the *D. immitis* antigen detection test. Dogs that had previously received any cardiovascular medication were not considered candidates for the study. Likewise, animals that showed clinical signs and echocardiographic evidence of cardiac conditions other than heartworm disease (i.e., left heart disease, dilated cardiomyopathy, congenital diseases) were excluded from the study. All owners were informed and gave consent to participate in the study.

Infected dogs were considered as symptomatic when presence of one or more symptoms related to heartworm disease (dyspnea, cough, exercise intolerance, weakness, loss of weight and syncope) was observed. In addition, the occurrence of ascites, jugular venous distension, and hepatomegaly were also observed in dogs with right-sided congestive heart failure (R-CHF). Echocardiographic examinations were performed on all animals prior to the beginning of adulticide treatment.

## 2.2. Echocardiography

Dogs were subjected to an echocardiographic examination, using an ultrasound equipment with spectral and color Doppler and multifrequency probes (2.5–10 MHz, Viviq Iq<sup>®</sup>, General Electric, Boston, MA, USA). All dogs were conscious, sedation-free, and under electrocardiographic monitoring during the whole test. For each measurement, three continuous cardiac cycles were recorded. All echocardiographic recordings were made by the same cardiologist.

The absence or presence of PH, as well as the severity, was based on the determination of the RPAD index as previously described [2,6], and an index < 29.5% correlated with moderate or severe PH (>50 mmHg) [6,11]. According to clinical status and the results of the RPAD index, dogs were divided into three groups: Group A included healthy dogs, all of them with absence of PH. Group B consisted of heartworm-infected dogs and absence of PH. Group C comprised heartworm-infected dogs with PH.

For measurement of the PV:AP ratio, a 4-chamber view of the right parasternal long axis was optimized to simultaneously visualize a longitudinal section of the right ostium of the right cranial pulmonary veins and the transverse section of the right pulmonary artery branch. Measurements of PV and PA diameters were taken in M (time–motion) and in 2D (two-dimensional) modes as previously described and validated [8,9]. For both measurements, the inner-edge-to-inner-edge method was used with timed measurements at the end of the T wave (end-systole), drawing a line perpendicular to the medial PV diameter (Figure 1) and 3 measurements were averaged. The interobserver variability of PV:PA image acquisition and PV:PA measurement was evaluated separately in 10 dogs. In order to demonstrate the presence/absence of PH as well as severity in the animals analyzed, the following echocardiographic parameters were also determined: pulmonary trunk to aorta ratio (PT:Ao ratio), tricuspid regurgitation pressure gradient (TRPG), and the velocity of the outflow tract of the right ventricle through the relationship between acceleration times (AT) and ejection times (ET) using the AT:ET ratio.

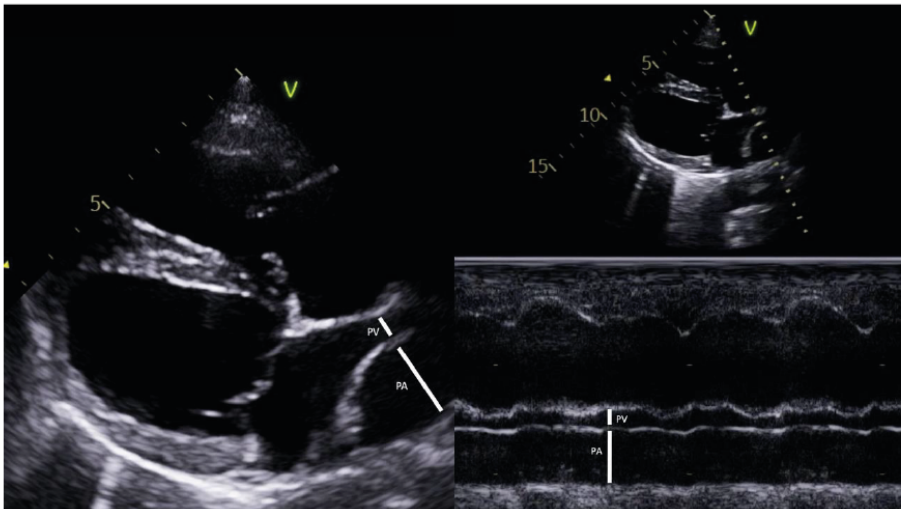


**Figure 1.** The image shows representative measurement and calculation of the pulmonary vein (PV) to pulmonary artery (PA) ratio in two-dimensional (2D) and time–motion mode (M mode) echocardiography. PV:PA ratio (2D and M mode) was obtained in a heartworm-infected dog with an RPAD index < 29.5% (Right parasternal long axis four-chamber view).

On the other hand, the presence of visible parasites in the pulmonary arteries and right heart chambers was assessed according to Venco et al., 2003 [12]. From low to high burden: parasite burden 1 was determined when the parasites were not observed, parasite burden 2 when they were observed in the right pulmonary branch, parasite burden 3 when they were observed in the pulmonary trunk, and parasite burden 4 when adult parasites were observed in the right heart chambers (caval syndrome).

### 2.3. Statistical Analysis

Statistical analyses were performed using commercially available software (BM SPSS® Statistics 25.0, New York, NY, USA). For categorical variables, frequencies and percentages are shown. The differences in parameters between groups were evaluated with Pearson's non-parametric Chi<sup>2</sup> test and, just in the case of 2 × 2 tables, Fisher's exact test was applied. For continuous variables, the differences in the parameters between groups were evaluated by means of Mann-Whitney/Kruskal-Wallis tests (non-parametric) or T-student/ANOVA (parametric) based on the normality of the variables to be evaluated by means of Shapiro-Wilks test. When significant differences were identified, post hoc pairwise comparisons were made using Pearson's *p* test with Bonferroni corrections. The results of the statistical procedures with respect to PV:PA ratio were also graphed by scatter plot. A simple linear regression was performed between the RPAD index values and the PV:PA ratio. To identify the best one-variable model, a regression analysis of all subsets was performed with a maximum improvement in R<sup>2</sup> as a selection criterion. Receiver operator characteristic curve (ROC) analyses were performed to determine the optimal cut-off values for the prediction of RPAD index < 29.5% (moderate or severe PH). For all analyses, *p* < 0.01 was considered statistically significant.

## 3. Results

Detailed epidemiological and clinical results of the studied dogs are summarized in Table 1. According to the results obtained, group A included 66/217 (30.4%) dogs, group B consisted of 81/217 (37.3%) dogs, and group C comprised 70/217 (32.3%) dogs. In this study, 28 different breeds were evaluated, with mongrel dogs (46.1%), Canary hound (8.3%), and American pit bull terrier (5.1%) being the main breeds analyzed. No statistical differences in age, body weight, and number of males/females were found between the three groups. Based on the RPAD index, PH was present in 46.36% of dogs infected by *Dirofilaria immitis*. The presence of symptoms was significantly higher in dogs from group C (87.1%) than in groups B (30.9%) and A (0%) (*p* < 0.01). Dogs with R-CHF were only reported in group C (*p* < 0.01). The most common clinical sign found was cough (50%), followed by exercise intolerance (21.0%), cyanosis (10.3%), dyspnea (8.5%), syncope (6.2%), and weight loss (1.3%).

The results of the echocardiographic parameters measured in each group are described in Table 1. The PV:PA ratio, measured by both the 2D mode and the M mode, decreased significantly with the presence of PH (Figure 2). Echocardiographic data showed that this decrease was mainly due to an increase in the size of the PA, compared with the diameter of the PV. A decrease in the AT:ET ratio was also observed, as well as an increase in the variables PT:Ao ratio and TRPG, related to the presence of PH (Table 1). When the parasite burden was assessed, healthy dogs obviously showed an absence of adult parasites, while parasite burden was higher in dogs from group C than in dogs from group B. All dogs from group C showed the echocardiographic presence of heartworms (scores 2 to 4), while no worms were echocardiographically visible in 8.6% (7/81) of dogs from group B (score 1).

**Table 1.** Clinical, epidemiological, and echocardiographic parameters of the studied dogs (group A: healthy dogs, group B: heartworm-infected dogs and absence of PH, group C: heartworm-infected dogs with PH). Data represent median and standard deviation (min–max) unless otherwise stated: RPAD index, right pulmonary artery distensibility index; TRPG, peak tricuspid regurgitation systolic pressure gradient; PT, pulmonary trunk; Ao, aorta; PV:PA pulmonary vein to pulmonary artery ratio; M mode, time–motion mode; 2D mode, two-dimensional mode; AT:ET, right acceleration time to ejection time ratio. Results for female, respiratory symptoms, and right-sided CHF are expressed as *n* (%). Results for parasite burden are expressed as median (range). Significant differences were found when *p*-value < 0.01. (\*): significant differences observed between groups C and B; (†): significant differences observed between groups C and A; (●): significant differences observed between groups B and A.

Clinical, Epidemiological, and Echocardiographic Parameters.	All Dogs (n = 217)	Group A (n = 66)	Group B (n = 81)	Group C (n = 70)	<i>p</i> -Value
Body weight (kg)	18.04 ± 11.24	16.76 ± 11.15	17.90 ± 12.35	18.65 ± 12.83	0.23
Age (years)	7.17 ± 4.66	8.08 ± 5.83	6.53 ± 4.08	8.21 ± 5.51	0.47
Female: number (%)	116 (53.5%)	30 (45.5%)	50 (61.7%)	36 (50.4%)	0.46
Respiratory symptom (%)	86 (39.6%)	0 (0.0%)	25 (30.9%)	61 (87.1%)	0.00 (*,†)
Right-sided CHF (%)	26 (12.0%)	0 (0%)	0 (0%)	26 (37.1%)	0.00 (*,†)
TRPG (mmHg)	21.05 ± 33.12	4.42 ± 3.11	3.95 ± 2.43	56.51 ± 39.18	0.00 (*,†)
RPAD index (%)	34.80 ± 11.52	42.11 ± 5.04	40.08 ± 6.88	20.62 ± 6.82	0.00 (*,†)
PT:Ao ratio	1.05 ± 0.18	0.96 ± 0.07	0.95 ± 0.15	1.26 ± 0.15	0.00 (*,†)
PV:PA ratio (M mode)	0.86 ± 0.33	1.08 ± 0.12	1.03 ± 0.20	0.47 ± 0.21	0.00 (*,†)
PV:PA ratio (2D mode)	0.88 ± 0.33	1.09 ± 0.13	1.05 ± 0.20	0.48 ± 0.23	0.00 (*,†)
AT:ET	0.33 ± 0.09	0.37 ± 0.06	0.38 ± 0.07	0.24 ± 0.06	0.00 (*,†)
Parasitic burden (1–4)	2.00 (1–4)	0.00 (0–0)	2.00 (1–3)	3.00 (2–4)	0.00 (†,●)

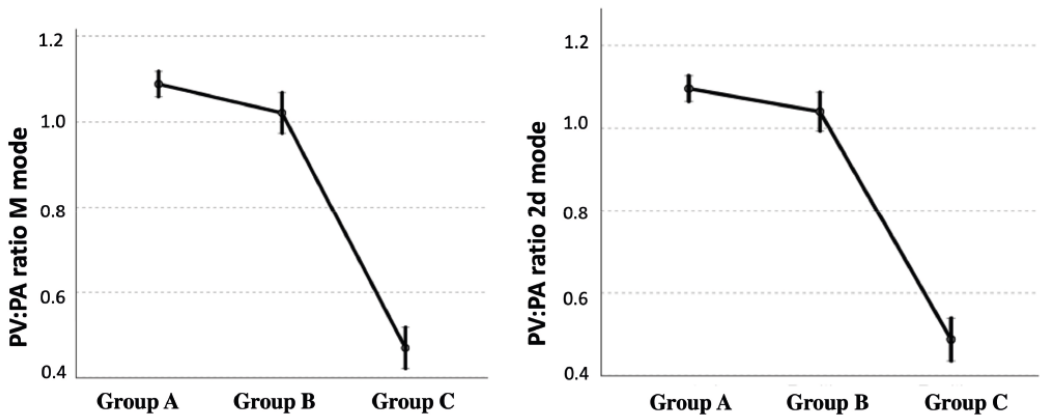


**Figure 2.** Scatterplots illustrating the right pulmonary vein to pulmonary artery (PV:PA) ratios in time–motion mode (M mode) and two-dimensional mode (2D mode), obtained in healthy dogs (group A), in dogs with heartworm and absence of PH (group B), and in dogs with heartworm and presence of PH (group C). The results show the estimated marginal means and their CI 95%.

Furthermore, the coefficient of determination ( $R^2$ ) of the regressions that allow comparing the quality of the PV:PA relationship, in the M and 2D modes, with respect to the RPAD index, were studied. The results showed that the M and 2D PV:PA ratios were highly positively correlated ( $r = 0.928$ ) (Figure 3). Furthermore, these two ratios were positively correlated with the RPAD index with  $r$  between 0.788 and 0.774, and  $R^2$  of 0.628 and 0.606, respectively (Table 2).

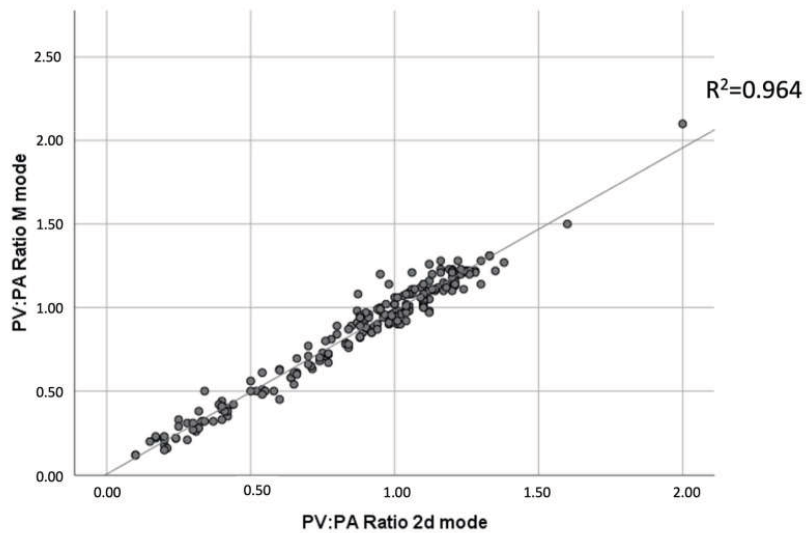


Figure 3. Linear regression illustrating right pulmonary vein to pulmonary artery (PV:PA) ratios in motion mode over time (M mode) and two-dimensional mode (2D mode). The M and 2D modes of the PV:PA ratios were highly positively correlated ( $r = 0.928$ ). The correlation was significant at the 0.01 level (bilateral).

Table 2. Results of simple regression analyses for the prediction of RPAD index  $< 29.5\%$ . CI 95%: confidence interval 95%;  $p$ : Pearson correlations; PV:PA: pulmonary vein to pulmonary artery ratio;  $R^2$ : coefficient of determination; RPAD index: right pulmonary artery distensibility index.

Method	$R^2$	$p$ -Value	CI 95%	Regression Equation
PV:PA ratio (M mode)	0.628	$<0.0001$	(24.654, 30.328)	RPAD index = $10.634 + 27.492 \times$ PV:PA ratio (M mode)
PV:PA ratio (2D mode)	0.605	$<0.0001$	(23.914, 29.711)	RPAD index = $10.809 + 26.812 \times$ PV:PA ratio (2D mode)

The results of the ROC curves of the PV:PA ratio measurement in the M mode and in the 2D mode to estimate the event of suffering from PH (RPAD index  $< 29.5\%$ ), and the cut-off points of the parameters that maximize sensitivity and specificity (through the Youden index) are shown in Table 3. The AUCs of the two ratios were excellent ( $>0.9$ ). For the PV:PA ratio in the M and 2D modes, any value  $\leq 0.845$  was suggestive of the presence of PH in 97% and 96%, respectively, and a value  $> 0.845$  was suggestive of the absence of PH in 94% and 93%, respectively.

Table 3. Sensitivity, specificity, and Youden index of cut-off points of PV:PA for predicting PH estimation of right pulmonary artery distensibility index (RPAD index)  $< 29.5\%$ . AUC: area under receiver operating characteristic curve; CI 95%: confidence interval 95%;  $p$ : Pearson correlations; PV:PA: pulmonary vein to pulmonary artery ratio; Se: sensitivity; Sp: specificity.

Method	AUC	CI 95%	$p$ -Value	Cut-off	Se	Sp	Youden Index
PV:PA ratio (M mode)	0.988	(0.967, 1.000)	$<0.0001$	$\leq 0.845$	0.97	0.94	0.91
PV:PA ratio (2D mode)	0.983	(0.970, 1.000)	$<0.0001$	$\leq 0.845$	0.96	0.93	0.89

#### 4. Discussion

PH is a serious, frequent, and non-reversible condition in dogs with heartworm disease [5,13]. The clinical signs that these dogs present are often due to the progression of PH, which, in the final stages, can lead to the development of R-CHF. Therefore, determining the presence of PH using effective methods is essential in heartworm disease since they will provide information about the chronicity of the disease, and will help establish the most accurate treatment protocol and prognosis.

The parasite load is also normally evaluated in the study of PH in dogs parasitized by *D. immitis* [2,4,6]. Although, in this study, burden was higher in dogs with PH, the influence of the parasite load in the development of proliferative pulmonary endarteritis and subsequent PH was not clear, and several authors have stated that the chronicity, immune reaction, and the lifestyle of the infected dog (animals that exercise frequently), have a more notable influence on the development of damage at the vascular level. However, a high parasite load has been shown to be subjective in increasing the proportion of moderate or severe HP in the infected dogs [4,6].

Currently, the RPAD index is used as the gold standard for determining the presence and severity of PH in dogs infected by *D. immitis*, and its utility in accurately estimating PH in these dogs has been demonstrated [1,2,5,6,13]. However, new diagnostic methods should continue to be studied to help in the measurement of PH in dogs with heartworm. In this study, the analysis of the other indirect echocardiographic predictors of PH in canine heartworm reported a significant increase in the PT:Ao ratio and the TRPG, as well as a decrease in the AT:ET ratio in proportion to the presence of PH, which supports the previously published studies [14–16]. Moreover, the results of this study demonstrated the validity of the PV:PA ratio to determine the presence of PH in dogs with heartworm disease, as the results in the PV:PA ratio showed significant variations depending on the presence/absence of PH. The lower values of the PV:PA ratio found in dogs with heartworm with PH may be as a result of the pulmonary artery distention caused by the chronic proliferative endarteritis resulting from the direct contact of the parasites with the intima layer of the pulmonary artery [17,18]. Likewise, significantly lower PV:PA ratio values have been found in dogs with precapillary PH caused by other pathologies, in comparison to animals without PH [9]. These findings suggest that the PV:PA ratio is an adequate tool to determine the presence of PH, regardless of the pathology that produced the increase in pulmonary arterial pressure.

In this study, both measurements of PV:PA ratio—the M and 2D modes—highly correlated, corroborating that both can be accurately used to study the presence/absence of PH in dogs infected by *D. immitis*. These results are similar to those reported in a previous study, using both the M and the 2D modes, which also found no significant variations between the two methods in healthy dogs [19]. Although, in the present study, the PV:PA ratio in the M mode showed slightly more accurate values in the estimation of an RPAD index < 29.5% in dogs with heartworm, the results showed that both measurements can be safely used.

In this study, an average value of PV:PA ratio of approximately 1.0 was found in healthy dogs, similar to values previously described by other authors [19,20]. Furthermore, a cut-off point of 0.845 was described for both the M and 2D modes to estimate pulmonary pressures > 50 mmHg, as correlated with an RPAD index < 29.5%. Recently, other authors studied the PV:PA ratio for the estimation of precapillary PH caused by pathologies other than heartworm disease, using the M and 2D modes, and reported a cut-off point of <0.70 (sensitivity 96%, specificity 82%) for the estimation of moderate PH (TRPG > 50 mmHg) [8,9]. The PV:PA ratio has also been used to estimate the survival of West Highland terrier dogs that presented pulmonary fibrosis and developed PH using the cut-off level of <0.70, demonstrating the usefulness of the measurement performed in the 2D mode and the M mode [9]. The cut-off value of <0.70 reported by these authors is lower than that observed in this study, which may be due to the difference in the sample size (67 vs. 217 dogs), the echocardiographic method established to estimate the

presence of PH (TRPG vs. RPAD index), or the different pathologies studied by other authors (angiostrongylosis, bronchomalacia, precapillary PH of unknown origin, brachycephalic syndrome, pulmonary thromboembolism, eosinophilic bronchopneumopathy, etc.). Another considerable difference is the average weight of the animals studied, which is considerably higher in the animals suffering from heartworm disease compared to the study by Roels et al. (2019), (7.4 kg vs. 18.65 kg) [9], and the precise echocardiographic measurement of the vascular structures is more difficult to determine in small dogs compared to heavier animals [21]. Finally, sensitivity and specificity varied between studies, both being higher in the present study.

The use of the PV:PA ratio is an easy, fast, and precise way to determine the hemodynamic status in dogs with heartworm, being a good option for inexperienced sonographers. Since the variation in the diameter of these vessels is a direct reflection of the pathology, the determination of the PV:PA ratio allows the severity of the disease to be established. Moreover, it is a very reliable intraoperative method and is a useful tool to assess patient follow-up. In the same echocardiographic view (right parasternal long axis four-chamber view) it is possible to visualize the presence of parasites and measure the RPAD index, so both measures complement each other, and it is possible to compare results in the same image and cardiac cycle.

The main limitation of this study is that the animals did not undergo right heart catheterization for the determination of pulmonary arterial pressure, which is considered the gold standard method, but instead underwent transthoracic echocardiography, considered an alternative tool to estimate the presence of PH. In this sense, the only echocardiographic measure used in this study to estimate the presence of PH in dogs with heartworm disease was the RPAD index, which, despite having shown an excellent correlation with the invasive pulmonary artery pressure measurement [6], presents limitations [3]. Therefore, to confirm the usefulness of the PV:PA ratio to determine the presence of PH, it is necessary to carry out new studies using other parameters for estimating the presence of PH, in addition to a larger sample size, which would allow standardizing protocols and obtaining objective reference values to satisfactorily establish the diagnosis and severity of PH in dogs with heartworm.

## 5. Conclusions

The echocardiographic measurement of the PV:AP ratio was able to discriminate between dogs without PH—being healthy or infected by *D. immitis*—and heartworm-infected dogs with PH (RPAD index < 29.5%). Therefore, the PV:PA ratio may be a useful tool to echocardiographically evaluate vascular status in patients with heartworm disease. The PV:PA ratio  $\leq 0.845$ , both in the M and 2D modes, suggested an acceptable cut-off value to differentiate between dogs with PH and dogs without PH.

**Author Contributions:** J.I.M., J.A.M.-A. and E.C. designed the study. J.I.M., A.C.-V. and E.C. wrote the manuscript. J.I.M., Y.F.-C., S.N.G.-R. and N.C.-R. performed the fieldwork, collected the data, and performed the experiments. All authors participated in the discussion of the results, corrected, read, and approved the final manuscript. All authors have read and agreed to the published version of the manuscript.

**Funding:** The presented study was partially supported by MERCK SHARP & DOHME ANIMAL HEALTH: S.L (CN-240/030/158). N.C.-R. was supported by the “Grants for the predoctoral training program for researchers” program of the Government of the Canary Islands (TESIS2021010010), and J.I.M. and S.N.R.-G. were supported by the “Grants for the financing of predoctoral contracts” program of the Universidad de Las Palmas de Gran Canaria; J.I.M. (PIFULPGC-2017-CCSALUD-3); S.N.R.-G. (PIFULPGC-2020-2-CCSALUD-2).



**Institutional Review Board Statement:** Ethical review and approval were not required for the animal study because the present study was conducted on client-owned animals/ clinical cases and no experimental animals were used. All of the dog owners were informed about the present study and consented to participate. The study was carried out in accordance with the current Spanish and European legislation on animal protection (Spanish Royal Decree 53/2013 and 2010/63/UE Directive).

**Informed Consent Statement:** Not applicable.

**Data Availability Statement:** The raw data supporting the conclusions of this article will be made available by the authors, without undue reservation.

**Acknowledgments:** The authors would like to thank the Hospital Clínico Veterinario of the Universidad de Las Palmas de Gran Canaria (ULPGC) for their support.

**Conflicts of Interest:** The authors declare no conflict of interest.

## References

- Maerz, I. Clinical and diagnostic imaging findings in 37 rescued dogs with heartworm disease in Germany. *Vet. Parasitol.* **2020**, *283*, 174–181. [[CrossRef](#)] [[PubMed](#)]
- Serrano-Parreño, B.; Carretón, E.; Caro-Vadillo, A.; Falcón-Cordón, Y.; Falcón-Cordón, S.; Montoya-Alonso, J.A. Evaluation of pulmonary hypertension and clinical status in dogs with heartworm by Right Pulmonary Artery Distensibility Index and other echocardiographic parameters. *Parasites Vectors* **2017**, *10*, 106–112. [[CrossRef](#)] [[PubMed](#)]
- Reinero, C.; Visser, L.C.; Kelliham, H.B.; Masseau, I.; Rozanski, E.; Clercx, C.; Williams, K.; Abbot, J.; Borgarelli, M.; Scansen, B.A. ACVIM consensus statement guidelines for the diagnosis, classification, treatment, and monitoring of pulmonary hypertension in dogs. *J. Vet. Intern. Med.* **2020**, *34*, 549–573. [[CrossRef](#)] [[PubMed](#)]
- Romano, A.E.; Saunders, A.B.; Gordon, S.G.; Wesselowski, S. Intracardiac heartworms in dogs: Clinical and echocardiographic characteristics in 72 cases (2010–2019). *J. Vet. Intern. Med.* **2021**, *35*, 88–97. [[CrossRef](#)] [[PubMed](#)]
- Falcón-Cordón, Y.; Montoya-Alonso, J.A.; Caro-Vadillo, A.; Matos, J.I.; Carretón, E. Persistence of pulmonary endarteritis in canine heartworm infection 10 months after the eradication of adult parasites of *Dirofilaria immitis*. *Vet. Parasitol.* **2019**, *273*, 1–4. [[CrossRef](#)] [[PubMed](#)]
- Venco, L.; Mihaylova, L.; Boon, J.A. Right Pulmonary Artery Distensibility Index (RPAD Index). A field study of an echocardiographic method to detect early development of pulmonary hypertension and its severity even in the absence of regurgitant jets for Doppler evaluation in heartworm-infected dogs. *Vet. Parasitol.* **2014**, *206*, 60–66. [[PubMed](#)]
- Patata, V.; Caivano, D.; Porciello, F.; Rishniw, M.; Domenech, O.; Marchesotti, F.; Giorgi, M.E.; Guglielmini, C.; Poser, H.; Spina, F.; et al. Pulmonary vein to pulmonary artery ratio in healthy and cardiomyopathic cats. *J. Vet. Cardiol.* **2019**, *27*, 23–33. [[CrossRef](#)] [[PubMed](#)]
- Roels, E.; Fastrès, A.; Merveille, A.C.; Bolen, G.; Teske, E.; Clercx, C.; Entee, K.M. The prevalence of pulmonary hypertension assessed using the pulmonary vein-to-right pulmonary artery ratio and its association with survival in West Highland White terriers with canine idiopathic pulmonary fibrosis. *BMC Vet. Res.* **2021**, *17*, 171–177. [[CrossRef](#)] [[PubMed](#)]
- Roels, E.; Merveille, A.C.; Moysé, E.; Gomart, S.; Clercx, C.; Entee, K.M. Diagnostic value of the pulmonary vein-to-right pulmonary artery ratio in dogs with pulmonary hypertension of precapillary origin. *J. Vet. Cardiol.* **2019**, *24*, 85–94. [[CrossRef](#)] [[PubMed](#)]
- Montoya-Alonso, J.A.; Morchón, R.; Costa-Rodríguez, N.; Matos-Rivero, J.I.; Falcón-Cordón, Y.; Carretón, E. Current Distribution of Selected Vector-Borne Diseases in Dogs in Spain. *Front. Vet. Sci.* **2020**, *7*, 28–37. [[CrossRef](#)] [[PubMed](#)]
- Visser, L.C.; Im, M.K.; Johnson, L.R.; Stern, J.A. Diagnostic Value of Right Pulmonary Artery Distensibility Index in Dogs with Pulmonary Hypertension: Comparison with Doppler Echocardiographic Estimates of Pulmonary Arterial Pressure. *J. Vet. Intern. Med.* **2016**, *30*, 543–552. [[CrossRef](#)] [[PubMed](#)]
- Venco, L.; Genchi, C.; Vigevani Colson, P.; Kramer, L. Relative utility of echocardiography, radiography, serologic testing and microfilariae counts to predict adult worm burden in dogs naturally infected with heartworms. In *Recent Advances in Heartworm Disease, Symposium '01*; Seward, R.L., Knight, D.H., Eds.; American Heartworm Society: Batavia, IL, USA, 2003; pp. 111–124.
- Serrano-Parreño, B.; Carretón, E.; Caro-Vadillo, A.; Falcón-Cordón, S.; Falcón-Cordón, Y.; Montoya-Alonso, J.A. Pulmonary hypertension in dogs with heartworm before and after the adulticide protocol recommended by the American Heartworm Society. *Vet. Parasitol.* **2017**, *236*, 34–37. [[CrossRef](#)] [[PubMed](#)]
- Matos, J.I.; Falcón-Cordón, Y.; García-Rodríguez, S.; Costa-Rodríguez, N.; Montoya-Alonso, J.A.; Carretón, E. Evaluation of Pulmonary Hypertension in Dogs with Heartworm Disease Using the Computed Tomographic Pulmonary Trunk to Aorta Diameter Ratio. *Animals* **2022**, *12*, 2441. [[CrossRef](#)] [[PubMed](#)]
- Gentile-Solomon, J.M.; Abbott, J.A. Conventional echocardiographic assessment of the canine right heart: Reference intervals and repeatability. *J. Vet. Cardiol.* **2016**, *18*, 234–247. [[CrossRef](#)] [[PubMed](#)]
- Vezzosi, T.; Domenech, O.; Iacona, M.; Marchesotti, F.; Zini, E.; Venco, L.; Tognetti, R. Echocardiographic evaluation of the right atrial area index in dogs with pulmonary hypertension. *J. Vet. Intern. Med.* **2018**, *32*, 42–47. [[CrossRef](#)] [[PubMed](#)]
- Carretón, E.; Falcón-Cordón, Y.; Falcón-Cordón, S.; Morchón, R.; Matos, J.I.; Montoya, J.A. Variation of the adulticide protocol for the treatment of canine heartworm infection: Can it be shorter? *Vet. Parasitol.* **2019**, *271*, 54–56. [[CrossRef](#)] [[PubMed](#)]

18. Falcón-Cordón, Y.; Tvarijonaviciute, A.; Montoya-Alonso, J.A.; Muñoz-Prieto, A.; Caro-Vadillo, A.; Carretón, E. Evaluation of acute phase proteins, adiponectin and endothelin-1 to determine vascular damage in dogs with heartworm disease (*Dirofilaria immitis*), before and after adulticide treatment. *Vet. Parasitol.* **2022**, *309*, 109759. [[CrossRef](#)] [[PubMed](#)]
19. Biretoni, F.; Caivano, D.; Patata, V.; Moïse, N.S.; Guglielmini, C.; Rishniw, M.; Porciello, F. Canine pulmonary vein-to-pulmonary artery ratio: Echocardiographic technique and reference intervals. *J. Vet. Cardiol.* **2016**, *18*, 326–335. [[CrossRef](#)] [[PubMed](#)]
20. Merveille, A.C.; Bolen, G.; Krafft, E.; Roles, E.; Gomart, S.; Etienne, A.L.; Clercx, C.; Entee, K.M. Pulmonary Vein-to-Pulmonary Artery Ratio is an Echocardiographic Index of Congestive Heart Failure in Dogs with Degenerative Mitral Valve Disease. *J. Vet. Intern. Med.* **2015**, *29*, 1502–1509. [[CrossRef](#)] [[PubMed](#)]
21. Kim, S.Y.; Park, H.Y.; Lee, J.Y.; Lee, Y.W.; Choi, H.J. Comparison of radiographic and echocardiographic features between small and large dogs with heartworm disease. *J. Vet. Clin.* **2019**, *36*, 207–211. [[CrossRef](#)]

**Disclaimer/Publisher’s Note:** The statements, opinions and data contained in all publications are solely those of the individual author(s) and contributor(s) and not of MDPI and/or the editor(s). MDPI and/or the editor(s) disclaim responsibility for any injury to people or property resulting from any ideas, methods, instructions or products referred to in the content.





## 4.2.

# Usefulness of Tissue Doppler Imaging for the Evaluation of Pulmonary Hypertension in Canine Heartworm Disease

**Matos, J.I.;** García-Rodríguez, S.N.; Costa-Rodríguez, N.; Caro-Vadillo, A.; Carretón, E.; Montoya-Alonso, J.A. Usefulness of Tissue Doppler Imaging for the Evaluation of Pulmonary Hypertension in Canine Heartworm Disease. *Animals* 2023, 13, 3647. <https://doi.org/10.3390/ani13233647>

JOURNAL CITATION REPORTS:  
JCR-Q1 (VETERINARY SCIENCES)  
CiteScore-Q1 (GENERAL VETERINARY)  
Impact Factor: 3.231  
SCImago Journal Rank: 0.684

## Article

# Usefulness of Tissue Doppler Imaging for the Evaluation of Pulmonary Hypertension in Canine Heartworm Disease

Jorge Isidoro Matos <sup>1</sup>, Sara Nieves García-Rodríguez <sup>1</sup>, Noelia Costa-Rodríguez <sup>1</sup>, Alicia Caro-Vadillo <sup>1,2</sup>, Elena Carretón <sup>1,\*</sup> and José Alberto Montoya-Alonso <sup>1</sup>

- <sup>1</sup> Internal Medicine, Faculty of Veterinary Medicine, Research Institute of Biomedical and Health Sciences (IUIBS), University of Las Palmas de Gran Canaria, 35016 Las Palmas de Gran Canaria, Spain; jorge.matos@ulpgc.es (J.I.M.); saranieves.garcia@ulpgc.es (S.N.G.-R.); noelia.costa@ulpgc.es (N.C.-R.); aliciac@vet.ucm.es (A.C.-V.); alberto.montoya@ulpgc.es (J.A.M.-A.)
- <sup>2</sup> Hospital Clínico Veterinario, Faculty of Veterinary Medicine, Universidad Complutense de Madrid (UCM), 28040 Madrid, Spain
- \* Correspondence: elena.carreton@ulpgc.es

**Simple Summary:** Tissue Doppler imaging is a useful echocardiographic technique to evaluate the systolic and diastolic function of the right ventricle and has been used as an estimator of pulmonary hypertension. The objective of this study was to evaluate the diagnostic value of tissue Doppler echocardiography to determine the presence of pulmonary hypertension in dogs with heartworm disease. A total of 116 heartworm-infected dogs and 33 healthy dogs were included in the study. Echocardiographic determinations were performed following established protocols to determine the presence of pulmonary hypertension in 47.4% of dogs infected with heartworm. Subsequently, a total of eight echocardiographic measurements were performed using tissue Doppler imaging to determine their usefulness in the diagnosis of pulmonary hypertension. Overall, the results showed significant differences with respect to the presence or absence of pulmonary hypertension. Furthermore, acceptable cut-off values were reported to estimate the presence of pulmonary hypertension in most echocardiographic measurements determined using tissue Doppler imaging. The measures analysed have demonstrated their usefulness as a complementary tool to determine pulmonary hypertension in dogs with *Dirofilaria immitis*.



**Citation:** Matos, J.I.; García-Rodríguez, S.N.; Costa-Rodríguez, N.; Caro-Vadillo, A.; Carretón, E.; Montoya-Alonso, J.A. Usefulness of Tissue Doppler Imaging for the Evaluation of Pulmonary Hypertension in Canine Heartworm Disease. *Animals* **2023**, *13*, 3647. <https://doi.org/10.3390/ani13233647>

Academic Editor: Sylvia García-Belenguier

Received: 17 October 2023  
Revised: 13 November 2023  
Accepted: 21 November 2023  
Published: 25 November 2023



**Copyright:** © 2023 by the authors. Licensee MDPI, Basel, Switzerland. This article is an open access article distributed under the terms and conditions of the Creative Commons Attribution (CC BY) license (<https://creativecommons.org/licenses/by/4.0/>).

**Abstract:** Background: *Dirofilaria immitis* is a nematode that produces proliferative pulmonary endarteritis in dogs due to direct contact of the adult parasites with the intima layer of the pulmonary arteries, leading to irreversible severe structural damage and sustained pulmonary hypertension (PH), which can produce severe cardiorespiratory disorders. The purpose of this study was to assess the diagnostic value of the echocardiography tissue Doppler imaging (TDI) in determining the presence of PH in dogs with heartworm disease. Methods: There were 116 heartworm-infected dogs with PH and 33 healthy dogs included in the study. Based on the right pulmonary artery distensibility index (RPADi) < 29.5%, PH was present in 47.4% of infected dogs. Additionally, the animals were evaluated using other standard alternative echocardiographic measures to estimate PH. Moreover, a total of eight echocardiographic measurements were analysed using the TDI to determine its usefulness in diagnosing PH (E', A', S, E':A', global TDI, HRI-IVCT, HRI-IVRT, R-TEI). Results: The TDI measurements showed significant differences between dogs with and without PH, demonstrating a positive correlation with respect to the RPADi. In addition, cut-off values for the detection of PH with excellent sensitivity and specificity were found for E':A', global TDI, HRI-IVCT, HRI-IVRT and R-TEI. Conclusions: The TDI mode may be useful as an adjunct diagnostic method for the determination of PH in dogs with *Dirofilaria immitis*.

**Keywords:** heartworm; *Dirofilaria immitis*; pulmonary hypertension; echocardiography; tissue Doppler imaging

## 1. Introduction

Heartworm disease is a parasitic disease caused by *Dirofilaria immitis* (Leidy, 1856), found worldwide and mainly affecting domestic and wild canids and felids. Heartworm disease produces severe cardiorespiratory disorders in dogs which require significant economic investment in endemic areas where regular prophylactic measures must be performed [1]. Chronic contact of the adult parasite of *D. immitis* with the intimal layer of the pulmonary vessel causes proliferative endarteritis, inducing dilatation, loss of lumen and loss of elasticity. Obstruction of blood flow can also occur, raising the pressure in the pulmonary arteries due to increased pulmonary vascular resistance. This increase is known as precapillary pulmonary hypertension (PH) [2], responsible for most of the clinical signs observed in dogs infected by *D. immitis*. Chronically, PH can cause hypertrophy and dilation of the right ventricle in its attempt to compensate for lung perfusion complications, leading to fatal right heart failure [3].

Nowadays, echocardiography sets the best technique for the detection of PH in daily veterinary practice, due to its accuracy and convenience [2]. To determine PH caused by *D. immitis*, previous research has determined that the right pulmonary artery distensibility index (RPADi) is the most accurate non-invasive measure to estimate the presence of increased pulmonary artery pressure, especially when tricuspid regurgitation velocity and pulmonary regurgitation are not evaluable [4–6].

Tissue Doppler imaging (TDI) is an echocardiographic method focused on the analysis of segmental myocardial movements in the systolic and diastolic phase. The degree of movement is determined by the cardiac contractility, the volume of the cardiac chambers and pressure differences, and allows for analysis of the systolic and diastolic functions [7]. Currently, most of the published studies have considered the use of TDI as a fundamental echocardiographic mode for analysing cardiac ventricular function and its use has been standardised in routine cardiac assessment [8,9]. A few studies have demonstrated the usefulness of TDI in estimating right ventricular dysfunction caused by PH in dogs, and have studied the diagnostic value of TDI in canine patients with PH caused by several conditions [10–14]. These studies concluded that TDI measurements of the systolic and diastolic phases of the right heart acted as an effective tool to estimate PH because a slight increase in pulmonary artery pressure alters the systolic and diastolic myocardial functions in the right heart. To date, the diagnostic value of TDI in the evaluation of PH has focused mainly on post-capillary causes in small animals, in which the changes originate from abnormalities in the left heart structures such as myxomatous mitral valve disease, canine dilated cardiomyopathy or feline hypertrophic cardiomyopathy [10–17]. Therefore, the use of TDI in heartworm disease has not been previously reported in dogs.

The haemodynamic changes that can be detected using TDI in the right heart chambers, caused by the presence of adult parasites, might be a useful tool for the evaluation of PH in canine heartworm disease. Thus, the aim of this study was to assess the utility of the measurements obtained via echocardiographic examination in TDI mode ( $E'$ ,  $A'$ ,  $S$ ,  $E':A'$ , global TDI, HRI-IVCT, HRI-IVRT, R-TEI) to detect the presence of PH in dogs infected by *D. immitis*.

## 2. Materials and Methods

### 2.1. Studied Animals

This prospective study included 149 client-owned dogs that visited the Veterinary Teaching Hospital of the University of Las Palmas de Gran Canaria (Canary Islands, Spain) between September 2021 and July 2022 and lived in a hyperendemic area of *D. immitis* [18]. A complete record was kept for each animal, including identification (age, sex, breed and weight), determination of body condition score (BCS) [19], as well as evaluation of the presence/absence of respiratory symptoms (i.e., cough, dyspnoea, exercise intolerance) and signs of right-sided congestive heart failure (R-CHF) mainly based on evidence of ascites, pleural effusion, jugular pulse and cava vein distention.

The presence/absence of heartworm was diagnosed by the detection of circulating *D. immitis* antigens, using a commercial kit (Uranotest Dirofilaria<sup>®</sup>, Urano Vet SL, Barcelona, Spain). Dogs with a negative test were used as healthy control animals, based on history, physical examination, cardiovascular evaluation and echocardiographic exam. In all cases, dogs with evidence of cardiac conditions coexisting with heartworm disease or dogs that had previously received any cardiovascular medication were excluded from the study.

## 2.2. Echocardiography

Echocardiographic exams were performed with the animals conscious and restrained without the use of any sedation, using an ultrasound equipment with spectral and colour Doppler and multifrequency phased-array transducers (2.5–12 MHz, Viviq Iq<sup>®</sup>, General Electric, Boston, MA, USA). Electrocardiographic monitoring was performed in all patients. Dogs were placed in right and left lateral decubitus with the transducer placed in the third-fourth intercostal space according to the described and validated methods [7,8]. Three consecutive cardiac cycles were performed to determine each of the measurements studied. All echocardiographic examinations were performed by the same researcher.

The presence or absence of PH was determined in accordance with the guidelines of the American College of Veterinary Internal Medicine (ACVIM) (REF). The RPADi and the tricuspid regurgitation systolic flow, among other measures taken routinely, were used as previously described [2,4,20,21]. The animals were classified with the presence of moderate/severe PH when they presented an RPADi < 29.5%, a tricuspid regurgitation systolic flow > 3.4 m/s, as well as other standard echocardiographic indicators ensuring the presence/absence of PH, as described below [21–25]. The pulmonary-vein-to-pulmonary-artery ratio in a right parasternal long axis view (PV:PA ratio) and the relation between the pulmonary trunk and ascending aorta taken in a right parasternal short axis view (PT:Ao) were recorded. The right ventricular outflow tract velocity was measured, and the relationship between the acceleration times (AT) and ejection times (ET) was determined using the AT:ET ratio. The peak of the tricuspid regurgitation velocity was also measured to obtain the tricuspid regurgitation pressure gradient (TRPG), along with the systolic displacement of the tricuspid annulus (TAPSE).

Right TDI examinations were performed as previously described and validated [7,10] (Figure 1). Longitudinal velocities were measured in a basal segment of the mid-inner portion of the right myocardium, focusing on the tricuspid valve annulus, using a longitudinal four-chamber left apical view optimised for the visualisation of the right ventricle and atrium [10]. The maximum myocardial velocities were measured in early diastole ( $E'$ ), late diastole ( $A'$ ), and systole (S), calculating the  $E':A'$  ratio. A global TDI index of the myocardial function (global TDI), based on the formula  $\text{global TDI} = S \times E':A'$ , was also calculated.

The RR interval was established on the same 3 consecutive cardiac cycles due to the significance of heart rate in the measurements. Therefore, TDI time indices were indexed to the RR interval, defining heart-rate-indexed (HRI) time indices, as previously published [9,10]. Myocardial time indices were measured, including the isovolumic contraction time (HRI-IVCT) and isovolumic relaxation time (HRI-IVRT). The HRI-IVCT was defined as the time between the end of the  $A'$  wave and the beginning of the S wave and the HRI-IVRT as the time between the end of the S wave and the beginning of the  $E'$  wave. The R-TEI index was calculated using the following formula  $(\text{HRI-IVRT} + \text{HRI-IVCT})/\text{ET}$  [23,24].

Finally, the presence or absence of worms in the pulmonary arteries and right heart chambers was evaluated, and the parasite burden was classified as low or high, according to the guidelines previously published [26].

Based on the RPADi and clinical status, dogs were classified into 3 groups. Group A comprised healthy control animals, Group B included heartworm-infected dogs without PH and group C was formed of heartworm-infected dogs with PH.

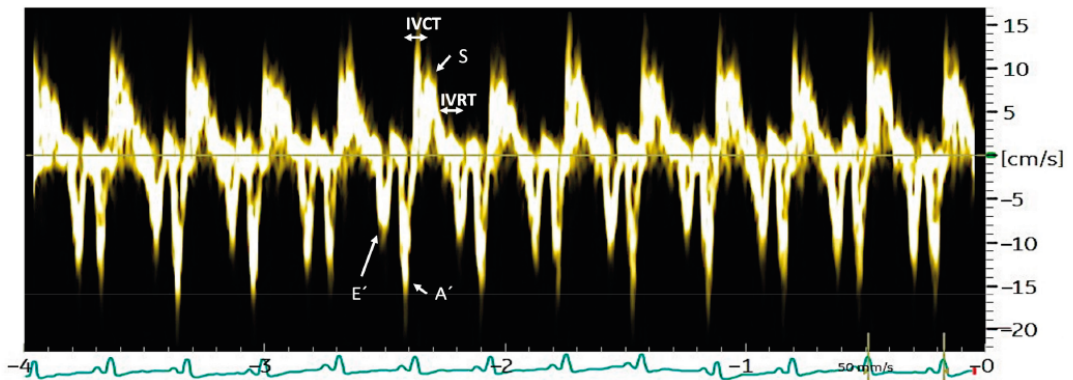


**Figure 1.** Measurement of the TDI parameters  $E'$ ,  $A'$ ,  $S$ , HRI-IVCT and HRI-IVRT in a dog with heartworm disease that presented pulmonary hypertension (right pulmonary artery distensibility index  $< 29.5\%$ ). Left parasternal position, apical four-chamber, longitudinal section in TDI mode, focusing on the tricuspid valve annulus.

### 2.3. Statistical Analysis

Frequencies and percentages were shown for categorical variables. The differences in parameters between groups were evaluated using Pearson's non-parametric  $\chi^2$  test and, only in the case of  $2 \times 2$  tables, Fisher's exact test was applied. For continuous variables, the differences in the parameters between groups were evaluated by means of Mann-Whitney/Kruskal-Wallis tests (non-parametric) or T-student/ANOVA (parametric) based on the normality of the variables to be evaluated by means of a Shapiro-Wilks test. To establish the correlation and explanatory capacity of the methods with the gold standard (RPADi), linear regression was applied and the non-standardised beta coefficients, their 95% CI, the  $R^2$  and the equation were shown. To determine the ability of the different echocardiographic measurements to classify the presence/absence of PH, the receiver operating characteristic (ROC) curve was used. All multiple comparisons were adjusted using the Bonferroni correction. All the contrasts were accompanied by the effect size estimator to complete the interpretation of the results. For categorical variables, it was Cramer's  $V$  and, for continuous variables, it was Cohen's  $d$ . The criteria for the classification of the magnitude of the effect were as follows: Cohen's  $d$ : small ( $d = 0.2$ – $0.4$ ), medium ( $d = 0.5$ – $0.8$ ) and large ( $d = \text{greater than } 0.8$ ). Cramer's  $V$ : 0.00–0.09 as negligible, 0.10–0.29 as low, 0.30–0.49 as medium and from 0.50 as high. For all cases, the significance level used was 5% ( $\alpha = 0.05$ ).

### 2.4. Ethical Statement

All owners were informed and gave their consent to participate in the study. Ethical approval was not required for this study, as it was a purely observational study with voluntary enrolment and did not involve additional invasive clinical diagnostic procedures. The evaluation of the study included ethical considerations and legal aspects regarding animal protection and welfare, and was conducted in accordance with the current Spanish and European legislation on animal protection.

## 3. Results

Presence of heartworm was diagnosed in 116 dogs (77.85%) while 33 (22.15%) dogs were used as healthy control animals. Based on the RPADi, all healthy dogs were normotensive (Group A,  $n = 33$ ), whilst PH was absent in 52.6% of dogs infected with *D. immitis* (Group B,  $n = 61$ ). Group C included 55 dogs with heartworm and presence of PH.

The results of the descriptive analytical study of the clinical variables and the standard and TDI mode echocardiographic measurements in the studied dogs are shown in Table 1.



All the animals studied presented age ranges from 3 to 14 years and showed similar proportions of both sexes (50.3% females and 49.7% males). The BCS ranged from 1 to 9 [19] and the weight range varied between 3.2 and 45.9 kg. The presence of mongrel dogs was greater than the remaining breeds analysed (49.1%), with a total of 29 different breeds recorded. No significant differences in age, sex, BCS, weight or breed were reported between the groups A, B and C.

**Table 1.** Clinical characteristics and echocardiography parameters of study dogs (n = 149). Data represent median unless otherwise stated. CHF: congestive heart failure; BCS: body condition score; HR: heart rate. Group A comprised healthy control animals, Group B included heartworm-infected dogs without pulmonary hypertension (PH) and group C was formed of heartworm-infected dogs with PH. RPADi: right pulmonary artery distensibility index; TRPG: tricuspid regurgitation pressure gradient; PT: pulmonary trunk; PV:PA: pulmonary vein to pulmonary artery ratio; TASPSE: tricuspid annular plane systolic excursion; AT:ET: right ventricle outflow Doppler acceleration time to ejection time ratio; HRI-IVCT: isovolumic contraction time indexed to heart rate; HRI-IVRT: isovolumic relaxation time indexed to heart rate; Global TDI: global TDI index defined as  $S \times E':A'$ ; R-TEI index: Tei index of right ventricular myocardial performance.

	DOGS (N = 149)	GROUP A (N = 33)	GROUP B (N = 61)	GROUP C (N = 55)	p-Value
Age (years)	7.67 ± 3.50	8.51 ± 3.75	6.43 ± 2.78	8.54 ± 3.64	0.01 (0.60) <sup>1</sup>
Female: number (%)	75 (50.33%)	15 (10.07%)	36 (24.16%)	24 (16.11%)	0.21 <sup>3</sup>
Body weight (kg)	18.45 ± 10.34	16.44 ± 10.15	18.70 ± 10.42	19.31 ± 10.40	0.47 <sup>2</sup>
BCS (1–9)	5.28 ± 0.99	5.36 ± 0.99	5.31 ± 0.77	5.20 ± 1.14	0.36 <sup>2</sup>
Breed: mongrel (%)	75 (50.34%)	10 (6.71%)	38 (25.50%)	27 (18.12%)	0.01 (0.61) <sup>3</sup>
Respiratory symptom (%)	69 (46.31%)	0 (0%)	21 (14.10%)	48 (32.21%)	0.01 (0.68) <sup>3</sup>
Right-sided CHF (%)	17 (11.41%)	0 (0%)	1 (0.67%)	16 (10.74%)	0.01 (0.43) <sup>3</sup>
Parasite burden (1–4)	1.88 ± 0.91	0 ± 0.00	2.13 ± 0.87	2.78 ± 0.76	0.01 (0.79) <sup>3</sup>
HR (beats per minute)	130.71 ± 24.45	129.63 ± 21.27	132.10 ± 30.51	129.82 ± 18.22	0.848 <sup>1</sup>
RPADi (%)	33.10 ± 12.07	41.48 ± 4.85	40.32 ± 7.34	20.07 ± 7.14	0.01 (1.77) <sup>2</sup>
TRPG (mmHg)	24.79 ± 36.92	5.15 ± 3.49	4.08 ± 3.40	59.53 ± 42.10	0.01 (−1.47) <sup>2</sup>
PT:Ao	1.05 ± 0.20	0.95 ± 0.07	0.92 ± 0.10	1.25 ± 0.16	0.01 (−1.51) <sup>2</sup>
PV:PA Ratio	0.84 ± 0.34	1.08 ± 0.12	1.05 ± 0.20	0.48 ± 0.21	0.01 (1.76) <sup>2</sup>
TASPSE	1.45 ± 0.41	1.71 ± 0.32	1.66 ± 0.27	1.06 ± 0.26	0.01 (1.58) <sup>2</sup>
AT:ET	0.33 ± 0.10	0.39 ± 0.06	0.39 ± 0.07	0.24 ± 0.06	0.01 (1.55) <sup>2</sup>
E' (cm/s)	8.94 ± 3.16	10.67 ± 2.26	10.25 ± 2.76	6.45 ± 2.42	0.01 (1.33) <sup>1</sup>
A' (cm/s)	10.20 ± 2.98	9.97 ± 1.55	9.79 ± 3.14	10.80 ± 3.38	0.17 <sup>1</sup>
S (cm/s)	13.44 ± 4.58	14.45 ± 2.36	16.11 ± 3.84	9.85 ± 3.99	0.01 (1.00) <sup>1</sup>
E':A'	0.92 ± 0.37	1.08 ± 0.23	1.11 ± 0.37	0.61 ± 0.19	0.01 (1.26) <sup>1</sup>
HRI-IVCT (ms)	25.01 ± 14.61	15.18 ± 4.81	16.59 ± 6.04	40.45 ± 12.21	0.01 (1.21) <sup>1</sup>
HRI-IVRT (ms)	47.93 ± 20.26	34.27 ± 6.9	35.95 ± 7.13	69.42 ± 17.13	0.01 (1.73) <sup>1</sup>
Global TDI	12.99 ± 7.83	15.55 ± 3.75	17.88 ± 7.95	6.05 ± 3.03	0.01 (1.73) <sup>1</sup>
R-TEI index	0.41 ± 0.19	0.27 ± 0.04	0.30 ± 0.06	0.626 ± 0.17	0.01 (1.80) <sup>1</sup>

<sup>1</sup>  $p < 0.01 =$  ANOVA and Cohen's  $d$  value in brackets. <sup>2</sup>  $p < 0.01 =$  Mann-Whitney/Kruskal-Wallis and Cohen's  $d$  value in brackets. <sup>3</sup>  $p < 0.01 =$  Chi<sup>2</sup> test and Cramer's  $V$  in brackets.

The parasite burden ranged from 1 to 4 [21,26] in the dogs of groups B and C, with no significant differences observed between them, although a higher mean value was observed in dogs from group C. The parasite load was obviously 1 (no worms visible) in dogs from group A. The presence of respiratory symptoms and signs of R-CHF were directly related to the presence of heartworm and PH, since all dogs with R-CHF occurred in group C, and respiratory symptoms increased considerably in the animals suffering from PH.

The statistical study revealed significant differences in the RPADi between group C in comparison to groups A and B ( $p = 0.000$ ), and no differences were found between groups A and B. The results of the additional standard echocardiographic measurements to estimate the presence of PH showed significantly higher values for TRPG and PT:Ao in group C when compared with groups A and B ( $p = 0.000$ ). There were also significantly lower values

for the A':E' ratio, TAPSE and PV:PA ratio in group C when compared with groups A and B ( $p = 0.000$ ). However, no differences were observed in the echocardiographic parameters studied between groups A and B.

Similarly, ANOVA tests found significant differences between the values of the TDI parameters in the studied groups. The Bonferroni post hoc tests for multiple comparisons indicated that, for all the parameters, except for the A' measurement, there were significant differences in dogs from group C when compared to groups A and B. The values of E', S, E':A' and global TDI were significantly lower in dogs from group C, whilst the values of HRI-IVCT, HRI-IVRT and R-TEI were significantly higher in dogs from group C ( $p = 0.000$ ) (Figure 2). The results obtained in the A' measurement did not report differences between the groups of animals studied ( $p = 0.166$ ).

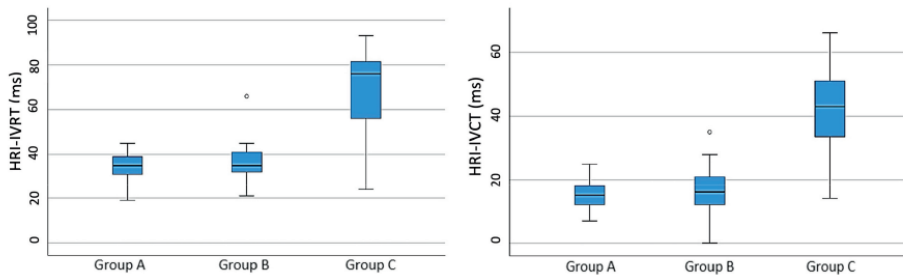


Figure 2. Scatter plots illustrating echocardiography TDI measurements of HRI-IVRT and HRI-IVCT obtained in dogs without heartworm infection (group A), in dogs with heartworm and without pulmonary hypertension (PH) (group B) and in dogs with heartworm and PH (group C).

Linear regression was carried out for each TDI parameter studied, showing that the parameters that best correlated with the RPADi were HRI-IVCT, HRI-IVRT and R-TEI, with  $R^2 > 0.5$  (Figure 3). The parameters E', S, E':A' and global TDI had an  $R^2$  close to 0.3. The result obtained for A' showed that this measurement did not correlate with the RPADi ( $R^2 < 0.1$ ).

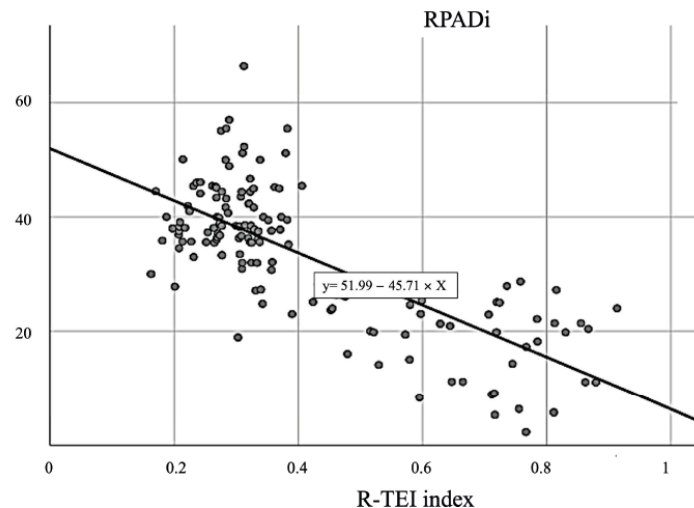


Figure 3. Scatter plots illustrating significant (all  $p < 0.01$ ) correlations (R) between right pulmonary artery distensibility index (RPADi) and R-TEI index. The solid line within each scatter plot represents the line of best fit. Lineal  $R^2 = 0.555$ .

The results of the ROC curves for each of the TDI measurements to determine the presence or absence of PH and the cut-off points of the parameters that maximise sensitivity and specificity (using the Youden index) are collected in Table 2, showing excellent areas under the curve (AUCs) (>0.9) for E':A', global TDI, HRI-IVCT, HRI-IVRT and R-TEI. The sensitivity and specificity of the cut-off points established for these measures for the diagnosis of PH obtained excellent results for E':A' (87.3%, 92.6%, respectively), HRI-IVCT (83.6% and 95.7%, respectively) and HRI-IVRT (87.3% and 98.9%), highlighting global TDI (94.5% and 98.9%, respectively) and R-TEI index (90.9% and 98.9%, respectively). The values of S and E' showed acceptable AUCs (>0.8), while the worst model was A' with an AUC of 0.572.

**Table 2.** Results of simple regression analysis of the cut-off points of TDI measurements by echocardiography to predict the presence of PH using the right pulmonary artery distensibility index (RPADi < 29.5%). R<sup>2</sup> (coefficient of determination); sensitivity (Se); specificity (Sp); Youden index; area under receiver operating characteristic curve (AUC); confidence interval 95% (CI 95%); tissue Doppler imaging (TDI); global TDI (global TDI index defined as S × E':A'); isovolumic contraction time indexed to heart rate (HRI-IVCT); isovolumic relaxation time indexed to heart rate (HRI-IVRT); Tei index of right ventricular myocardial performance (R-TEI index).

	R <sup>2</sup>	AUC	CI 95%	Cut-Off Point	Se	Es	p-Value	Youden Index (Se + Es - 1)
E' (cm/s)	0.284	0.863	(0.802, 0.924)	≤8.50	0.818	0.766	0.000	0.584
A' (cm/s)	0.012	0.572	(0.474, 0.670)	≥11.50	0.455	0.755	0.093	0.210
S (cm/s)	0.281	0.881	(0.816, 0.947)	≤12.50	0.818	0.862	0.000	0.680
E':A'	0.312	0.938	(0.869, 0.980)	≤0.839	0.873	0.926	0.000	0.798
Global TDI	0.336	0.984	(0.961, 1.000)	≤10.20	0.945	0.989	0.000	0.935
HRI-IVCT (ms)	0.513	0.958	(0.926, 0.990)	≥26.50	0.836	0.957	0.000	0.794
HRI-IVRT (ms)	0.533	0.954	(0.915, 0.994)	≥46.50	0.873	0.989	0.000	0.862
R-TEI index	0.555	0.965	(0.927, 1.000)	≥0.387	0.909	0.989	0.000	0.898

#### 4. Discussion

The presence of PH is a severe hemodynamic condition that usually occurs in dogs parasitised by *D. immitis* and is responsible for multiple cardiorespiratory complications that characterise canine heartworm disease [3,4], including chronic systolic and diastolic dysfunction in the right cardiac chambers. So far, echocardiographic measurement of the RPADi has proven useful for the diagnosis and staging of PH in dogs with heartworm [5,6]. However, new non-invasive methods must be incorporated to assess in a more exact and precise way the cardiovascular repercussions of this disease. In this sense, the TDI mode is proposed as an effective complementary tool for the echocardiographic analysis of the haemodynamic repercussions in heartworm disease.

In this study, the guidelines of the ACVIM for the diagnosis of PH have been used [2]. Since some standardised measures, such as pulmonary and tricuspid regurgitation, are not always detectable [20,22], the RPADi was used as a gold-standard measure to identify the presence of PH in dogs with heartworm disease [3–6], whilst other echocardiographic parameters were used to confirm the presence of PH [23–25]. In the present study, the measurements of PT:Ao, AT:ET, TRPG, TAPSE and PV:PA ratio were used, which have a widely demonstrated diagnostic value in the study of canine PH caused by *D. immitis* [21–23]. The results for all the studied standard echocardiographic measures obtained in the present research have obtained highly similar values to those previously published in heartworm disease and confirm their usefulness in the study of this parasitic disease [5,6,21].

The TDI echocardiographic mode is widely used in veterinary medicine and its effectiveness is particularly important in providing information on systolic and diastolic function triggered by cardiovascular diseases. Previously, the use of echocardiographic measurements using the TDI mode has shown its efficacy for the assessment of volume overload and its effects on left ventricular dysfunction in dogs with myxomatous mitral valve disease and dilated cardiomyopathy [8,11,13–15]. Furthermore, it has demonstrated

its usefulness in the echocardiographic study of other species, such as cats with hypertrophic cardiomyopathy [16,17], horses with heart disease [27] and in the evaluation of cardiac function in healthy animals such as rabbits and goats [28,29].

Regarding the detection of PH, the study of TDI mode has already demonstrated its usefulness in dogs, specifically in the diagnosis of PH in dogs mainly suffering from left heart pathologies [7–9]. The results of the present study agree with those from previous authors [10,11,14], who reported severe decreases in the values of  $E'$ ,  $E':A'$  and  $S$ , as well as increases in the values of HRI-IVCT and HRI-IVRT; moreover, these authors noted excellent sensitivities and specificities for global TDI and  $E':A'$  (Se 89%; Sp 93% and 90%, respectively) [10], with similar cut-off points to those reported in the present study. Therefore, although the methodologies varied and other pathologies that cause PH were evaluated, the results showed the great usefulness of the TDI mode to determine the presence of PH, as seen in the present study, in which the results confirm the utility of the TDI mode to determine PH in dogs with heartworm. Thus, this method shows important value in the clinical study of infections by *D. immitis*, by demonstrating excellent correlations between TDI measurements (HRI-IVCT, HRI-IVRT and R-TEI) and the presence and severity of PH, as well as high sensitivity and specificity values when establishing cut-off points for the detection of PH for most TDI measurements. Another study, unlike the present one, found significant differences in the value of  $A'$  in dogs with PH [11], although, again, this can be justified by the difference in the methodology and pathologies studied. In any case, the results of the present study suggest that the presence of PH can be estimated by means of TDI measurements regardless of its origin, and therefore bestows great value in being used in veterinary cardiology.

The results observed agree with the cardiovascular alterations present in canine heartworm. In this sense, the presence of adult parasites in the lumen of the pulmonary arteries generates proliferative endarteritis that causes a decrease in the distension capacity during the cardiac cycle, an increase in pulmonary arterial pressure and therefore morphological changes with loss of myocardial functionality. When this event becomes chronic, tricuspid insufficiency occurs due to the increased pressure in the right ventricle. Finally, at the final stages, signs of atrial dilation and retrograde venous congestion are generated with a decrease in the speed of passive diastolic filling ( $E'$ ) and also a decrease in systolic velocity ( $S$ ) due to volume overload. However, the active diastolic filling rate ( $A'$ ) remains unchanged because it does not depend on pressure differences in the cardiac chambers. Likewise, it is logical that the aforementioned pressure and volume overloads cause increases in the relaxation (HRI-IVRT) and contraction (HRI-IVCT) times adjacent to ventricular systole. Similarly, measures that adjust these haemodynamic changes to analyse them more precisely, such as the global TDI and the R-TEI using diastolic and systolic measurements in TDI mode, have shown satisfactory results in the present study.

No significant differences were found according to age, sex, weight, breed or BCS between groups, coinciding with previous studies that determined that *D. immitis* infection does not show preferences regarding these epidemiological parameters, nor does the development of PH in the presence of this pathology [3,5,18,20].

A higher parasite burden was reported in animals with heartworm suffering PH, although the statistical differences were not significant. The influence of the parasitic load on the development of PH is not clear. Some authors claim that the greatest influence on the development of endarteritis and PH corresponds to the chronicity of the disease, the intensity of exercise and the immune response of the host to the parasite [4,5,26], whilst other authors attribute an important role also to the parasite load [3,30,31].

Most dogs with cardiorespiratory symptoms corresponded with those with PH; previous studies have demonstrated that approximately 50% of infected animals developed PH and, therefore, associated symptoms [4–6,21]. The presence of PH is a negative prognostic factor in infected dogs [2,23] and, considering the severity and frequency of PH, which also appears to be irreversible in many patients [3,4,21], it is crucial to keep developing non-invasive and affordable techniques to detect this condition in dogs with *D. immitis*.

## 5. Conclusions

The results showed that the TDI measurements of  $E'$ ,  $S$ ,  $E':A'$ , HRI-IVRT, HRI-IVCT, global TDI and R-TEI differentiated between normotensive dogs and those with PH (RPADI < 29.5%). Therefore, they can be a helpful alternative for evaluating patients with heartworm via transthoracic echocardiography. Similarly, the  $A'$  measure proved to be an inadequate indicator for estimating PH in dogs with heartworm disease. The HRI-IVCT, HRI-IVRT and R-TEI showed higher levels of efficiency in the detection of PH in dogs parasitised by *D. immitis*, although further studies are indicated with the aim of obtaining standardised protocols and exact reference values to satisfactorily establish the diagnosis and estimate the severity of PH in dogs with heartworm disease.

**Author Contributions:** J.I.M., J.A.M.-A. and E.C. designed the study. J.I.M., A.C.-V. and E.C. wrote the manuscript. J.I.M., S.N.G.-R. and N.C.-R. performed the fieldwork, collected the data and performed the experiments. All authors participated in the discussion of the results, corrected, read and approved the final manuscript. All authors have read and agreed to the published version of the manuscript.

**Funding:** The presented study was supported by own funds from the Servicio de Medicina Veterinaria FULP/ULPGC (SD-240/030/0026). N.C.-R. was supported by the “Grants for the predoctoral training program for researchers” program of the Government of the Canary Islands (TESIS2021010010) and J.I.M. and S.N.R.-G. were supported by the “Grants for the financing of predoctoral contracts” program of the Universidad de Las Palmas de Gran Canaria (PIFULPGC-2017-CCSALUD-3 and PIFULPGC-2020-2-CCSALUD-2, respectively).

**Institutional Review Board Statement:** Ethical review and approval were not required for the animal study because the present study was conducted on client-owned animals/clinical cases and no experimental animals were used. All dog owners were informed about the present study and consented to participate. The study was carried out in accordance with the current Spanish and European legislation on animal protection (Spanish Royal Decree 53/2013 and 2010/63/UE Directive).

**Informed Consent Statement:** Not applicable.

**Data Availability Statement:** The raw data supporting the conclusions of this article will be made available by the authors, without undue reservation. Data are contained within the article.

**Acknowledgments:** The authors would like to thank Uranovet for kindly providing the Uranotest *Dirofilaria*<sup>®</sup>. Also, they would like to thank to the Hospital Clínico Veterinario of the Universidad de Las Palmas de Gran Canaria (ULPGC) for its support.

**Conflicts of Interest:** The authors declare no conflict of interest.

## References

1. Simón, F.; Siles-Lucas, M.; Morchón, R.; González-Miguel, J.; Mellado, I.; Carretón, E.; Montoya-Alonso, J.A. Human and Animal *Dirofilaria* Infection: The Emergence of a Zoonotic Mosaic. *J. Clin. Microbiol.* **2012**, *25*, 507–544. [[CrossRef](#)]
2. Reiner, C.; Visser, L.C.; Kellihan, H.B.; Masseur, I.; Rozanski, E.; Clercx, C.; Williams, K.; Abbott, J.; Borgarelli, M.; Scansen, B.A. ACVIM consensus statement guidelines for the diagnosis, classification, treatment, and monitoring of pulmonary hypertension in dogs. *J. Vet. Intern. Med.* **2020**, *34*, 549–573. [[CrossRef](#)]
3. Romano, A.E.; Saunders, A.B.; Gordon, S.G.; Wesselowski, S. Intracardiac heartworms in dogs: Clinical and echocardiographic characteristics in 72 cases (2010–2019). *J. Vet. Intern. Med.* **2021**, *35*, 88–97. [[CrossRef](#)] [[PubMed](#)]
4. Falcón-Cordón, Y.; Montoya-Alonso, J.A.; Caro-Vadillo, A.; Matos, J.I.; Carretón, E. Persistence of pulmonary endarteritis in canine heartworm infection 10 months after the eradication of adult parasites of *Dirofilaria immitis*. *Vet. Parasitol.* **2019**, *273*, 1–4. [[CrossRef](#)] [[PubMed](#)]
5. Serrano-Parreño, B.; Carretón, E.; Caro-Vadillo, A.; Falcón-Cordón, Y.; Falcón-Cordón, S.; Montoya-Alonso, J.A. Evaluation of pulmonary hypertension and clinical status in dogs with heartworm by Right Pulmonary Artery Distensibility Index and other echocardiographic parameters. *Parasites Vectors* **2017**, *10*, 106–112. [[CrossRef](#)] [[PubMed](#)]
6. Venco, L.; Mihaylova, L.; Boon, J.A. Right Pulmonary Artery Distensibility Index (RPAD Index). A field study of an echocardiographic method to detect early development of pulmonary hypertension and its severity even in the absence of regurgitant jets for Doppler evaluation in heartworm-infected dogs. *Vet. Parasitol.* **2014**, *206*, 60–66. [[PubMed](#)]

7. Chetboul, V.; Sampedrano, C.C.; Gouni, V.; Concordet, D.; Lamour, T.; Ginesta, J.; Nicolle, A.P.; Pouchelon, J.L.; Lefebvre, H.P. Quantitative Assessment of Regional Right Ventricular Myocardial Velocities in Awake Dogs by Doppler Tissue Imaging: Repeatability, Reproducibility, Effect of Body Weight and Breed, and Comparison with Left Ventricular Myocardial Velocities. *J. Vet. Intern. Med.* **2005**, *19*, 837–844. [[CrossRef](#)] [[PubMed](#)]
8. Chetboul, V.; Gouni, V.; Sampedrano, C.C.; Tissier, R.; Serres, F.; Pouchelon, J.L. Assessment of regional systolic and diastolic myocardial function using tissue Doppler and strain imaging in dogs with dilated cardiomyopathy. *J. Vet. Intern. Med.* **2007**, *21*, 719–730. [[CrossRef](#)] [[PubMed](#)]
9. Koffas, H.; Dukes-McEwan, J.; Corcoran, B.M.; Moran, C.M.; French, A.; Sboros, V.; Simpson, K.; McDicken, W.N. Pulsed tissue Doppler imaging in normal cats and cats with hypertrophic cardiomyopathy. *J. Vet. Intern. Med.* **2006**, *20*, 65–77. [[CrossRef](#)]
10. Serres, F.; Chetboul, V.; Gouni, V.; Tissier, R.; Sampedrano, C.C.; Pouchelon, J.L. Diagnostic value of echo-Doppler and tissue Doppler imaging in dogs with pulmonary arterial hypertension. *J. Vet. Intern. Med.* **2007**, *21*, 1280–1289.
11. Toaldo, M.; Poser, H.; Menciotti, G.; Battaia, S.; Contiero, B.; Cipone, M.; Diana, A.; Mazzotta, E.; Guglielmini, C. Utility of Tissue Doppler Imaging in the Echocardiographic Evaluation of Left and Right Ventricular Function in Dogs with Myxomatous Mitral Valve Disease with or without Pulmonary Hypertension. *J. Vet. Intern. Med.* **2016**, *30*, 697–705. [[CrossRef](#)] [[PubMed](#)]
12. Morita, T.; Nakamura, K.; Osuga, T.; Morishita, K.; Sasaki, N.; Ohta, H.; Takiguchi, M. Right ventricular function and dyssynchrony measured by echocardiography in dogs with precapillary pulmonary hypertension. *J. Vet. Cardiol.* **2019**, *23*, 1–14. [[CrossRef](#)] [[PubMed](#)]
13. Yuchi, Y.; Suzuki, R.; Yasumura, Y.; Saito, T.; Teshima, T.; Matsumoto, H.; Koyama, H. Prognostic value of pulmonary vascular resistance estimated by echocardiography in dogs with myxomatous mitral valve disease and pulmonary hypertension. *J. Vet. Intern. Med.* **2023**, *37*, 856–865. [[CrossRef](#)] [[PubMed](#)]
14. Morita, T.; Nakamura, K.; Osuga, T.; Takiguchi, M. Incremental predictive value of echocardiographic indices of right ventricular function in the assessment of long-term prognosis in dogs with myxomatous mitral valve disease. *J. Vet. Cardiol.* **2022**, *39*, 51–62. [[CrossRef](#)] [[PubMed](#)]
15. Tidholm, A.; Ljungvall, I.; Höglund, K.; Westling, A.B.; Häggström, J. Tissue Doppler and strain imaging in dogs with myxomatous mitral valve disease in different stages of congestive heart failure. *J. Vet. Intern. Med.* **2009**, *23*, 1197–1207. [[CrossRef](#)] [[PubMed](#)]
16. Tuleski, G.; Wolf, M.; Pscheidt, M.; Dos Santos, J.P.; Sousa, M.G. Tissue motion annular displacement to assess the left ventricular systolic function in healthy cats. *Vet. Res. Commun.* **2022**, *8*, 10–17. [[CrossRef](#)] [[PubMed](#)]
17. Sampedrano, C.C.; Chetboul, V.; Gouni, V.; Nicolle, A.P.; Pouchelon, J.L.; Tissier, R. Systolic and diastolic myocardial dysfunction in cats with hypertrophic cardiomyopathy or systemic hypertension. *J. Vet. Intern. Med.* **2006**, *20*, 1106–1115. [[CrossRef](#)]
18. Montoya-Alonso, J.A.; Morchón, R.; García, S.; Falcón-Cordón, Y.; Costa-Rodríguez, N.; Matos, J.; Escolar, I.R.; Carretón, E. Expansion of Canine Heartworm in Spain. *Animals* **2022**, *12*, 1268. [[CrossRef](#)]
19. Laflamme, D.P. Development and Validation of a Body Condition Score System for Dogs. *Canine Pract.* **1997**, *22*, 10–15.
20. Visser, L.C.; Im, M.K.; Johnson, L.R.; Stern, J.A. Diagnostic Value of Right Pulmonary Artery Distensibility Index in Dogs with Pulmonary Hypertension: Comparison with Doppler Echocardiographic Estimates of Pulmonary Arterial Pressure. *J. Vet. Intern. Med.* **2016**, *30*, 543–552. [[CrossRef](#)]
21. Matos, J.I.; Caro-Vadillo, A.; Falcón-Cordón, Y.; García-Rodríguez, S.N.; Costa-Rodríguez, N.; Carretón, E.; Montoya-Alonso, J.A. Echocardiographic Assessment of the Pulmonary Vein to Pulmonary Artery Ratio in Canine Heartworm Disease. *Animals* **2023**, *13*, 703. [[CrossRef](#)]
22. Kellihan, H.B.; Stepien, R.L. Pulmonary hypertension in canine degenerative mitral valve disease. *J. Vet. Cardiol.* **2012**, *14*, 149–164. [[CrossRef](#)] [[PubMed](#)]
23. Teshima, K.; Asano, K.; Iwanaga, K.; Koie, H.; Uechi, M.; Kato, Y. Evaluation of right ventricular Tei index (index of myocardial performance) in healthy dogs and dogs with tricuspid regurgitation. *J. Vet. Med.* **2006**, *68*, 1307–1313. [[CrossRef](#)] [[PubMed](#)]
24. Morita, T.; Nakamura, K.; Osuga, T.; Lim, S.Y.; Yokoyama, N.; Morishita, K. Repeatability and reproducibility of right ventricular Tei index values derived from three echocardiographic methods for evaluation of cardiac function in dogs. *Am. J. Vet. Res.* **2016**, *77*, 15–20. [[CrossRef](#)] [[PubMed](#)]
25. Silva, V.B.C.; Wolf, M.; Lucina, S.B.; Sarraff-Lopes, A.P.; Sousa, M.G. Assessment of right ventricular systolic function by tissue motion annular displacement in healthy dogs. *J. Vet. Cardiol.* **2020**, *32*, 40–48. [[CrossRef](#)]
26. Venco, L.; Genchi, C.; Vigevani, D.; Colson, P.; Kramer, L. Relative utility of echocardiography, radiography, serologic testing and microfilariae counts to predict adult worm burden in dogs naturally infected with heartworms. In *Recent Advances in Heartworm Disease, Symposium '01*; American Heartworm Society: Batavia, IL, USA, 2014; pp. 24–111.
27. Koenig, T.R.; Mitchell, K.J.; Schwarzwald, C.C. Echocardiographic Assessment of Left Ventricular Function in Healthy Horses and in Horses with Heart Disease Using Pulsed-Wave Tissue Doppler Imaging. *J. Vet. Intern. Med.* **2017**, *31*, 556–567. [[CrossRef](#)] [[PubMed](#)]
28. Fontes-Sousa, A.P.; Moura, C.; Carneiro, C.S.; Teixeira-Pinto, A.; Azeias, J.C.; Leite-Moreira, A.F. Echocardiographic evaluation including tissue Doppler imaging in New Zealand white rabbits sedated with ketamine and midazolam. *Vet. J.* **2009**, *181*, 326–331. [[CrossRef](#)]
29. Mandour, A.S.; Samir, H.; Yoshida, T.; Matsuura, K.; Abdelmageed, H.A.; Elbadawy, M.; Al-Rejaie, S.; El-Husseiny, H.M.; Elfadadny, A.; Ma, D.; et al. Assessment of the Cardiac Functions Using Full Conventional Echocardiography with Tissue Doppler Imaging before and after Xylazine Sedation in Male Shiba Goats. *Animals* **2020**, *10*, 2320. [[CrossRef](#)]

30. Dillon, R.A.; Brawner, W.R.; Hanrahan, L. Influence of number of parasites and exercise on the severity of heartworm disease in dogs. In *Proceedings of the Heartworm Symposium'95*; Sol, M.D., Knight, D.H., Eds.; American Heartworm Society: Vatavia, IL, USA, 1995; p. 113.
31. Méndez, J.C.; Carretón, E.; Martínez-Subiela, S.; Tvarijonaviciute, A.; Cerón, J.J.; Montoya-Alonso, J.A. Acute phase protein response in heartworm-infected dogs after adulticide treatment. *Vet. Parasitol.* **2015**, *209*, 197–201. [[CrossRef](#)]

**Disclaimer/Publisher's Note:** The statements, opinions and data contained in all publications are solely those of the individual author(s) and contributor(s) and not of MDPI and/or the editor(s). MDPI and/or the editor(s) disclaim responsibility for any injury to people or property resulting from any ideas, methods, instructions or products referred to in the content.



## 4.3.

### **Right Ventricle Strain Assessed by 2-Dimensional Speckle Tracking Echocardiography (2D-STE) to Evaluate Pulmonary Hypertension in Dogs with *Dirofilaria immitis***

**Matos, J.I.;** García-Rodríguez, S.N.; Costa-Rodríguez, N.; Caro-Vadillo, A.; Carretón, E.; Montoya-Alonso, J.A. Usefulness of Tissue Doppler Imaging for the Evaluation of Pulmonary Hypertension in Canine Heartworm Disease. *Animals* 2023, 14, 26. <https://doi.org/10.3390/ani14010026>

JOURNAL CITATION REPORTS:  
JCR-Q1 (VETERINARY SCIENCES)  
CiteScore-Q1 (GENERAL VETERINARY)  
Impact Factor: 3.231  
SCImago Journal Rank: 0.684



## Article

# Right Ventricle Strain Assessed by 2-Dimensional Speckle Tracking Echocardiography (2D-STE) to Evaluate Pulmonary Hypertension in Dogs with *Dirofilaria immitis*

Jorge Isidoro Matos <sup>1</sup>, Sara Nieves García-Rodríguez <sup>1</sup>, Noelia Costa-Rodríguez <sup>1</sup>, Alicia Caro-Vadillo <sup>1,2</sup>, Elena Carretón <sup>1,\*</sup> and José Alberto Montoya-Alonso <sup>1</sup>

- <sup>1</sup> Internal Medicine, Faculty of Veterinary Medicine, Research Institute of Biomedical and Health Sciences (IUIBS), University of Las Palmas de Gran Canaria, 35001 Las Palmas de Gran Canaria, Spain; jorge.matos@ulpgc.es (J.I.M.); sarnieves.garcia@ulpgc.es (S.N.G.-R.); alberto.montoya@ulpgc.es (J.A.M.-A.)  
<sup>2</sup> Hospital Clínico Veterinario, Faculty of Veterinary Medicine, Universidad Complutense de Madrid (UCM), 28040 Madrid, Spain  
\* Correspondence: elena.carreton@ulpgc.es

**Simple Summary:** The development of new echocardiographic techniques, such as two-dimensional speckle tracking echocardiography and assessment of longitudinal myocardial deformation, may be new alternative tools to analyse the presence and severity of pulmonary hypertension in heartworm disease. A total of 93 dogs were used, of which 71% were diagnosed with heartworm infection and 41% were found to have PH. The measurements evaluated were obtained using Right Ventricular Automated Function Imaging (RV AFI<sup>®</sup>) software. The results showed significant differences between animals with and without pulmonary hypertension. Cut-off values with high sensitivity and specificity were also obtained for the detection of pulmonary hypertension in the animals analysed. Echocardiographic measurements for functional assessment of the right ventricle using myocardial longitudinal strain have demonstrated their usefulness in heartworm-infected dogs.

**Citation:** Matos, J.I.; García-Rodríguez, S.N.; Costa-Rodríguez, N.; Caro-Vadillo, A.; Carretón, E.; Montoya-Alonso, J.A. Right Ventricle Strain Assessed by 2-Dimensional Speckle Tracking Echocardiography (2D-STE) to Evaluate Pulmonary Hypertension in Dogs with *Dirofilaria immitis*. *Animals* **2023**, *14*, 26. <https://doi.org/10.3390/ani14010026>

Academic Editor: Clive J. C. Phillips

Received: 30 October 2023

Revised: 7 December 2023

Accepted: 19 December 2023

Published: 20 December 2023



**Copyright:** © 2023 by the authors. Licensee MDPI, Basel, Switzerland. This article is an open access article distributed under the terms and conditions of the Creative Commons Attribution (CC BY) license (<https://creativecommons.org/licenses/by/4.0/>).

**Abstract:** Echocardiographic assessment of the right ventricle is helpful for analysing the pathophysiology of heartworm disease and detecting pulmonary hypertension (PH) in dogs. In veterinary cardiology, the study of myocardial deformation using two-dimensional speckle tracking (2D-STE) echocardiography has become increasingly acknowledged as useful for quantifying right ventricular function. The aim of this study was to evaluate the usefulness of myocardial deformation strain of the right ventricular free wall (FWS), global deformation strain of the right ventricle, including the interventricular septum (GS), and tissue motion annular displacement of the tricuspid valve (TMAD) in a cohort of dogs with heartworm (*Dirofilaria immitis*) disease and to determine cut-off values for detecting the presence of PH. Out of the 93 dogs tested, 71% were diagnosed with heartworm infection. PH was identified in 41% of the infected dogs following the American College of Veterinary Internal Medicine (ACVIM) guidelines, based on the peak tricuspid regurgitation velocity to calculate the tricuspid regurgitation pressure gradient (TRPG), while other routine measurements were used, including the right pulmonary artery distensibility index (RPADi). The 2D-STE mode measurements were determined using Right Ventricular Automated Function Imaging (RV AFI<sup>®</sup>) software. The statistical analysis showed significant differences in the studied parameters among dogs with and without PH. Additionally, sensitivity (sen) and specificity (sp) cut-off values were obtained (GS  $\geq -21.25\%$ , sen 96%, sp 86.4%; FWS  $\geq -21.95\%$ , sen 92.56%, sp 95.5%; TMAD  $\leq 0.85$  cm, sen 70.4%, sp 83.3%). These results demonstrated that GS, FWS, and TMAD could be used as supplementary and alternative variables to conventional echocardiographic measurements when detecting PH in dogs with heartworm disease.

**Keywords:** *Dirofilaria immitis*; heartworm; echocardiography; speckle tracking; strain; pulmonary hypertension

## 1. Background

Canine heartworm disease (*Dirofilaria immitis*) has a major impact on the cardiovascular system of infected animals, primarily causing pulmonary endarteritis in all and chronic and irreversible precapillary pulmonary hypertension (PH) in some dogs [1,2]. The increase in pulmonary vascular resistance results in a pressure overload in the right ventricle, which can lead to systolic or diastolic dysfunction and right congestive heart failure (R-CHF) [2].

The contractile functionality of the right ventricle is difficult to assess due to its unique anatomical and functional characteristics [3]. Several studies have confirmed that the right ventricle contracts centripetally, with each myocardial segment moving towards the centre. In addition, the base and apex rotate in opposite directions while the ventricle shortens along the longitudinal axis [4,5]. Echocardiographic two-dimensional speckle tracking (2D-STE) allows the analysis of the percentage change in length or thickness of a myocardial segment during the cardiac cycle, which is called myocardial deformation or strain [6]. The free wall of the right ventricle has predominantly longitudinal fibres and, to a lesser extent, circumferential fibres, whereas the interventricular septum has crossed fibres coming from the left ventricular segments and shows a different deformation behaviour. Therefore, analysis of the right ventricular free wall has been considered more specific to the intrinsic function of the right ventricle [7]. However, evaluation of the global functionality of the entire right ventricular myocardium, including the interventricular septum, is commonly used in cardiology [6–8].

Longitudinal strain, as measured by 2D-STE, provides an opportunity to quantify both the magnitude and timing of regional, systolic, and diastolic function in specific segments of the myocardium [8]. Many echocardiographic studies have assessed myocardial deformation of the right ventricular free wall (FWS) and global deformation of the right ventricle, including the interventricular septum (GS), in humans [3–5]. In veterinary studies, FWS and GS have been considered normal in healthy dogs when less than  $-20.8\%$  [9–12] and  $-18.35\%$  [11,12], respectively. In general, more negative strain values express better systolic function.

Many publications have confirmed the value and clinical utility of right ventricular strain in the study of PH, either independently or in addition to conventional clinical and echocardiographic parameters. In human medicine, a significant correlation has been found between GS and FWS and increased mortality in patients with PH, demonstrating prognostic value [3–5]. Recently, in veterinary practice, several studies have reported FWS and GS values in dogs with precapillary and postcapillary PH caused by different diseases [13–16].

Recently, the use of tissue motion annular displacement of the tricuspid valve (TMAD) has been reported as a measure to study systolic function obtained by echocardiographic study in 2D-STE mode in pets [17]. This parameter evaluates the displacement of the valve annulus towards the apex of the heart, and several studies have shown an adequate correlation of this echocardiographic determination with respect to ventricular function with the tricuspid valve in healthy dogs [18–20]. In addition, significantly lower TMAD values have been reported in humans with PH compared to healthy individuals [3].

Due to the high prevalence of PH in dogs with heartworm disease and the difficulty of detecting it echocardiographically in some dogs, it would be prudent to investigate if right ventricular longitudinal strain and tricuspid annular displacement are measurements that might be useful for helping to detect PH in these animals. Therefore, the aim of this study was to evaluate the usefulness of GS, FWS, and TMAD measurements in *D. immitis*-infected dogs and to determine cut-off values for detecting the presence of PH.

## 2. Materials and Methods

### 2.1. Animals

A convenience sample of 93 privately owned dogs was prospectively analysed. The tests were performed at the Veterinary Teaching Hospital of the University of Las Palmas de Gran Canaria (Canary Islands, Spain) between September 2022 and April 2023 during the routine examination of canine patients prior to treatment for heartworm disease or as regular controls in healthy animals. All dogs lived in a hyperendemic area for *D. immitis* [21]. A complete

record was kept of each animal, including identification (age, sex, breed, and weight), clinical history, and demographic data. In addition, all were carefully examined for the presence of R-CHF (i.e., one or more of these signs: ascites, pleural effusion, jugular pulse, and/or vena cava distension). A commercial immunochromatography test kit (Urano test *Dirofilaria*®, Urano Vet SL, Barcelona, Spain) was used to determine the presence or absence of *D. immitis* antigen (94.4% sensitivity, 100% specificity). Control dogs were considered free of the disease on the basis of their clinical history (healthy animals, good owner compliance with chemoprophylaxis, dogs are on heartworm prevention year-round), clinical examination, absence of heartworm antigen, no visualisation of worms by echocardiography, and no radiographic evidence of heartworm disease.

Any animal receiving cardiovascular medication was excluded from the study. Similarly, dogs with clinical signs of heart disease (i.e., valvular heart disease, cardiomyopathy, and congenital defects) were excluded. The presence of other respiratory diseases that could cause precapillary PH was also excluded by radiological examination [1].

### 2.2. Conventional Echocardiography

Echocardiographic examinations were performed using an ultrasound machine with spectral and colour Doppler and multifrequency phased array transducers (2.5–12 MHz, Vivid Iq®, General Electric, Boston, MA, USA). Examinations were performed with the animals conscious and without the use of sedation. Dogs were placed in right and left lateral recumbency, with the transducer placed in the third-fifth intercostal space, according to previously described techniques [22]. Electrocardiographic monitoring was performed in all cases, allowing assessment of heart rate by measurement of the R–R interval. An average of 3 consecutive cardiac cycles in sinus rhythm was used for each measurement. All echocardiographic examinations were performed by the same researcher.

The presence or absence of PH was determined according to the American College of Veterinary Internal Medicine (ACVIM) guidelines [1]. The peak tricuspid regurgitation velocity to calculate the tricuspid regurgitation pressure gradient (TRPG) was the main measurement, while other routine measurements were used as previously described [1,23–25], such as the right pulmonary artery distensibility index (RPADi), the ratio of the pulmonary trunk to the ascending aorta in the right parasternal short-axis view (PT:Ao), the systolic displacement of the tricuspid annular muscle using a one-dimensional mode (TAPSE), and the maximum myocardial velocity ( $S'$ ) measured in the lateral portion of the tricuspid annulus by tissue Doppler imaging [26–28]. The RPADi results were used to evaluate the results, based on previous studies in dogs with heartworm disease and PH [23,24], which demonstrated strong correlation with invasive “gold standard” systolic pulmonary artery pressures.

Relative parasite burden was assessed based on the score published by Venco et al., 2014 [29], which ranges from 1 to 4: 1, no worms visualised; 2, few compatible images in the distal part of the right pulmonary artery; 3, compatible images in the right pulmonary artery extending to the main pulmonary artery; and 4, images of worms occupying the entire right pulmonary artery and the main pulmonary artery to the level of the pulmonary valve.

### 2.3. 2D-STE Echocardiography

Two-dimensional strain measurements were obtained using the same ultrasound equipment, from a left apical 4-chamber view optimised for adequate visualisation of the right chambers of the heart [22]. All studies achieved optimal frame rates > 40 frames per second. Images from all examinations were analysed using Right Ventricle Automated Function Imaging (RV AFI®) software (General Electric, Boston, MA, USA).

RV AFI® software used spot-tracking technology to quantify specific right ventricular myocardial motion, with some custom adaptations to better capture right ventricular free wall motion. The region of interest was defined by the operator to include the entire right ventricular myocardium and the interventricular septum. The operator placed two points on the parietal and septal annuli of the tricuspid valve and one point on the right ventricular apex, starting with end-systole and followed by end-diastole. The system then

automatically provided an estimate of the area of interest, which could be regionally edited if desired. RV AFI® software tracked the acquired image over time, extracting information on regional and longitudinal strain. The software provided segmental longitudinal strain values for the following 6 segments: apical FW, mid FW, baseline FW, apical IVS, mid IVS, baseline IVS. Finally, the results were provided, showing the quality of the follow-up and the values in percentage of GS, percentage of FWS, and centimetres of TMAD (Figure 1).

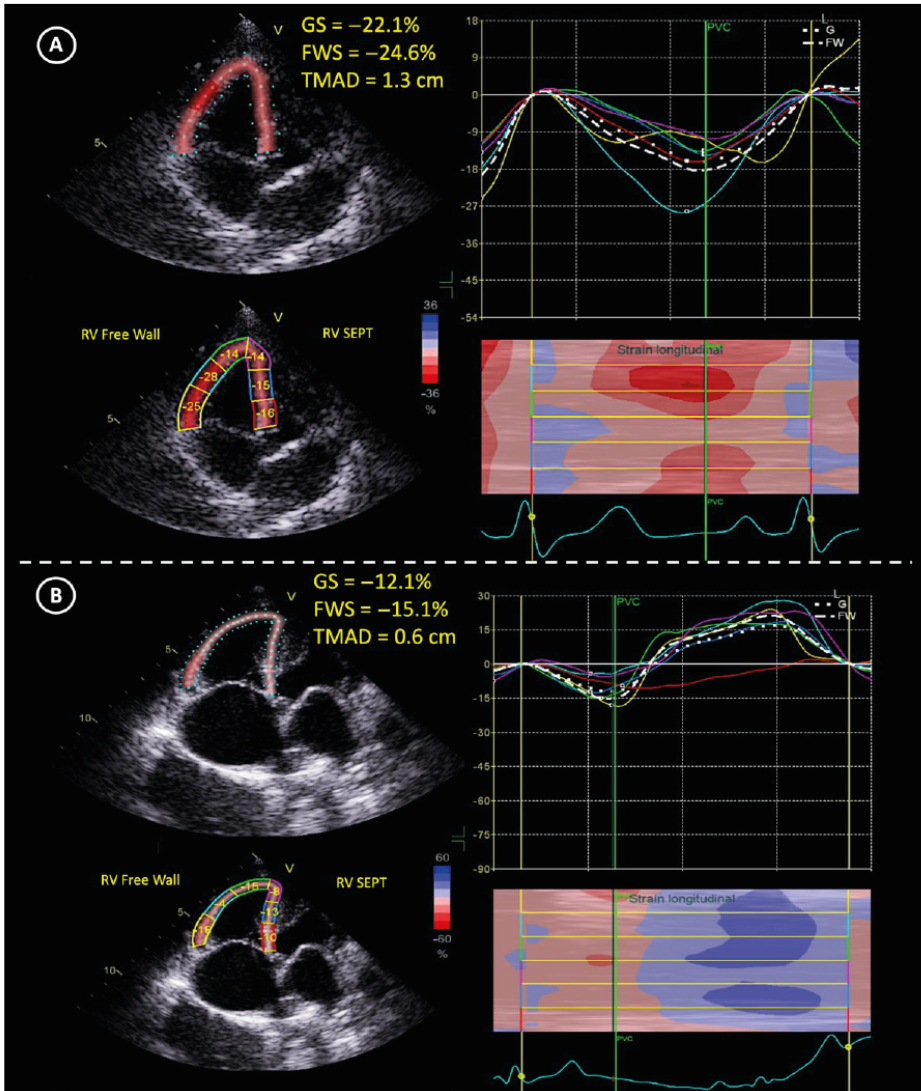


**Figure 1.** Representation of the analysis of the right strain through the RV AFI® software to obtain the values of GS (%), FWS (%), and TMAD (cm) in (A) a patient with heartworm disease without PH, and (B) in a patient with heartworm disease that presented PH (RPADi < 30%). Left parasternal position, left apical four-chamber view with >40 frames per second. The graphs show the movement and deformation of each of the myocardial segments in specific colours during the cardiac cycle (apical FW, mean FW, reference FW, apical IVS, mean IVS, baseline IVS). The mean FWS value is

represented by a segmented white line, and the mean GS value is represented by a white dotted line. Legend: PVC: peak ventricular contraction; RV: right ventricle.

#### 2.4. Statistical Analysis

Statistical analysis of echocardiographic values was performed using commercially available software (BM SPSS Statistics 25.0, New York, NY, USA). Frequencies and percentages were calculated for categorical variables. Parameter differences between groups were assessed using Pearson's non-parametric Chi-squared test and, only in the case of  $2 \times 2$  tables, Fisher's exact test. For continuous variables, parameter differences between groups were evaluated using the Mann-Whitney/Kruskal-Wallis test (non-parametric) or t-student/ANOVA (parametric), depending on the normality of the variables to be evaluated, as determined by the Shapiro-Wilk test. Linear regressions were used to determine the correlation and explanatory power of the methods with the gold standard (RPADi), and the non-standardised beta coefficients, their 95% CIs, R<sup>2</sup>, and equations were presented. The receiver operating characteristic (ROC) curve was used to determine the ability of the different echocardiographic measurements to classify the presence/absence of PH. All multiple comparisons were adjusted by Bonferroni correction. All contrasts were accompanied by an effect size estimate to complete the interpretation of the results. For categorical variables, this was Cramer's V, and for continuous variables, Cohen's d. The criteria for classifying the size of the effect were as follows: Cohen's d: small ( $d = 0.2-0.4$ ), medium ( $d = 0.5-0.8$ ), and large ( $d = \text{greater than } 0.8$ ). Cramer's V: 0.00-0.09 as negligible, 0.10-0.29 as low, 0.30-0.49 as medium, and from 0.50 as high. In the case of effect size estimator values obtained from inversely correlated variables, the results were expressed as negative (-). In all cases, the significance level used was 5% ( $\alpha = 0.05$ ).

#### 2.5. Ethical Statement

All owners were informed and gave consent for their dogs to be included in the study. Ethical approval was not required for this study as it was a purely observational study with voluntary enrolment and did not involve any additional invasive clinical diagnostic procedures. The evaluation of the study included ethical considerations and legal aspects of animal protection and welfare and was carried out in accordance with current Spanish and European legislation on animal protection.

### 3. Results

Based on the immunochromatographic test kit, 71% ( $n = 66$ ) of the dogs were infected with *D. immitis*, and 29% ( $n = 27$ ) were considered healthy based on the absence of *D. immitis* antigens, clinical signs, history, physical examination, and echocardiographic and radiographic evaluations.

Following the ACVIM consensus criteria [1], PH was present in 41% ( $n = 27$ ) of heartworm-infected dogs, whereas PH was absent in all healthy dogs. According to heartworm status and the presence of PH, three groups were created: group A (healthy dogs,  $n = 27$ ), group B (heartworm-infected dogs without PH,  $n = 39$ ), and group C (dogs with heartworm and PH,  $n = 27$ ). All dogs with PH showed an RPADi < 30%. The clinical characteristics, conventional echocardiographic parameters, and 2D-STE echocardiographic measurements of the total animal population and in each of the different groups are shown in Table 1.

**Table 1.** Clinical and echocardiographic parameters of the dogs studied ( $n = 93$ ). Data represent median and standard deviation, unless otherwise indicated. Group A: healthy dogs; group B: dogs with heartworms and absence of PH; group C: dogs with heartworms and with PH (RPADi < 30%). Legend: CHF: congestive heart failure; HR: heart rate; RPADi: right pulmonary artery distensibility index; TRPG: tricuspid regurgitation pressure gradient; PT: pulmonary trunk; Ao: aorta; TAPSE: systolic displacement of the tricuspid annular muscle; S: maximum myocardial velocity; GS: global strain; FWS: free-wall strain; TMAD: tissue motion annular displacement of the tricuspid valve. Results for female, mongrel, and right-sided CHF symptoms are expressed as  $n$  (%). Parasite burden scores and TRPG are expressed as median (range). Significant differences were found when  $p < 0.01$ .

	Group A ( $n=27$ )	Group B ( $n=39$ )	Group C ( $n=27$ )	$p$ -value ( <sup>4</sup> Cramer's V; <sup>5,6</sup> Cohen's d)
Age (years)	8.0 ± 3.9	6.8 ± 2.8	8.3 ± 3.2	0.164 <sup>1</sup>
Female: number (%)	15 (55.6%)	24 (61.5%)	9 (33.3%)	0.07 <sup>2</sup>
Body weight (kg)	15.6 ± 10.2	19.5 ± 11.1	19.6 ± 9.7	0.51 <sup>1</sup>
Mongrel: number (%)	9 (33.3%)	20 (51.3%)	13 (48.1%)	0.02 (0.60) <sup>4</sup>
Right-sided CHF (%)	0 (0%)	0 (0.0%)	12 (44.4%)	0.00 (0.60) <sup>4</sup>
Parasite burden score (1–4)	1	2 (1–3)	3 (2–4)	0.00 (0.72) <sup>4</sup>
HR (Beats per minute)	134.4 ± 25.1	131.4 ± 28.1	129.2 ± 21.8	0.871 <sup>3</sup>
RPADi (%)	42.2 ± 4.7	41.4 ± 8.0	18.8 ± 7.6	0.00 (1.79) <sup>5</sup>
TRPG (mmHg)	4.49 (2.43–7.07)	3.5 (2.10–5.23)	49.44 (38.21–152.15)	0.00 (–1.32) <sup>5</sup>
PT:Ao	1.0 ± 0.1	0.9 ± 0.1	1.3 ± 0.2	0.00 (–1.47) <sup>5</sup>
TAPSE (cm)	1.7 ± 0.3	1.6 ± 0.3	1.1 ± 0.3	0.00 (1.62) <sup>5</sup>
S (cm/s)	14.7 ± 2.5	15.7 ± 3.4	9.3 ± 3.8	0.00 (1.08) <sup>6</sup>
TMAD (cm)	1.1 ± 0.2	1.0 ± 0.2	0.7 ± 0.3	0.00 (1.27) <sup>6</sup>
GS (%)	–25.6 ± 4.9	–25.2 ± 4.0	–15.8 ± 4.4	0.00 (1.58) <sup>6</sup>
FWS (%)	–26.7 ± 4.7	–26.2 ± 3.5	–16.9 ± 5.0	0.00 (1.6) <sup>6</sup>

<sup>1</sup> Mann–Whitney/Kruskal–Wallis. <sup>2</sup> Chi2 test. <sup>3</sup> ANOVA. <sup>4</sup> Chi2 test =  $p < 0.01$  (Cramer's V in parentheses). <sup>5</sup> Mann–Whitney/Kruskal–Wallis =  $p < 0.01$  (Cohen's d value in parentheses). <sup>6</sup> ANOVA =  $p < 0.01$  (Cohen's d value in parentheses).

A wide age range (2–15 years) was present in the dogs studied, both sexes were present in similar proportions (51.6% females and 48.4% males), and weights ranged from 3.2 to 45.9 kg. Twenty-four different breeds were included in the study, with mixed breeds being the most common (45.2%). There were no significant differences in age, sex, breed, or weight between the groups.

The observed parasite burden score ranged from 1 to 4 in dogs with heartworm. A higher burden was observed in dogs from group C compared to group B ( $p$  Chi2 value < 0.01; Cramer's V = 0.841). The relative parasite burden in healthy dogs was 1 (no visible worms). The signs of R-CHF were directly related to the presence of heartworm and PH ( $p$  Chi2 value < 0.01; Cramer's V = 0.602), as signs of R-CHF were present only in group C (44.4%).

All conventional echocardiographic measurements showed significant differences in group C when compared to groups A and B ( $p$ -value ANOVA < 0.01; Cohen's d > 1.00). The results showed higher values for TRPG and PT:Ao and lower values for TAPSE and S' in group C. No significant differences were observed between the animals in groups A and B in any of the parameters evaluated.

The ANOVA tests of the parameters obtained by 2D-STE indicate that there were significant differences in the values of GS, FWS, and TMAD between the groups studied (Figure 2). Bonferroni’s post hoc tests for multiple comparisons showed that the values obtained in dogs from group C were significantly lower than those obtained in groups A and B ( $p$ -value ANOVA < 0.01; Cohen’s  $d > 1.00$ ), whereas groups A and B did not differ from each other.

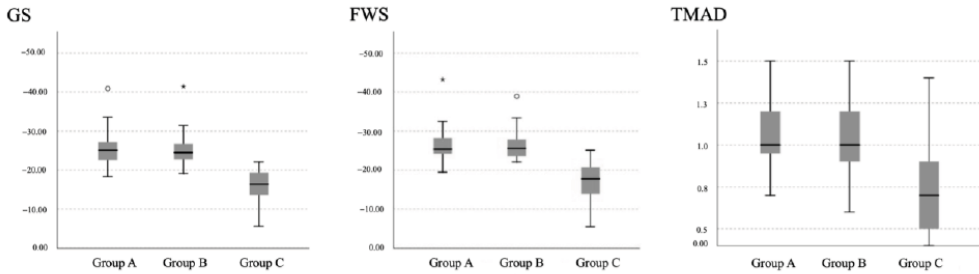


**Figure 2.** Echocardiographic 2D-STE measurements of GS (%), FWS (%), and TMAD (cm) obtained in healthy dogs (group A), dogs with heartworm without PH (group B), and dogs with heartworm with PH (group C). Box plots show median (solid horizontal lines within boxes), 25th and 75th percentiles (boxes), and minimum and maximum values (whiskers). Statistically significant differences were observed in group C when compared to groups A and B in all cases. Legend: white circle=outlier; asterisk=extreme outlier.

A total of three linear regressions were performed, one for each 2D-STE parameter, to determine which variables correlated best with the RPADi. Pearson’s correlations showed values of 0.733, 0.698, and 0.555 for the variables of GS, FWS, and TMAD, respectively (Figure 3). The measurements that correlated best with the RPADi were GS ( $R^2 = 0.537$ ), followed by FWS ( $R^2 = 0.488$ ) and TMAD ( $R^2 = 0.300$ ). All models were calculated in 93 cases.

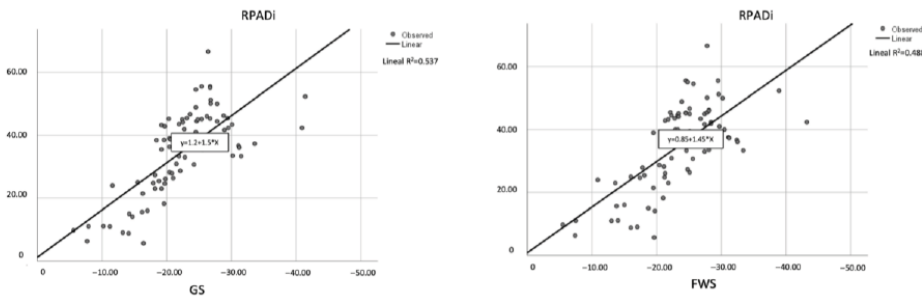


**Figure 3.** Scatter plots showing significant (both  $p < 0.01$ ) coefficient of determination ( $R^2$ ) between RPADi and 2D-STE measurements (GS and FWS). The solid line within each scatterplot represents the line of best fit.

The results of the ROC curves for each of the 2D-STE measurements to determine the presence or absence of PH and the cut-off points of the parameters that maximised sensitivity and specificity (using the Youden index) are summarised in Table 2. GS and FWS showed an excellent area under the curve (AUC) (>0.9), while TMAD had an optimal AUC

of 0.830. To detect PH, the cut-off values were  $\geq -21.25\%$  for GS (sensitivity 96.3%; specificity 86.4%),  $\geq -21.95\%$  for FWS (sensitivity 92.6%; specificity 95.5%), and  $\leq 0.85$  cm for TMAD (sensitivity 70.4%; specificity 83.3%).

**Table 2.** Results of simple regression analyses for the prediction of RPADi ( $R^2$ : coefficient of determination). Therefore, sensitivity (Se), specificity (Sp), and Youden index of cut-off points of echocardiographic 2D-STE measurements for predicting PH for detecting RPADi < 30%. AUC: area under the receiver operating characteristic curve; CI 95%: confidence interval 95%.

	$R^2$	AUC	IC 95%	Cut-off	Se	Sp	Youden Index (Se + Es - 1)
FWS (%)	0.482	0.962	(0.917, 1.000)	$\leq 21.95$	0.926	0.955	0.880
GS (%)	0.532	0.970	(0.943, 0.998)	$\geq -21.25$	0.963	0.864	0.827
TMAD (cm)	0.300	0.830	(0.725, 0.935)	$\leq 0.850$	0.704	0.833	0.537

#### 4. Discussion

The presence of heartworms in the pulmonary arteries causes endarteritis and embolization that leads to a loss of vascular elasticity and an increase in vascular resistance, which, when severe, leads to pre-capillary PH [30]. This produces an increase in right ventricular afterload, which leads to a decrease in ventricular contraction (strain). PH is common in dogs with heartworm disease (although it is often not present), occurring in 30–67% of infected dogs (41% in the current study) [2,23,24,28]. When severe, PH can lead to R-CHF [2,28].

Previous studies have found no evidence that sex, breed, weight, or age are risk factors for *D. immitis* infection [27–30]. In the present study, dogs with PH had a higher relative worm burden. While some previous studies have agreed with this assessment, others have found disease chronicity, exercise, and host immune response to be more important factors [2,23,24,28–30].

The employment of RPADi has been ratified by numerous studies as a useful method to help in the detection of PH in dogs infected with *D. immitis*. In this study, PH was identified in 41% of dogs with heartworm, and in all cases, RPADi was <30% [23,24,28,30]. Additionally, previous studies have demonstrated statistically significant differences in dogs with PH compared to those without, regardless of whether they were healthy or infected with *D. immitis* [1,2,8–12].

Speckle tracking is a technique used in echocardiography to assess myocardial strain, which refers to the deformation (contraction and relaxation) of the heart muscle during the cardiac cycle. Speckle tracking involves tracking the movement of small, natural acoustic markers (speckles) within the myocardial tissue. These speckles appear as small, bright dots in the ultrasound images. Specialised software is used to identify and track these speckles frame by frame throughout the cardiac cycle. As the heart contracts and relaxes, the speckle-tracking software analyses the displacement of the speckles in the myocardial tissue. The software calculates strain, which is a measure of the percentage change in length of the myocardial segments during contraction or relaxation. Much like fractional shortening, systolic strain is a measure of the percent change in the length of myocardial segments in systole. As opposed to fractional shortening, which only measures global shortening, strain can measure both global and regional functions [11]. While several studies have used strain to examine left ventricular function in dogs with left heart diseases [7,14,15,26,31], measuring strain in the right ventricle is particularly advantageous because of the unusual shape of the right ventricle.

The complex morphology of the right side of the heart makes the analysis of right ventricular function difficult. Blood flows are complicated to quantify in a simple form,



and the use of tissue Doppler provides limited information on systolic and diastolic function. Compared to conventional echocardiographic techniques, 2D STE evaluates longitudinal and circumferential right ventricular myocardial deformation (influenced by contractility, preload, and afterload) very efficiently and accurately [26,27]. The values obtained in animals without PH were similar to those previously reported in healthy dogs, which were values  $<-24.85\%$  for GS and  $<-26.12\%$  for FWS, in addition to values  $>0.95$  cm for TMAD [11,13–16,19,22].

Significant statistical differences were observed in the values of GS, FWS, and TMAD between dogs with PH and normotensive dogs. This suggests that these variables may be useful in helping to diagnose PH in dogs with heartworm disease. The established values and cut-off points for GS and FWS in this study align with prior research on dogs with precapillary PH due to various diseases [9,13]. However, the GS and FWS measurements were slightly different when compared to previous studies. This may be attributed to methodological differences, including sample size, the type of 2D-STE software used, and the specific diseases assessed (mainly myxomatous mitral valve disease) [7–14]. Interestingly, previous studies also found lower FWS values when compared to GS [12–15]. This may be due to the right ventricular free wall being the key component of right ventricular functionality. In contrast, circumferential strain measurements showed higher values in patients with various causes of PH, as reported by Caivano et al. (2020) [16]. The transverse strain of the right ventricle in our study did not aid in identifying the presence or absence of PH, suggesting that longitudinal measurements may be more sensitive for this diagnosis. No prior studies have recorded TMAD in dogs with PH. Our results suggest a cut-off value of  $\leq 0.85$  cm for detecting the presence of PH in dogs with heartworm disease.

In the present study, the GS method displayed the best correlation with the RPADi; however, FWS was the parameter with the highest sensitivity and specificity for detecting PH in the dogs analysed. This study's findings align with previous publications that demonstrated the higher specificity and sensitivity of FWS compared to GS for the detection of PH in both dogs and humans [3–5,9,13]. On the other hand, despite exhibiting a reasonable AUC, the TMAD measurement was the least helpful parameter in diagnosing PH in heartworm-infected dogs.

The high cost of specialised software is a key drawback to the use of 2D-STE echocardiography in veterinary cardiology. Furthermore, identification of the appropriate echocardiographic view, which should be optimised to facilitate the visualisation of the right chambers whilst maintaining high frames per second and good resolution, is crucial. However, 2D-STE studies are less sensitive to angle limitations compared to other traditional measurements, leading to more reliable outcomes and decreased intra- and inter-operator deviation [7,10,14]. Furthermore, it is acknowledged as an ultrasound imaging mode characterised by good reproducibility, although in certain studies, body weight, heart rate, and age have reportedly influenced measurements, which has not been documented in the present research [9,11,12,18]. The unique diagnostic value of being able to identify abnormalities in each myocardial segment sets this echocardiographic technique apart from others. However, caution must be exercised in interpreting the results, as they depend on the analysis software used.

## 5. Conclusions

This study demonstrated that measurements of right ventricular longitudinal strain may be useful to assist in the detection of PH in dogs with *D. immitis*. These measurements may be useful as additional or alternative measurements for the detection of PH alongside traditional echocardiographic measurements. This study has provided cut-off points for detecting PH in dogs with heartworm disease with optimal sensitivity and specificity. However, further research is required to validate these results.

**Author Contributions:** J.I.M., J.A.M.-A., and E.C. designed the study. J.I.M., A.C.-V., and E.C. wrote the manuscript. J.I.M., S.N.G.-R., and N.C.-R. performed the fieldwork, collected the data, and

performed the experiments. All authors have read and agreed to the published version of the manuscript.

**Funding:** The presented study was supported by funds from the Servicio de Medicina Veterinaria FULP/ULPGC (SD-240/030/0026). N.C.-R. was supported by the “Grants for the predoctoral training program for researchers” programme of the Government of the Canary Islands (TESIS2021010010), and J.I.M. and S.N.R.-G. were supported by the “Grants for the financing of predoctoral contracts” programme of the Universidad de Las Palmas de Gran Canaria (PIFULPGC-2017-CCSALUD-3 and PIFULPGC-2020-2-CCSALUD-2, respectively).

**Institutional Review Board Statement:** Ethical review and approval were not required for the animal study because the present study was conducted on client-owned animals/clinical cases and no experimental animals were used. All dog owners were informed about the present study and consented to participate. The study was carried out in accordance with the current Spanish and European legislation on animal protection (Spanish Royal Decree 53/2013 and 2010/63/UE Directive).

**Informed Consent Statement:** Not applicable.

**Data Availability Statement:** The raw data supporting the conclusions of this article will be made available by the authors, without undue reservation.

**Acknowledgements:** The authors would like to thank Uranovet for kindly providing the Urano test *Dirofilaria*<sup>®</sup>. Also, they would like to thank to the Hospital Clínico Veterinario of the Universidad de Las Palmas de Gran Canaria (ULPGC) for their support.

**Conflicts of Interest:** The authors declare no conflicts of interest.

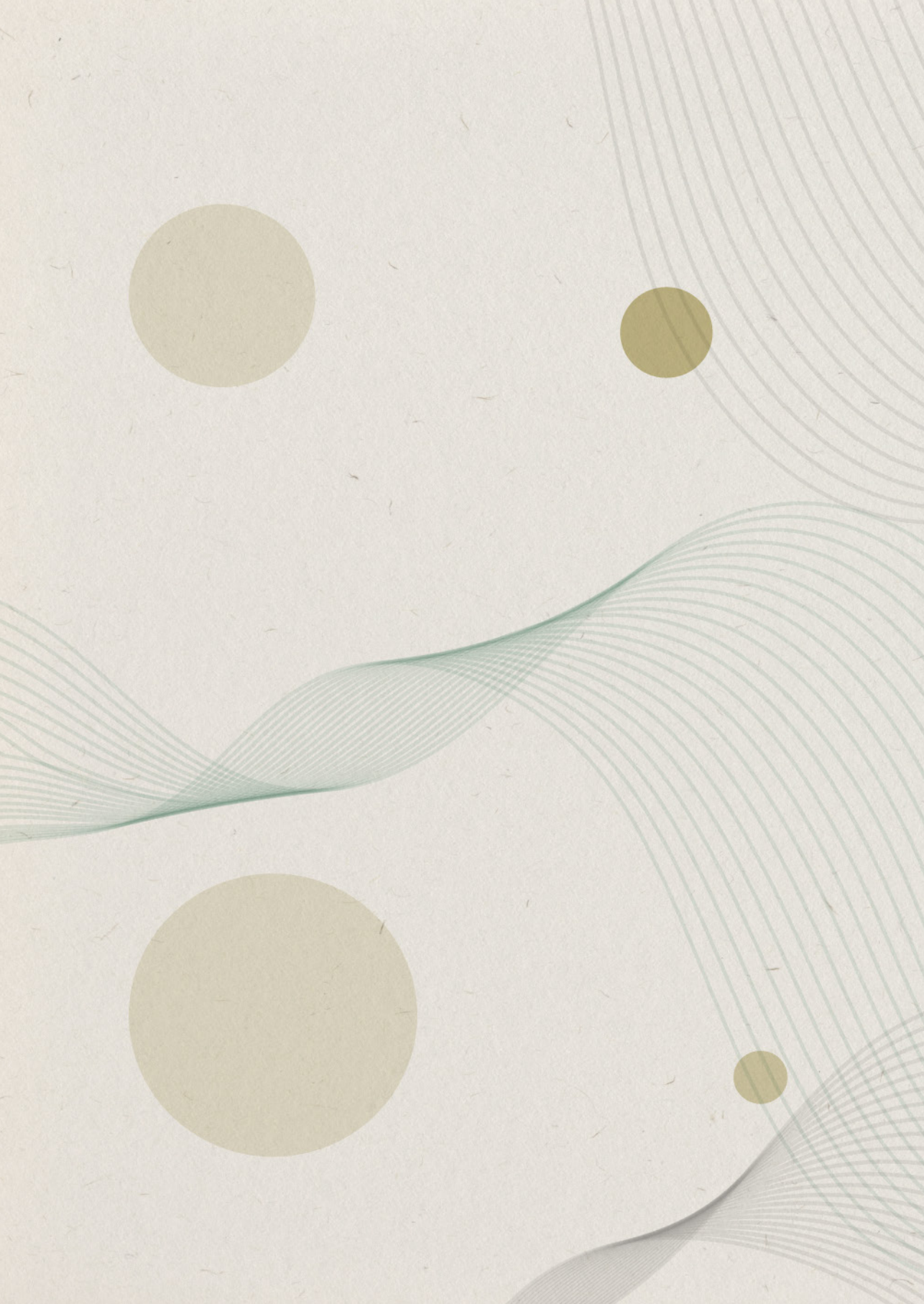
## References

- Reinero, C.; Visser, L.C.; Kellihan, H.B.; Masseau, I.; Rozanski, E.; Clercx, C.; Williams, K.; Abbott, J.; Borgarelli, M.; Scansen, B.A. ACVIM consensus statement guidelines for the diagnosis, classification, treatment, and monitoring of pulmonary hypertension in dogs. *J. Vet. Intern. Med.* **2020**, *34*, 549–573.
- Romano, A.E.; Saunders, A.B.; Gordon, S.G.; Wesselowski, S. Intracardiac heartworms in dogs: Clinical and echocardiographic characteristics in 72 cases (2010–2019). *J. Vet. Intern. Med.* **2021**, *35*, 88–97.
- Theres, L.; Hübscher, A.; Stangl, K.; Dreger, H.; Knebel, F.; Brand, A.; Hewing, B. Associations of 2D speckle tracking echocardiography-based right heart deformation parameters and invasively assessed hemodynamic measurements in patients with pulmonary hypertension. *Cardiovasc. Ultrasound* **2020**, *18*, 13.
- Liu, B.-Y.; Wu, W.-C.; Zeng, Q.-X.; Liu, Z.-H.; Niu, L.-L.; Tian, Y.; Cheng, X.-L.; Luo, Q.; Zhao, Z.-H.; Huang, L.; et al. Two-dimensional speckle tracking echocardiography assessed right ventricular function and exercise capacity in pre-capillary pulmonary hypertension. *Int. J. Cardiovasc. Imaging* **2019**, *10*, 1055–1064.
- Vitarelli, A.; Mangieri, E.; Terzano, C.; Gaudio, C.; Salsano, F.; Rosato, E.; Capotosto, L.; D’Orazio, S.; Azzano, A.; Truscetti, G.; et al. Three-Dimensional Echocardiography and 2D-3D Speckle-Tracking Imaging in Chronic Pulmonary Hypertension: Diagnostic Accuracy in Detecting Hemodynamic Signs of Right Ventricular (RV) Failure. *J. Am. Heart Assoc.* **2015**, *4*, e001584.
- Feldhütter, E.K.; Domenech, O.; Vezzosi, T.; Tognetti, R.; Sauter, N.; Bauer, A.; Eberhard, J.; Friederich, J.; Wess, G. Echocardiographic reference intervals for right ventricular indices, including 3-dimensional volume and 2-dimensional strain measurements in healthy dogs. *J. Vet. Intern. Med.* **2022**, *36*, 8–19.
- Chapel, E.H.; Scansen, B.A.; Schober, K.E.; Bonagura, J.D. Echocardiographic Estimates of Right Ventricular Systolic Function in Dogs with Myxomatous Mitral Valve Disease. *J. Vet. Intern. Med.* **2017**, *12*, 14–22.
- Visser, L.C.; Scansen, B.A.; Schober, K.E.; Bonagura, J.D. Echocardiographic assessment of right ventricular systolic function in conscious healthy dogs: Repeatability and reference intervals. *J. Vet. Cardiol.* **2015**, *17*, 83–96.
- Feldhütter, E.K.; Domenech, O.; Vezzosi, T.; Tognetti, R.; Eberhard, J.; Friederich, J.; Wess, G. Right ventricular size and function evaluated by various echocardiographic indices in dogs with pulmonary hypertension. *J. Vet. Intern. Med.* **2022**, *36*, 1882–1891.
- Visser, L.C.; Scansen, B.A.; Brown, N.V.; Schober, K.E.; Bonagura, J.D. Echocardiographic assessment of right ventricular systolic function in conscious healthy dogs following a single dose of pimobendan versus atenolol. *J. Vet. Cardiol.* **2015**, *17*, 161–172.
- Chetboul, V.; Serres, F.; Gouni, V.; Tissier, R.; Pouchelon, J.L. Radial strain and strain rate by two-dimensional speckle tracking echocardiography and the tissue velocity based technique in the dog. *J. Vet. Cardiol.* **2007**, *9*, 69–81.
- Morita, T.; Nakamura, K.; Osuga, T.; Yokoyama, N.; Khoirun, N.; Morishita, K.; Sasaki, N. The repeatability and characteristics of right ventricular longitudinal strain imaging by speckle-tracking echocardiography in healthy dogs. *J. Vet. Cardiol.* **2017**, *19*, 351–362.
- Morita, T.; Nakamura, K.; Osuga, T.; Morishita, K.; Sasaki, N.; Ohta, H.; Takiguchi, M. Right ventricular function and dyssynchrony measured by echocardiography in dogs with precapillary pulmonary hypertension. *J. Vet. Cardiol.* **2019**, *23*, 1–14.

14. Yuchi, Y.; Suzuki, R.; Yasumura, Y.; Saito, T.; Teshima, T.; Matsumoto, H.; Koyama, H. Prognostic value of pulmonary vascular resistance estimated by echocardiography in dogs with myxomatous mitral valve disease and pulmonary hypertension. *J. Vet. Intern. Med.* **2023**, *1*, 1–10.
15. Tidholm, A.; Ljungvall, I.; Hoglund, K.; Westling, A.B.; Haggstrom, J. Tissue Doppler and Strain Imaging in Dogs with Myxomatous Mitral Valve Disease in Different Stages of Congestive Heart Failure. *J. Vet. Intern. Med.* **2009**, *23*, 1197–1207.
16. Caivano, D.; Rishniw, M.; Birettoni, F.; Petrescu, V.S.; Porciello, F. Transverse Right Ventricle Strain and Strain Rate Assessed by 2-Dimensional Speckle Tracking Echocardiography in Dogs with Pulmonary Hypertension. *Vet. Sci.* **2020**, *7*, 19.
17. Tuleski, G.L.R.; Wolf, M.; Garcia-Ribeiro, M.J.; Dos Santos, J.P.; Sousa, M.G. Tissue motion annular displacement to assess the left ventricular systolic function in healthy cats. *Vet. Res. Commun.* **2022**, *46*, 823–836.
18. Visser, L.C.; Sintov, D.J.; Oldach, M.S. Evaluation of tricuspid annular plane systolic excursion measured by two dimensional echocardiography in healthy dogs: Repeatability, reference intervals, and comparison with M-mode assessment. *J. Vet. Cardiol.* **2018**, *20*, 165–174.
19. Silva, V.B.C.; Wolf, M.; Lucina, S.B.; Sarraff-Lopes, A.P.; Sousa, M.G. Assessment of right ventricular systolic function by tissue motion annular displacement in healthy dogs. *J. Vet. Cardiol.* **2020**, *32*, 40–48.
20. Wolf, M.; Lucina, S.B.; Bruler, B.S.; Tuleski, G.L.R.; Silva, V.B.C.; Sousa, M.G. Assessment of longitudinal systolic function using tissue motion annular displacement in healthy dogs. *J. Vet. Cardiol.* **2018**, *20*, 175–185.
21. Montoya-Alonso, J.A.; Morchón, R.; García, S.N.; Falcón-Cordón, Y.; Costa-Rodríguez, N.; Matos, J.I.; Escolar, I.R.; Carretón, E. Expansion of Canine Heartworm in Spain. *Animals* **2022**, *12*, 12–25.
22. Chetboul, V.; Damoiseaux, C.; Lefebvre, H.P.; Concordet, D.; Desquilbet, L.; Vassiliki, G.; Poissonnier, C.; Pouchelon, J.L.; Renaud, T. Quantitative assessment of systolic and diastolic right ventricular function by echocardiography and speckle-tracking imaging: A prospective study in 104 dogs. *Vet. Sci.* **2018**, *19*, 683–692.
23. Serrano-Parreño, B.; Carretón, E.; Caro-Vadillo, A.; Falcón-Cordón, Y.; Falcón-Cordón, S.; Montoya-Alonso, J.A. Evaluation of pulmonary hypertension and clinical status in dogs with heartworm by Right Pulmonary Artery Distensibility Index and other echocardiographic parameters. *Parasit. Vectors* **2017**, *10*, 106–112.
24. Venco, L.; Mihaylova, L.; Boon, J.A. Right Pulmonary Artery Distensibility Index (RPAD Index). A field study of an echocardiographic method to detect early development of pulmonary hypertension and its severity even in the absence of regurgitant jets for Doppler evaluation in heartworm-infected dogs. *Vet. Parasitol.* **2014**, *206*, 60–66.
25. Visser, L.C.; Im, M.K.; Johnson, L.R.; Stern, J.A. Diagnostic Value of Right Pulmonary Artery Distensibility Index in Dogs with Pulmonary Hypertension: Comparison with Doppler Echocardiographic Estimates of Pulmonary Arterial Pressure. *J. Vet. Intern. Med.* **2016**, *30*, 543–552.
26. Chetboul, V.; Gouni, V.; Sampedrano, C.C.; Tissier, R.; Serres, F.; Pouchelon, J.L. Assessment of Regional Systolic and Diastolic Myocardial Function Using Tissue Doppler and Strain Imaging in Dogs with Dilated Cardiomyopathy. *J. Vet. Intern. Med.* **2007**, *21*, 719–730.
27. Locatelli, C.; Spalla, I.; Zanaboni, A.M.; Brambilla, P.G.; Bussadori, C. Assessment of right ventricular function by feature-tracking echocardiography in conscious healthy dogs. *Res. J. Vet. Sci.* **2016**, *105*, 103–110.
28. Matos, J.I.; Caro-Vadillo, A.; Falcón-Cordón, Y.; García-Rodríguez, S.N.; Costa-Rodríguez, N.; Carretón, E.; Montoya-Alonso, J.A. Echocardiographic Assessment of the Pulmonary Vein to Pulmonary Artery Ratio in Canine Heartworm Disease. *Animals* **2023**, *13*, 703.
29. Venco, L.; Genchi, C.; Vigevani, C.P.; Kramer, L. Relative utility of echocardiography, radiography, serologic testing and microfilariae counts to predict adult worm burden in dogs naturally infected with heartworms. In *Recent Advances in Heartworm Disease. Symposium '01*; American Heartworm Society: Batavia, IL, USA, 2014; pp. 24–111.
30. Falcón-Cordón, Y.; Montoya-Alonso, J.A.; Caro-Vadillo, A.; Matos, J.I.; Carretón, E. Persistence of pulmonary endarteritis in canine heartworm infection 10 months after the eradication of adult parasites of *Dirofilaria immitis*. *Vet. Parasitol.* **2019**, *273*, 1–4.
31. Hamabe, L.; Mandour, A.S.; Shimada, K.; Uemura, A.; Yilmaz, Z.; Nagaoka, K.; Tanaka, R. Role of Two-Dimensional Speckle-Tracking Echocardiography in Early Detection of Left Ventricular Dysfunction in Dogs. *Animals* **2021**, *11*, 2361.

**Disclaimer/Publisher's Note:** The statements, opinions and data contained in all publications are solely those of the individual author(s) and contributor(s) and not of MDPI and/or the editor(s). MDPI and/or the editor(s) disclaim responsibility for any injury to people or property resulting from any ideas, methods, instructions or products referred to in the content.





The background features a textured, light beige surface with faint, wavy lines in shades of grey and green. Three solid olive-green circles are scattered across the page: one in the upper right, one in the lower left, and a smaller one in the lower right.

# 5. CONCLUSIONS



5.1. Echocardiographic measurement of the pulmonary vein to pulmonary artery ratio was able to discriminate between dogs without pulmonary hypertension (healthy or infected with *Dirofilaria immitis*) and dogs infected with cardiopulmonary dirofilariosis with pulmonary hypertension. Therefore, the pulmonary vein to pulmonary artery ratio may be a useful tool to echocardiographically evaluate vascular status in patients with heartworm disease. The pulmonary vein to pulmonary artery ratio of 0.845, in both the one-dimensional and two-dimensional modes, suggested an acceptable cut-off value to differentiate between dogs with pulmonary hypertension and dogs without pulmonary hypertension.

*5.1. La medición ecocardiográfica de la proporción vena pulmonar y arteria pulmonar fue capaz de discriminar entre perros sin hipertensión pulmonar (sanos o infectados con Dirofilaria immitis) y perros infectados con dirofilariosis cardiopulmonar con hipertensión pulmonar. Por lo tanto, la proporción vena pulmonar y arteria pulmonar podría ser una herramienta útil para evaluar ecocardiográficamente el estado vascular en pacientes con dirofilariosis cardiopulmonar. La relación de la proporción vena pulmonar a arteria pulmonar de 0,845, tanto en los modos monodimensionales como bidimensional, sugirió un valor de corte aceptable para diferenciar entre perros con hipertensión pulmonar y perros sin hipertensión pulmonar.*



5.2. The results showed that the tissue Doppler imaging measures of E', S, E':A', HRI-IVRT, HRI-IVCT, Global-TDI and R-TEI discriminated between normotensive and dogs with pulmonary hypertension and, therefore, can be a useful alternative tool to evaluate patients with cardiopulmonary dirofilariosis by using transthoracic echocardiography. Likewise, the A' measure was shown to be a poor indicator in estimating the presence of pulmonary hypertension in dogs with canine cardiopulmonary dirofilariosis. The HRI-IVCT, HRI-IVRT and R-TEI showed higher levels of efficiency in the detection of pulmonary hypertension in dogs parasitized by *Dirofilaria immitis*.

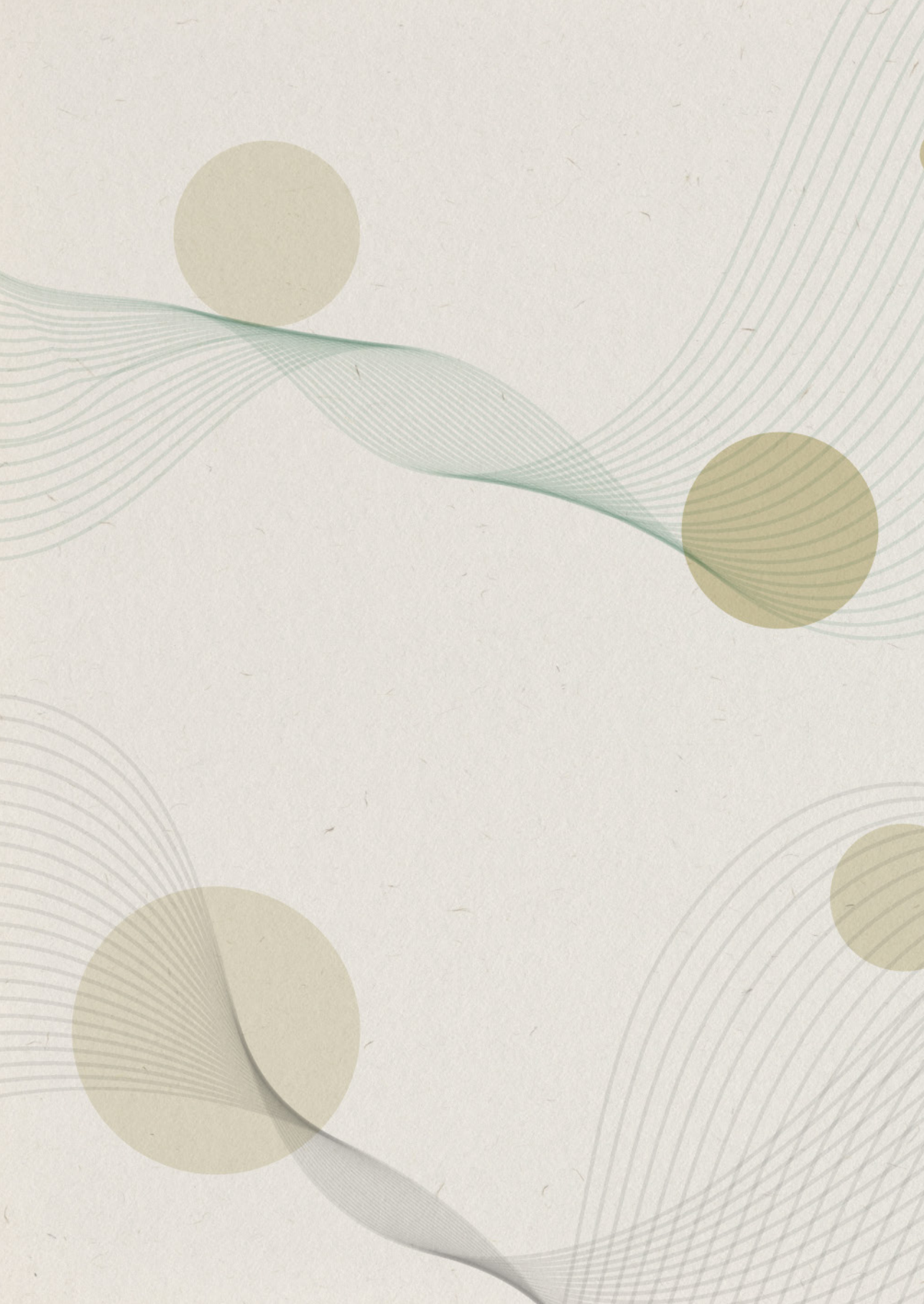


5.2. Los resultados mostraron que las medidas de imagen de Doppler miocárdico, como  $E'$ ,  $S$ ,  $E':A'$ , HRI-IVRT, HRI-IVCT, Global-TDI y R-TEI, discriminaron entre perros normotensos y perros con hipertensión pulmonar, y por lo tanto, pueden ser una herramienta alternativa útil para evaluar a pacientes con dirofilariosis cardiopulmonar mediante el uso de ecocardiografía transtorácica. Asimismo, la medida  $A'$  se mostró como un indicador deficiente para estimar la presencia de hipertensión pulmonar en perros con dirofilariosis cardiopulmonar. Las medidas HRI-IVCT, HRI-IVRT y R-TEI mostraron niveles más altos de eficiencia en la detección de hipertensión pulmonar en perros parasitados por *Dirofilaria immitis*.

5.3. This study has shown that the longitudinal measurements studied in two-dimensional speckle tracking echocardiography mode are useful for the determination of pulmonary hypertension in dogs parasitized by *Dirofilaria immitis*. According to obtained results, the GS, FWS and TAMD measurements can be considered as additional and alternative parameters to other conventional echocardiographic measurements for pulmonary hypertension estimation in canine heartworm disease. Optimized use for right ventricular analysis using the RV AFI® software has been effective in assessing myocardial strain percentage. Adequate statistical results were reported for the estimation of the presence of pulmonary hypertension and cut-off values were: GS  $\geq -21.25\%$  (Sen 96%, Sp 86.4%), FWS  $\geq -21.95\%$  (Sen 92.56%, Sp 95.5%) and TAMD  $\leq 0.850$  (Sen 70.4%, Sp 83.3%).

5.3. Este estudio ha demostrado que las mediciones longitudinales estudiadas en el modo de ecocardiografía speckle tracking son útiles para la determinación de la hipertensión pulmonar en perros parasitados por *Dirofilaria immitis*. Según los resultados obtenidos, las mediciones de GS, FWS y TAMD pueden considerarse como parámetros adicionales y alternativos a otras mediciones ecocardiográficas convencionales para la estimación de la hipertensión pulmonar en la dirofilariosis cardiopulmonar. El uso optimizado para el análisis del ventrículo derecho utilizando el software RV AFI® ha sido efectivo en la evaluación del porcentaje de deformación miocárdica. Se informaron resultados estadísticos adecuados para la estimación de la presencia de hipertensión pulmonar y los valores de corte fueron: GS  $\geq -21,25\%$ , (Sensibilidad 96%, Especificidad 86,4%), FWS  $\geq -21,95\%$  (Sensibilidad 92,56%, Especificidad 95,5%) y TAMD  $\leq 0,850$  (Sensibilidad 70,4%, Especificidad 83,3%).





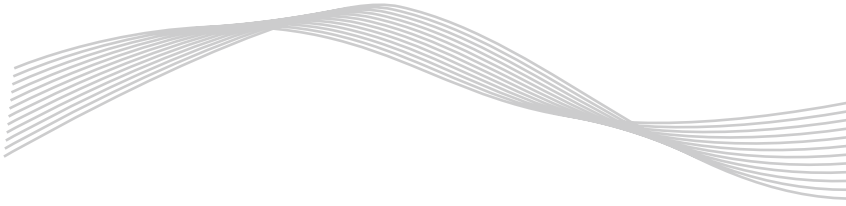
The background features a light beige, textured paper surface. It is decorated with several sets of thin, parallel, wavy lines in a muted sage green color. These lines are arranged in a way that creates a sense of depth and movement, with some lines curving and overlapping. Interspersed among these lines are four solid, olive-green circles of varying sizes, positioned in the upper left, upper right, lower left, and lower right areas of the page.

# 6. EXTENDED SUMMARY



# 6.1.

## State of the art



*Dirofilaria immitis*, a parasitic nematode causing cardiopulmonary heartworm disease, belongs to the *Onchocercidae* family and is the largest species among medically and veterinary significant filarids. Its life cycle involves an arthropod intermediate host, commonly mosquitoes, and exhibits a symbiotic relationship with *Wolbachia pipientis*. Canine cardiopulmonary dirofilariosis is globally distributed, with increasing prevalence due to climate change and vector habitat alterations (Bowman & Atkins, 2009; Anvari *et al.*, 2020). In Spain, the prevalence is 6.25%, varying regionally, and the disease is expanding in the north (Montoya-Alonso *et al.*, 2022; Morchón *et al.*, 2022).

Clinical signs of heartworm disease range from mild cough to severe tachypnea, syncope, and cardiorespiratory shock. Diagnosis involves serological tests, microscopic examination for *microfilariae*, and auxiliary tests. Treatment complexity depends on disease severity, and a standard protocol includes melarsomine injections, doxycycline, and macrocyclic lactones (Carretón *et al.*, 2019; Pariaut *et al.*, 2020).

*D. immitis* parasitosis induces a combination of acute and chronic immune responses in hosts, leading to a multisystem disorder affecting the lungs, heart, liver, and kidneys. The severity of lesions depends on factors such as nematode number, infection duration, and the host's immune reaction. Adult forms are primarily found in the pulmonary vascular surface, with potential migration to the main PA, right heart, and vena cava in severe cases (Simón *et al.*, 2015).

Pulmonary arterial pathology is central to *Dirofilaria immitis*-induced disease, resulting in functional and pathological alterations. Immunological responses, toxic substances, and physical trauma contribute to villous proliferation, inflammation, pulmonary hypertension, vascular integrity disruption, and fibrosis. *Wolbachia pipientis* exacerbates inflammatory reactions, leading to arterial lesions, peri-vascular inflammation, endothelial proliferation, and increased thrombus probability (McCall *et al.*, 2008).

Pulmonary hypertension in *D. immitis* parasitosis involves two mechanisms: endothelial damage from parasites and hypertension due to pulmonary emboli or thromboembolism. Vascular endothelium thickening and lumen narrowing

cause blood flow obstruction and decreased PA distension capacity. Smaller vessels may be occluded by parasitic or thromboembolic emboli, contributing to PA dilation (Venco *et al.*, 2014; Serrano-Parreño *et al.*, 2017).

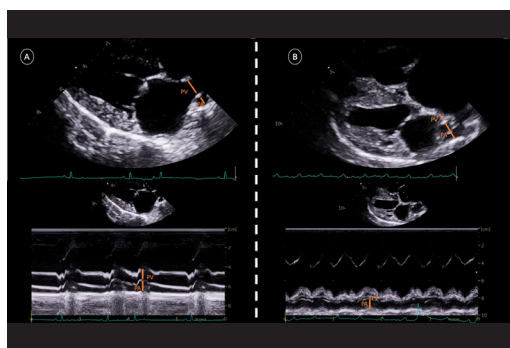
The pulmonary circulation functions in blood gas exchange, acts as a volume reservoir, and filters against thromboembolisms and respiratory infections. It operates at low pressure, with the RV pumping blood to the PA for gas exchange, and oxygenated blood returning to the left heart through PV. Unlike systemic circulation, pulmonary circulation has arteries carrying deoxygenated blood and veins returning oxygenated blood, with higher compliance, capacitance, and lower resistance. Local, hormonal, and neural controls regulate it. Pulmonary hypertension, marked by increased pulmonary vascular resistance and elevated arterial pressure, has various causes, including precapillary pulmonary hypertension in dogs with cardiopulmonary heartworm disease (Chan *et al.*, 2019; Reiner *et al.*, 2020).

In humans, pulmonary hypertension diagnosis involves right heart catheterization. Still, this invasive procedure is not routinely feasible in veterinary practice due to cost, anesthesia risks, and time. Pulmonary hypertension in dogs may be precapillary or postcapillary, linked to increased blood flow, vascular resistance, or venous pressures. Echocardiography is crucial for non-invasive estimation, but its limitations include operator skill, equipment variability, and imprecision. Despite these challenges, it is essential for assessing clinical signs and guiding further diagnoses (Lang *et al.*, 2015; Nijhawan *et al.*, 2019; Reiner *et al.*, 2020).

Pulmonary hypertension classification traditionally involves mild, moderate, or severe categories based on echocardiographic assessments. However, the international consensus suggests considering the clinical impact, and tricuspid regurgitation pressure gradient  $>46$  mmHg is proposed for clinical definition. Standardizing the study of pulmonary hypertension is discouraging, emphasizing tailored methods and protocols for each pathological condition (Kelliher & Stepien, 2012; Visser *et al.*, 2016; Reiner *et al.*, 2020). Future research should explore reliable, repeatable, and non-invasive methods with high Sen and Sp for diagnosing pulmonary hypertension in veterinary medicine (Schober *et al.*, 2006; Toaldo *et al.*, 2016; Wolf *et al.*, 2021).

The PV and PA exhibit dynamic changes in diameter during the cardiac cycle,

influenced by flow volume, intravascular pressure, and vascular compliance. Veterinarians traditionally assess these vessels to gain insights into the hemodynamic status of canine patients, comparing PV and PA sizes on radiographs, CT or echocardiography and evaluating their ratios, offering optimal results in assessing pulmonary hypertension (Biretoni *et al.*, 2016) (Figure 14).



\*Figure 14. Representation of the echocardiographic measurement of the relationship between the pulmonary vein and the pulmonary artery (PV:PA ratio) by two-dimensional method and by one-dimensional method. Right parasternal view of 4 cardiac chambers in dog with canine cardiopulmonary heartworm without pulmonary hypertension (A), and in a dog with canine cardiopulmonary heartworm disease with pulmonary hypertension (B).

Recent studies, particularly using echocardiography, focus on the PV:PA ratio as a valuable index. The physiological relationship between PV and PA in healthy dogs approaches 1.0, and this ratio has been applied to predict CHF in both dogs and cats. This ratio, measured in both 2D and M-mode echocardiography, provides predictive value for CHF in dogs with myxomatous mitral valve disease. A PV:PA ratio of  $<1.8$  at the end of the T-waves has been shown to be sensitive and specific for detecting CHF (Merveille *et al.*, 2015).

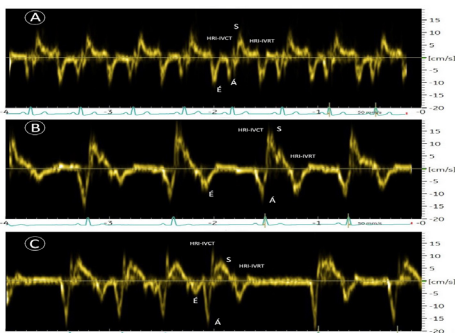
In cats, the PV:PA ratio has been used to discriminate those with CHF, showing higher accuracy compared to other measures. The ratio, obtained from a modified right parasternal long-axis view, using the inner-edge-to-inner-edge method, demonstrated its ability to differentiate between animals with CHF and those with subclinical heart disease. These findings suggest the potential clinical utility of the PV:PA ratio in identifying cardiac conditions in veterinary practice (Patata *et al.*, 2019). Furthermore, recent studies have explored the application of the PV:PA ratio in identifying pulmonary hypertension in dogs. Results indicate its effectiveness as a non-invasive tool for diagnosing at least moderate precapillary pulmonary hypertension, with promising predictive value for the presence of moderate pulmonary hypertension and potential applications in assessing survival in specific canine conditions such as idiopathic pulmonary fibrosis (Roels *et al.*, 2019; Roels *et al.*, 2021).



The PV:PA ratio obtained through various imaging techniques emerges as a valuable diagnostic tool in veterinary cardiology, offering insights into CHF and pulmonary hypertension in dogs and cats. This non-invasive approach holds promise for further applications in clinical practice, providing clinicians with an additional tool for assessing the cardiovascular status of their patients (Lee & Choi, 2022).

TDI revolutionized the quantitative evaluation of myocardial function in echocardiography since its introduction in 1989. TDI uses Doppler ultrasound to detect changes in the frequency of ultrasound signals reflected by moving cardiac structures, enabling the assessment of myocardial motion. TDI is particularly effective in evaluating the longitudinal component of myocardial contraction throughout the cardiac cycle. There are two main methods of obtaining TDI: pulsed-wave TDI and color tissue Doppler. Pulsed-wave TDI measures the longitudinal myocardial velocity peak of a single segment instantaneously, while color tissue Doppler allows simultaneous assessment of velocities from multiple sites but represents mean maximum velocity, being 25% lower than pulsed-wave Doppler. The two methods are not interchangeable (Chetboul *et al.*, 2007; Tidholm *et al.*, 2009).

TDI provides valuable information on myocardial function by analyzing peaks during a cardiac cycle: positive systolic peak (S velocity), early diastolic relaxation (E' velocity), and active atrial contraction (A' velocity). Additionally, periods of isovolumetric contraction (IVCT) and relaxation (IVRT) can be identified (Figure 15). TDI measurements have been extensively used in various cardiac conditions in small animals, including left and right ventricular systolic and diastolic dysfunction, dyssynchrony, and atrial function. TDI proves more sensitive than conventional echocardiography in detecting early myocardial alterations in both primary and secondary disorders (Boissiere *et al.*, 2005; Toaldo *et al.*, 2016).



\*Figure 15. Representation of different patterns of tissue Doppler imaging in the right ventricle in the analysis of the presence of pulmonary hypertension. A: dog without canine cardiopulmonary heartworm, B: dog with canine cardiopulmonary heartworm without pulmonary hypertension. C: dog with canine cardiopulmonary heartworm disease with pulmonary hypertension.

In particular, TDI has been employed in studying right ventricular function, an area often challenging to assess due to its retrosternal position. Parameters such as S velocity, E' velocity, and A' velocity have been studied in healthy dogs, demonstrating reproducibility and providing reference intervals. TDI has shown diagnostic value in dogs with pulmonary hypertension and predictive potential for dilated cardiomyopathy (Serres *et al.*, 2007; Chetboul *et al.*, 2007).

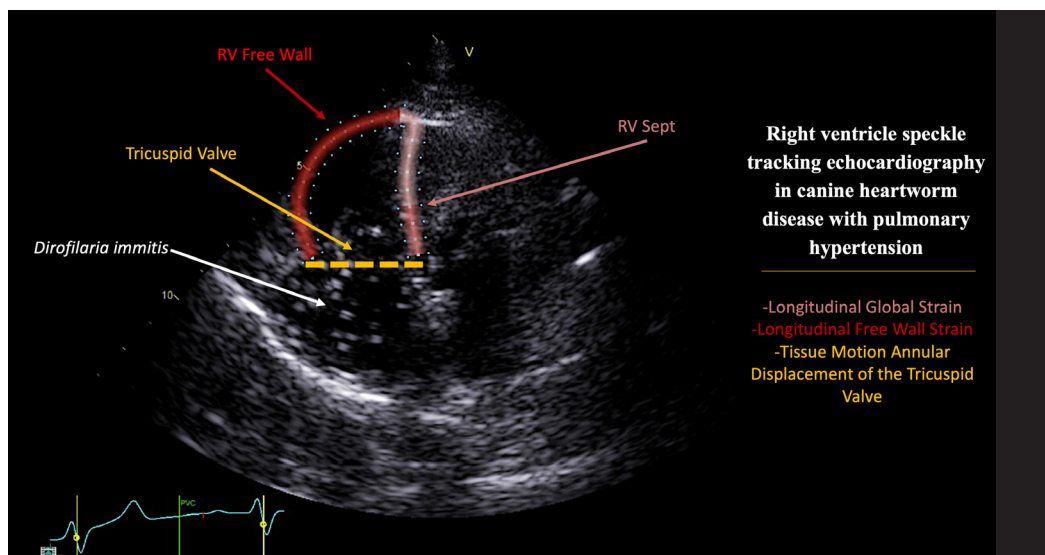
TDI is a powerful tool in echocardiography, offering detailed insights into myocardial function and proving particularly valuable in assessing conditions such as pulmonary hypertension in small animals. Despite its challenges, TDI's sensitivity to early myocardial alterations makes it a key modality in both clinical screening and evaluating therapeutic interventions. However, TDI has limitations, including the difficulty in distinguishing active myocardial contraction from tethering effects and challenges associated with accurate positioning of the sample volume. Learning curves and variations in machine algorithms may affect TDI rates, and the interrogation angle plays a crucial role. High frame rates are necessary for accurate imaging, and cursor position can impact synchronization, especially in desynchrony studies. Interpretation of pulsed TDI traces may be challenging, especially at high heart rates (Koffas *et al.*, 2006; Koenig *et al.*, 2017).

Echocardiography is a key diagnostic tool in both veterinary and human medicine for cardiovascular assessment, but accurately evaluating cardiac mechanics is challenging due to myocardial geometry and functional complexities. Conventional echocardiography struggles to depict twisting motions and overall wall thickening, and it cannot distinguish active from passive myocardial segment movement. Speckle tracking echocardiography, a non-Doppler technique, overcomes these limitations (Feldhutter *et al.*, 2021).

Speckle tracking uses computer software to analyze ultrasound images, identifying stable speckles as natural acoustic markers. It calculates motion and deformation parameters, including strain and strain rate, providing insights into myocardial mechanics. Strain, expressed as a percentage of change from the original length, reveals narrowing or shortening (negative values) or lengthening or thickening (positive values). Strain rate represents the average change in strain per unit of time (Hamabe *et al.*, 2021).

The double helical structure of myocardial fibers is vital for efficient cardiac function, enabling simultaneous shortening in longitudinal and circumferential directions, resulting in a twisting motion that enhances energy efficiency. Ventricular motion involves various deformations, such as narrowing, shortening, lengthening, widening, and twisting, leading to alterations in shape (Locatelli *et al.*, 2016; Chetboul *et al.*, 2018).

Speckle tracking has been applied in veterinary cardiology, particularly in dogs. It assesses longitudinal strain in both left and right ventricles and, to a lesser extent, circumferential fiber strain. Studies suggest its sensitivity in detecting right ventricular dysfunction compared to conventional indices. However, its application in canine cardiopulmonary heartworm disease, a condition causing precapillary pulmonary hypertension, remains unexplored (Morita *et al.*, 2017; Cavaino *et al.*, 2020) (Figure 16).



\*Figure 16. Representation of longitudinal endocardial strain analysis in the right ventricle of a patient with heartworm caval syndrome. The strain measurements determined by the speckle tracking method are longitudinal global strain (%), longitudinal free wall strain (%) and tissue motion annular displacement of the tricuspid valve (cm).

The process involves standardizing the assessment of mechanical events, with end diastole and end systole commonly identified as the beginning and end of the cardiac cycle. Speckle tracking provides reports on endocardial deformation, often dividing the ventricular wall into segments for analysis. Despite its promise,

the clinical utility of strain measurements is under scrutiny. Challenges include the need for high-quality image streams, time-intensive post-processing, and variations in software, leading to potential discrepancies in clinical outcomes. Additionally, strain measurement requires expertise to assess output validity, hindering routine use in standard cases. Despite these challenges, speckle tracking offers valuable insights into cardiac mechanics, making it a promising tool for evaluating cardiac function (Visser *et al.*, 2017; Morita *et al.*, 2019).

## 6.2. Objectives



1. Structural changes in the pulmonary vasculature reflect cardiorespiratory hemodynamic alterations. Assessment of pulmonary vein (PV) and pulmonary artery (PA) diameter in dogs and cats has previously been shown to be a valuable echocardiographic index. It was proposed to evaluate the relationship between the PV and PA (PV:PA) in dogs affected by cardiopulmonary dirofilariosis with the hypothesis that there must be a direct association with the presence or absence of pulmonary hypertension. Likewise, the investigation between the echocardiographic methods of determination, two-dimensional and one-dimensional mode, was analyzed to determine the degree of correlation between both measurements.
2. Tissue Doppler imaging (TDI) has been widely used in veterinary medicine to evaluate cardiac functionality. It was proposed to evaluate the hemodynamic changes that could be detected by TDI in the right heart chambers of dogs affected by cardiopulmonary dirofilariosis with the hypothesis that the determinations could be a useful tool for the evaluation of the presence of pulmonary hypertension in the animals analyzed. Thus, the objective of this study was to evaluate the usefulness of the measurements obtained by echocardiographic examination in TDI mode (E', A', S, E':A', Global TDI, HRI-IVCT, HRI-IVRT, R-TEI ), to detect the presence of pulmonary hypertension in dogs infected by *Dirofilaria immitis*.

3. Two-dimensional speckle tracking echocardiography has improved the assessment of cardiac functionality by being able to analyze specific segments of the ventricular myocardium influenced by diverse phenomena such as pulmonary hypertension. Therefore, due to the high percentage of canine patients who suffer from canine cardiopulmonary dirofilariosis and generate pulmonary hypertension, it is essential to know the diagnostic value of the longitudinal strain of the right ventricle (GS and FWS) and the measurements of the annular displacement of the tricuspid movement (TMAD) using two-dimensional speckle tracking echocardiography. The objective was to evaluate the usefulness of GS, FWS and TMAD measurements in a group of dogs infected with heartworm to determine the cut-off values to estimate the presence of pulmonary hypertension.

## 6.3.

### Scientific publications



#### 6.3.1. Echocardiographic Assessment Of The Pulmonary Vein To Pulmonary Artery Ratio In Canine Heartworm Disease

##### Background:

*Dirofilaria immitis* infection in dogs results in proliferative pulmonary endarteritis and pulmonary thromboembolism, causing irreversible structural damage and sustained precapillary pulmonary hypertension (PH). This study aimed to evaluate the diagnostic efficacy of the pulmonary vein to pulmonary artery ratio (PV:PA ratio) in identifying moderate or severe PH (>50 mmHg) in heartworm-infected dogs.

##### Methods:

The study included 151 naturally infected and 66 healthy dogs. PH presence/absence was determined by the right pulmonary artery distensibility index (RPAD index <29.5%), and the PV:PA ratio was measured using both time-motion mode (M mode) and two-dimensional mode (2D mode) echocardiography. Other echocardiographic parameters were also examined (pulmonary trunk to aorta ratio, tricuspid regurgitation pressure gradient, and AT:ET ratio).

### Results:

Results revealed a strong positive correlation between M and 2D modes' PV:PA ratios ( $r = 0.928$ ). The M mode's PV:PA ratio emerged as the strongest predictor for RPAD index ( $R^2 0.628$ ,  $p < 0.0001$ ) with high diagnostic accuracy ( $AUC = 0.99$ ). Similarly, the 2D mode's PV:PA ratio demonstrated significant predictive capability for the RPAD index ( $R^2 0.606$ ,  $p < 0.0001$ ) with good diagnostic accuracy ( $AUC = 0.98$ ). Both M and 2D modes' PV:PA ratios decreased significantly in the presence of PH. A cut-off value of 0.845 exhibited high sensitivity and specificity for both M mode (97% and 94%, respectively) and 2D mode (96% and 93%, respectively).

### Conclusion:

In conclusion, the PV:PA ratio serves as a valuable complementary diagnostic tool for estimating moderate or severe PH in heartworm-infected dogs.

## 6.3.2. Usefulness of Tissue Doppler Imaging for the Evaluation of Pulmonary Hypertension in Canine Heartworm Disease

### Background:

*Dirofilaria immitis*, a nematode causing proliferative pulmonary endarteritis in dogs, leads to severe and irreversible structural damage in pulmonary arteries, resulting in sustained pulmonary hypertension (PH). This condition can contribute to significant cardiorespiratory disorders. This study aimed to evaluate the diagnostic utility of echocardiography tissue Doppler imaging (TDI) in identifying PH in dogs with heartworm disease.

### Methods:

The study included 116 heartworm-infected dogs with PH and 33 healthy dogs. PH was determined based on the right pulmonary artery distensibility index (RPADi)  $< 29.5\%$ , indicating its presence in 47.4% of infected dogs. Alternative standard echocardiographic measures for PH estimation were also employed. TDI was used for eight echocardiographic measurements ( $E'$ ,  $A'$ ,  $S$ ,  $E':A'$ , global TDI, HRI-IVCT, HRI-IVRT, R-TEI) to assess its diagnostic efficacy.

### Results:

TDI measurements revealed significant differences between dogs with and without PH, displaying a positive correlation with RPADi. Furthermore, cut-off values for excellent sensitivity and specificity were identified for  $E':A'$ , global TDI, HRI-IVCT, HRI-IVRT, and R-TEI in detecting PH.

### Conclusion:

The TDI mode emerges as a valuable adjunct diagnostic tool for identifying PH in dogs with *Dirofilaria immitis*, providing additional insights into the assessment of this cardiovascular condition.

## **6. 3. 3. Right ventricle strain assessed by 2-dimensional speckle tracking echocardiography (2D-STE) to evaluate pulmonary hypertension in dogs with *Dirofilaria immitis***

### Background:

Echocardiographic assessment of the right ventricle is crucial for analysing the pathophysiology of heartworm disease and determining the presence of pulmonary hypertension (PH) in patients. In veterinary cardiology, the study of myocardial deformation using two-dimensional speckle tracking (2D-STE) echocardiography has become increasingly acknowledged as essential for quantifying right ventricular function. Therefore, the aim of this study was to evaluate the usefulness of myocardial deformation of the right ventricular free wall (FWS), global deformation of the right ventricle, including the interventricular septum (GS) and tissue motion annular displacement of the tricuspid valve (TMAD) in a cohort of dogs with heartworm disease (*Dirofilaria immitis*), and to determine cut-off values for detecting the presence of PH.

### Methods:

Out of 93 dogs tested, 71% were diagnosed with heartworm infection, while PH was identified in 41% of the infected canines by assessing the distensibility index of the right pulmonary artery (RPADi <30%). Other conventional echocardiographic measurements were determined to estimate cardiac function and detect PH. The 2D-STE mode measurements were determined using the Right Ventricular Automated Function Imaging (RV AFI®) software.

### Results:

The statistical analysis showed significant differences in the studied parameters among dogs with and without PH. Additionally, high sensitivity (sen) and specificity (sp) cut-off values were obtained (GS  $\geq$ -21.25%, sen 96%, sp 86.4%; FWS  $\geq$ -21.95%, sen 92.56%, sp 95.5%; TMAD  $\leq$ 0.85cm, sen 70.4%, sp 83.3%).

### Conclusion:

These results demonstrated that GS, FWS, and TMAD could be used as supplementary and alternative parameters to conventional echocardiographic measurements when detecting PH in dogs with heartworm disease.

## 6.4. Conclusions



1. Echocardiographic measurement of the pulmonary vein to pulmonary artery ratio was able to discriminate between dogs without pulmonary hypertension (healthy or infected with *Dirofilaria immitis*) and dogs infected with heartworms with pulmonary hypertension. Therefore, the pulmonary vein to pulmonary artery ratio may be a useful tool to echocardiographically evaluate vascular status in patients with heartworm disease. The pulmonary vein to pulmonary artery ratio of 0.845, in both the one-dimensional and two-dimensional modes, suggested an acceptable cut-off value to differentiate between dogs with pulmonary hypertension and dogs without pulmonary hypertension.
2. The results showed that the tissue Doppler imaging measures of E', S, E':A', HRI-IVRT, HRI-IVCT, Global-TDI and R-TEI discriminated between normotensive and dogs with pulmonary hypertension and, therefore, can be a useful alternative tool to evaluate patients with heartworm by using transthoracic echocardiography. Likewise, the A' measure was shown to be a poor indicator in estimating the presence of pulmonary hypertension in dogs with canine cardiopulmonary dirofilariosis. The HRI-IVCT, HRI-IVRT and R-TEI showed higher levels of efficiency in the detection of pulmonary hypertension in dogs parasitized by *Dirofilaria immitis*.



3. This study has shown that the longitudinal measurements studied in two-dimensional speckle tracking echocardiography mode are useful for the determination of pulmonary hypertension in dogs parasitized by *Dirofilaria immitis*. According to obtained results, the GS, FWS and TAMD measurements can be considered as additional and alternative parameters to other conventional echocardiographic measurements for pulmonary hypertension estimation in canine heartworm disease. Optimized use for right ventricular analysis using the RV AFI® software has been effective in assessing myocardial strain percentage. Adequate statistical results were reported for the estimation of the presence of pulmonary hypertension and cut-off values were: GS  $\geq -21.25\%$ , (Sen 96%, Sp 86.4%), FWS  $\geq -21.95\%$  (Sen 92.56%, Sp 95.5%) and TAMD  $\leq 0.850$  (Sen 70.4%, Sp 83.3%).





The background features a light beige, textured surface. Overlaid on this are several sets of thin, wavy, grey lines that create a sense of movement and depth. Interspersed among these lines are four solid gold circles of varying sizes, positioned in the upper left, upper right, lower left, and lower right areas.

# 7. SIMPLE SUMMARY



*Dirofilaria immitis*, a parasitic nematode causing canine cardiopulmonary dirofilariosis, is prevalent globally, with increasing cases due to climate change. In Spain, the prevalence is 6.25%, varying regionally. Clinical signs range from mild cough to severe respiratory distress. Diagnosis involves serological tests, microscopic examination, and auxiliary tests. Treatment includes melarsomine injections, doxycycline, and macrocyclic lactones.

The parasitosis induces acute and chronic immune responses, affecting multiple organs. Pulmonary arterial pathology is central, leading to villous proliferation, inflammation, and pulmonary hypertension. *Wolbachia pipientis* exacerbates inflammatory reactions. Pulmonary hypertension involves endothelial damage and hypertension due to emboli or thromboembolism, causing blood flow obstruction and vessel dilation.

The pulmonary circulation in dogs with heartworm disease experiences increased pulmonary vascular resistance and elevated arterial pressure, leading to pulmonary hypertension. Diagnosis involves echocardiography, but challenges include operator skill and imprecision. Despite challenges, non-invasive methods for diagnosing pulmonary hypertension in veterinary medicine are crucial. Currently research are focus on reliable, repeatable, and non-invasive methods with high sensitivity and specificity.

#### Structural Changes in Pulmonary Vasculature:

The study aimed to evaluate the relationship between the pulmonary vein and pulmonary artery in dogs with cardiopulmonary dirofilariosis, assessing its potential association with pulmonary hypertension. Echocardiographic measurement of the pulmonary vein to pulmonary artery ratio effectively distinguished dogs with pulmonary hypertension, suggesting a cut-off value of 0.845 in both one-dimensional and two-dimensional modes.

#### Tissue Doppler Imaging:

The research focused on using tissue Doppler imaging to assess hemodynamic changes in the right heart chambers of dogs with cardiopulmonary dirofilariosis. Various tissue Doppler imaging parameters, including E', A', S, E':A', Global TDI, HRI-IVCT, HRI-IVRT, and R-TEI, were examined for their utility in detecting the presence of pulmonary hypertension. Notably, the majority of parameters showed efficiency in discriminating between normotensive and hypertensive dogs.

#### Two-Dimensional Speckle Tracking Echocardiography:

The study explored the diagnostic value of two-dimensional speckle tracking echocardiography in dogs with cardiopulmonary dirofilariosis. Longitudinal measurements, such as Global Strain, Free Wall Strain, and Tissue Motion Annular Displacement, were investigated to determine cut-off values for estimating the presence of pulmonary hypertension. The RV AFI® software for right ventricular analysis was found effective, providing specific cut-off values for each parameter in detecting pulmonary hypertension by assessing myocardial strain percentage.

*Dirofilaria immitis*, un nematodo que causa la dirofilariosis cardiopulmonar en perros, es prevalente a nivel mundial, con un aumento de casos debido al cambio climático. En España, la prevalencia es del 6,25%, variando regionalmente. Los signos clínicos van desde una tos leve hasta una disnea severa. El diagnóstico incluye pruebas serológicas, examen microscópico y pruebas auxiliares. El tratamiento incluye inyecciones de melarsomina, doxiciclina e lactonas macrocíclicas.

La parasitosis induce respuestas inmunológicas agudas y crónicas, afectando a múltiples órganos. La patología arterial pulmonar es central, provocando endoarteritis pulmonar proliferativa, inflamación e hipertensión pulmonar. *Wolbachia pipientis* exacerba las reacciones inflamatorias. La hipertensión pulmonar implica daño endotelial e hipertensión debido a émbolos o tromboembolismos, causando obstrucción del flujo sanguíneo y dilatación vascular.

La circulación pulmonar en perros con dirofilariosis cardiopulmonar experimenta un aumento de la resistencia vascular pulmonar y una elevación de la presión arterial, lo que lleva a la hipertensión pulmonar. El diagnóstico implica la ecocardiografía, pero los desafíos incluyen la habilidad del operador y la imprecisión de las mediciones. A pesar de ello, los métodos no invasivos para diagnosticar la hipertensión pulmonar en medicina veterinaria son cruciales. La investigación actual se centra en métodos confiables, repetibles y no invasivos con alta sensibilidad y especificidad.

#### Cambios Estructurales en la Vasculatura Pulmonar:

El estudio tuvo como objetivo evaluar la relación entre la vena pulmonar y la arteria pulmonar en perros con dirofilariosis cardiopulmonar, evaluando su posible asociación con la hipertensión pulmonar. La medición ecocardiográfica de la relación vena pulmonar y arteria pulmonar distinguió eficazmente a perros con hipertensión pulmonar, sugiriendo un valor de corte de 0,845 en modos unidimensional y bidimensional.

#### Imagen de Doppler Miocárdico:

La investigación se centró en el uso de la imagen de Doppler miocárdico para evaluar cambios hemodinámicos en las cámaras cardíacas derechas de perros con dirofilariosis cardiopulmonar. Se examinaron varios parámetros de imagen de Doppler miocárdico, incluyendo  $E'$ ,  $A'$ ,  $S$ ,  $E':A'$ , Global TDI, HRI-IVCT, HRI-IVRT y R-TEI, para determinar su utilidad en la detección de la presencia de hipertensión pulmonar. Notablemente, la mayoría de los parámetros mostraron eficiencia para discriminar entre perros normotensos e hipertensos.

#### Ecocardiografía Bidimensional Speckle Tracking:

El estudio exploró el valor diagnóstico de la ecocardiografía bidimensional Speckle Tracking en perros con dirofilariosis cardiopulmonar. Se investigaron mediciones longitudinales, como la deformación global, la deformación de la pared Libre y el desplazamiento anular del movimiento tricúspide, para determinar valores de corte para estimar la presencia de hipertensión pulmonar. El software RV AFI® para el análisis del ventrículo derecho resultó efectivo, proporcionando valores de corte específicos para cada parámetro en la detección de la hipertensión pulmonar mediante la evaluación del porcentaje de deformación miocárdica.







The background features a textured, light beige paper surface. It is decorated with several sets of thin, wavy, light green lines that create a sense of movement and depth. Interspersed among these lines are three solid gold circles of varying sizes, positioned in the upper left, upper right, and lower right areas.

# 8. REFERENCE LIST



- Adams, D.S.; Marolf, A.J.; Valdés-Martínez, A.; Randall, E.K.; Bachand, A.M. Associations between thoracic radiographic changes and severity of pulmonary arterial hypertension diagnosed in 60 dogs via Doppler echocardiography: A retrospective study. *Vet Radiol Ultrasound*. 2017; 58:454-462.
- Adebayo, O.O.; Akande, F.A.; Adenubi, O.T. Canine Dirofilaria: A Case Report and Review of the Literature. *Folia Vet*. 2020; 64:75-81.
- Alho, A.M.; Fiarresga, A.; Landum, M.; Lima, C.; Gamboa, O.; Meireles, J.; et al. A Homemade Snare: an alternative method for mechanical removal of *Dirofilaria immitis* in Dogs. *Vet Med Int*. 2016; 23:34-41.
- Ames, M.K.; Atkins, C.E. Treatment of dogs with severe heartworm disease. *Vet parasitol*. 2020; 283:454-462.
- Antinoff, N. Clinical observations in ferrets with naturally occurring heartworm disease and preliminary evaluation of treatment with ivermectin with and without melarsomine. *Proc Heartworm Symp AHS*. 2002; 64:45-47.
- Anvari, D.; Narouei, E.; Daryani, A.; Sarvi, S.; Moosazadeh, M.; Hezarjaribi, Z.; et al. The global status of *Dirofilaria immitis* in dogs: a systematic review and meta-analysis based on published articles. *Res Vet Sci*. 2020; 131:104-116.
- Arita, N.; Yamane, I.; Takemura, I. Comparison of canine heartworm removal rates using flexible alligator forceps guided by transesophageal echocardiography and fluoroscopy. *J Vet Med Sci*. 2003; 65:259-261.
- Biretoni, F.; Caivano, D.; Patata, V.; Moïse, N.S.; Guglielmini, C.; Rishniw, M.; Porciello, F. Canine pulmonary vein-to-pulmonary artery ratio: echocardiographic technique and reference intervals. *J Vet Cardiol*. 2016; 18:326-335.
- Boissiere, J.; Gautier, M.; Machet, M.C.; Hanton, G.; Bonnet, P.; Eder, V. Doppler tissue imaging in assessment of pulmonary hypertension-induced right ventricle dysfunction. *Am J Physiol Heart Circ Physiol*. 2005;289:2450-2455.
- Bolio-González, M.E.; Rodríguez-Vivas, R.I.; Sauri-Arceo, C.H.; Gutiérrez-Blanco, E.; Ortega-Pacheco, A.; Colin-Flores, R.F. Prevalence of the *Dirofilaria immitis* infection in dogs from Merida, Yucatan. Mexico. *Vet Parasitol*. 2007;148:166-169.
- Borgarelli, M.; Savarino, P.; Crosara, S.; Santilli, R.A.; Chiavegato, D.; Poggi, M.; et al. Survival characteristics and prognostic variables of dogs with mitral regurgitation attributable to myxomatous valve disease. *J Vet Intern Med*. 2008; 22:120-128.
- Borthakur, S.K.; Deka, D.K.; Islam, S.; Sarma, D.K.; Sarmah, P.C. Prevalence and molecular epidemiological data on *Dirofilaria immitis* in dogs from Northeastern States of India. *Sci World J*. 2015; 15:265-285.
- Bové, C.M.; Gordon, S.G.; Saunders, A.B.; Miller, M.W.; Roland, R.M.; Ahen, S.E.; et al. Outcome of minimally invasive surgical treatment of heartworm caval syndrome in dogs: 42 cases (1999–2007). *J Am Vet Med Assoc*. 2010; 236:187-192.
- Bowman, D.D.; Atkins, C.E. Heartworm biology, treatment, and control. *Vet Clin North Am Small Anim Pract*. 2009; 39: 1127-1158.
- Bradbury, C.; Saunders, A.B.; Heatley, J.J.; Gregory, C.R.; Wilcox, A.L.; Russell, K.E. Transvenous heartworm extraction in a ferret with caval syndrome. *J Am Anim Hosp Assoc*. 2010; 46:31-35.
- Braz, J.B.; Camacho, A.A.; Canola, R.A.M.; Beluque, T.; Zacché, E.; Silva-Filho, J.C.; Zamora, W.A.; Sousa, M.G. Echocardiographic features of pre- and postcapillary pulmonary hypertension with a focus on the right ventricle in dogs. *Pesq Vet Bras*. 2021; 41:143-152.
- Caivano, D.; Cordal, A.; Rishniw, M.; Giorgi, M.E.; Parpaglia, M.L.; Conti, M.B.; Porciello, F.; Biretoni, F. Transthoracic M-mode echocardiographic assessment of pulmonary vein-to-pulmonary artery ratio in healthy horses. *PLoS ONE*. 2019; 14:8-12.

- Caivano, D.; Dickson, D.; Pariaut, R.; Stillman, M.; Rishniw, M. Tricuspid annular plane systolic excursion-to-aortic ratio provides a bodyweight independent measure of right ventricular systolic function in dogs. *J Vet Cardiol.* 2018a; 20:79-91.
- Caivano, D.; Rishniw, M.; Biretoni, F.; Patata, V.; Giorgi, M.E.; Dei, K.; Porciello, F. Right ventricular outflow tract fractional shortening: an echocardiographic index of right ventricular systolic function in dogs with pulmonary hypertension. *J Vet Cardiol.* 2018b; 20:354-363.
- Caivano, D.; Rishniw, M.; Biretoni, F.; Petrescu, V.S.; Porciello, F. Transverse Right Ventricle Strain and Strain Rate Assessed by 2-Dimensional Speckle Tracking Echocardiography in Dogs with Pulmonary Hypertension. *Vet Sci.* 2020; 1:7-19.
- Cancrini, G.; Kramer, L. Heartworm Infection in Humans and Animals. In: Simón F. & Genchi C., editors. *Insect vectors of Dirofilaria spp.* Ediciones Universidad de Salamanca. 2001; 63-82.
- Cannon, M.S.; Wisner, E.R.; Johnson, I.R.; Kass, P.H. Computed tomography bronchial lumen to pulmonary artery diameter ratio in dogs without clinical pulmonary disease. *J Vet Radiol Ultrasound.* 2009; 50:622-624.
- Carretón, E.; Falcón-Cordón, Y.; Rodon, J.; Matos, J.I.; Morchón, R.; Montoya-Alonso, J.A. Evaluation of serum biomarkers and proteinuria for the early detection of renal damage in dogs with heartworm (*Dirofilaria immitis*). *J Vet Parasitol.* 2020; 283:1-4.
- Carretón, E.; Falcón, Y.; Falcón, S.; Morchón, R.; Matos, J.I.; Montoya, J.A. Variation of the adulticide protocol for the treatment of canine heartworm infection: Can it be shorter? *J Vet Parasitol.* 2019; 271: 54–56.
- Carretón, E.; Montoya, J.A.; Morchón, R.; Silveir, A.L.; Falcón, Y.; Simón, F. The impact of the climate on the epidemiology of *Dirofilaria immitis* in the pet population of the Canary Islands. *J Vet Parasitol.* 2016; 216: 66-71.
- Carretón, E.; Morchón, R.; Falcón-Cordón, Y.; Falcón-Cordón, S.; Matos, J.I.; Montoya-Alonso, J.A. Evaluation of different dosages of doxycycline during the adulticide treatment of heartworm (*Dirofilaria immitis*) in dogs. *J Vet Parasitol.* 2020; 283:1-4.
- Cavaliere, L.; Romito, G.; Domenech, O.; Venco, L. Heartworm removal guided by transesophageal echocardiography in a dog with naturally acquired caval syndrome. *J Am Anim Hosp Assoc.* 2017; 53:96-100.
- Chan, P.; Chieh, M.; Hsueh, T.; Chang, Y.; Long, S. Prognostic value of right pulmonary artery distensibility in dogs with pulmonary hypertension. *Vet Sci.* 2019; 20: 34-38.
- Chetboul, V.; Damoiseaux, C.; Lefebvre, H.P.; Concordet, D.; Desquilbet, L.; Vassiliki, G.; Poissonnier, C.; Pouchelon, J.L.; Renaud, T. Quantitative assessment of systolic and diastolic right ventricular function by echocardiography and speckle-tracking imaging: A prospective study in 104 dogs. *Vet Sci.* 2018, 19: 683-692.
- Chetboul, V.; Gouni, V.; Sampedrano, C.C.; Tissier, R.; Serres, F.; Pouchelon, J.L. Assessment of regional systolic and diastolic myocardial function using tissue Doppler and strain imaging in dogs with dilated cardiomyopathy. *J Vet Intern Med.* 2007; 21:719-730.
- Chetboul, V.; Gouni, V.; Sampedrano, C.C.; Tissier, R.; Serres, F.; Pouchelon, J.L. Assessment of Regional Systolic and Diastolic Myocardial Function Using Tissue Doppler and Strain Imaging in Dogs with Dilated Cardiomyopathy. *J Vet Intern Med.* 2007; 21:719-730.
- Chetboul, V.; Serres, F.; Gouni, V.; Tissier, R.; Pouchelon, J.L. Radial strain and strain rate by two-dimensional speckle tracking echocardiography and the tissue velocity based technique in the dog. *J Vet Cardiol.* 2007; 9:69-81.
- Chetboul, V.; Tissier, R. Echocardiographic assessment of canine degenerative mitral valve disease. *J Vet Cardiol.* 2012; 14:127-148.
- Chikwetoa, A.; Bhaiyat, M.I.; Lanza-Perea, M.; Veytsman, S.; Tiwari, K.; Allie, C.D.; et al. Retrospective study of canine heartworm disease with caval syndrome in Grenada, West Indies. *Vet parasitol.* 2014; 205:721-724.

- Constantinoiu, C.; Croton, C.; Paterson, M.B.; Knott, J.; Henning, K.; Mallyon, J.; et al. Prevalence of canine heartworm infection in Queensland, Australia: comparison of diagnostic methods and investigation of factors associated with reduction in antigen detection. *Parasites Vectors*. 2023; 16:63-72.
- Cottrell, D.K. Use of moxidectin (ProHeart 6) as a heartworm adulticide in 4 ferrets. *Exot DVM*. 2004; 5:9-12.
- Das, M.; Patra, R.; Senapati, S.K.; Sahoo, R.; Panda, S.; Sahoo, P.K. Sensitivity of wet blood smear examination, modified Knott's method and Polymerase chain reaction for diagnosis of *Dirofilaria immitis* infestation in dogs, and its therapeutic management. *Ind J Vet Sci and Biotech*. 2023; 19:96-98.
- Davood, A.; Narouei, E.; Daryani, A.; Sarvi, S.; Moosazadehe, M.; Hezarjaribi, H.Z.; Narouei, M.R.; Gholami, S. The global status of *Dirofilaria immitis* in dogs: a systematic review and metaanalysis based on published articles. *Vet Scie*. 2020; 131: 104-116.
- Díaz-Regañón, D.; Roura, X.; Suárez, M.L.; León, M.; Sainz, Á. Serological evaluation of selected vector-borne pathogens in owned dogs from northern Spain based on a multicenter study using a commercial test. *Parasites vectors*. 2020; 13: 301-312.
- DiGangi, B.A.; Dworkin, C.; Stull, J.W.; O'Quin, J.; Elser, M.; Marsh, A.E.; et al. Impact of heat treatment on *Dirofilaria immitis* antigen detection in shelter dogs. *Parasites Vectors*. 2017; 10:123-128.
- Diosdado, A.; Gómez, P.J.; González-Miguel, J.; Simón, F.; Morchón, R. Current status of canine dirofilariosis in an endemic area of western Spain. *J Helminthol*. 2017; 92:520-523.
- Evason, M.; Stull, J.W.; Pearl, D.L.; Peregrine, A.S.; Jardine, C.; Buch, J.S.; et al. Prevalence of *Borrelia burgdorferi*, *Anaplasma* spp., *Ehrlichia* spp. and *Dirofilaria immitis* in Canadian dogs, 2008 to 2015: a repeat cross-sectional study. *Parasites Vectors*. 2019; 12:64:75.
- Falcón-Cordón, Y.; Montoya-Alonso, J.A.; Caro-Vadillo, A.; Matos, J.I.; Carretón, E. Persistence of pulmonary endarteritis in canine heartworm infection 10 months after the eradication of adult parasites of *Dirofilaria immitis*. *J Vet Parasitol*. 2019; 273:1-4.
- Feldhutter, E.K.; Domenech, O.; Vezzosi, T.; et al. Echocardiographic reference intervals for right ventricular indices, including 3-dimensional volume and 2-dimensional strain measurements in healthy dogs. *J Vet Intern Med*. 2022; 36:8-19.
- Figueredo, L.A.; Sales, K.G.D.S.; Deuster, K.; Pollmeier, M.; Otranto, D.; Dantas-Torres, F. Exposure to vector-borne pathogens in privately owned dogs living in different socioeconomic settings in Brazil. *Vet Parasitol*. 2017; 243:18-23.
- Fontes-Sousa, A.P.; Moura, C.; Carneiro, C.S.; Teixeira-Pinto, A.; Areias, J.C.; Leite-Moreira, A.F. Echocardiographic evaluation including tissue Doppler imaging in New Zealand white rabbits sedated with ketamine and midazolam. *Vet J*. 2009; 181: 326-331.
- Genchi, C.; Kramer, L.H. The prevalence of *Dirofilaria immitis* and *D. repens* in the Old World. *Vet parasitol*. 2020; 280:108-127.
- Gentile-Solomon, J.M.; Abbott J.A. Conventional echocardiographic assessment of the canine right heart: reference intervals and repeatability. *J Vet Cardiol*. 2016; 18: 234-247.
- Granger, L.A.; Pariaut, R.; Vila, J.; Coulter, C.E.; Rademacher, N.; Queiroz-Williams, P. Computed tomographic measurement of the main pulmonary artery to aortic diameter ratio in healthy dogs: a comparison to echocardiographically derived ratios. *J Vet Radiol Ultrasound*. 2016; 57: 376-386.
- Greet, V.; Bode, E.F.; Dukes-McEwan, J.; Oliveira, P.; Connolly, D.J.; Sargent, J. Clinical features and outcome of dogs and cats with bidirectional and continuous right-to-left shunting patent ductus arteriosus. *J Vet Intern Med*. 2021; 35:780-788.
- Hamabe, L.; Mandour, A.S.; Shimada, K.; Uemura, A.; Yilmaz, Z.; Nagaoka, K.; Tanaka, R. Role of Two-Dimensional Speckle-Tracking Echocardiography in Early Detection of Left Ventricular

Dysfunction in Dogs. *Animals*. 2021; 11:2361.

- Hayward, N.; Baines, S.J.; Baines, E.A.; Herrtage, M.E. The radiographic appearance of the pulmonary vasculature in the cat. *J Vet Radiol Ultrasound*. 2004; 45: 501-504.
- Heejin, O.; Juyeon, O.; Seoyeon, K.; Gahyun, L.; Sunghoon, J.; Hyunwook, K.; Junghee, Y.; Jihye, C. Measurements of the pulmonary vasculature on thoracic radiographs in healthy dogs compared to dogs with mitral regurgitation. *J Vet Radiol Ultrasound*. 2014; 56: 251–256.
- Hidaka, Y.; Hagio, M.; Murakami, T.; Okano, S.; Natsuhori, K.; Narita N. Three dogs under 2 years of age with heartworm caval syndrome. *J Vet Med Sci*. 2003; 65:1147-1149.
- Huang, H.; Tai, Z. Echocardiographic assessment of right heart indices in dogs with elevated pulmonary artery pressure associated with chronic respiratory disorders, heartworm disease, and chronic degenerative mitral valvular disease. *Vet Med Praha*. 2013; 12: 613-620.
- Hwang, S.H.; Park, H.J.; Seo, K.W.; Lee, S.E.; Song, K.H. Elevation of Plasma NTProBNP concentration in a Korean Jindo Dog infected with *Dirofilaria immitis*. *J Vet Clin*. 2013; 30: 496-498.
- Iizuka, T.; Hoshi, K.; Ishida, Y.; Sakata, I. Right atriotomy using total venous inflow occlusion for removal of heartworms in a cat. *J Vet Med Sci*. 2009; 71:489-491.
- Keene B.W.; Atkins, C.E.; Bonagura, J.D.; Fox, P.R.; Häggström, J.; Fuentes, V.L.; et al. ACVIM consensus guidelines for the diagnosis and treatment of myxomatous mitral valve disease in dogs. *J Vet Intern Med*. 2019; 33:1127-1140.
- Kellihan, H.B.; Stepien, R.L. Pulmonary hypertension in canine degenerative mitral valve disease. *J Vet Cardiol*. 2012; 14:149-164.
- Kim, S.; Oh, D.; Lee, S.; Hong, S.; Choi, M.; Yoon, J. Determination of tricuspid regurgitation velocity/pulmonary artery flow velocity time integral in dogs with pulmonary hypertension. *J Vet Clin*. 2020; 37:185-190.
- Kitagawa, H.; Kitoh, K.; Iwasaki, T.; Sasaki, Y. Comparison of laboratory data in dogs with heartworm caval syndrome surviving and non-surviving after surgical treatment. *J Vet Med Sci*. 1997; 59:609-611.
- Koenig, T.R.; Mitchell, K.J.; Schwarzwald, C.C. Echocardiographic Assessment of Left Ventricular Function in Healthy Horses and in Horses with Heart Disease Using Pulsed-Wave Tissue Doppler Imaging. *J Vet Intern Med*. 2017; 31:556-567.
- Koffas, H.; Dukes-McEwan, J.; Corcoran, B.M.; Moran, C.M.; French, A.; Sboros, V.; et al. Pulsed tissue Doppler imaging in normal cats and cats with hypertrophic cardiomyopathy. *J Vet Intern Med*. 2006; 20: 65-77.
- Laflamme, D.P. Development and Validation of a Body Condition Score System for Dogs. *Canine Practice*. 1997; 22:10-15.
- Lane, J.N.; Litster, A.; Little, S.E.; Rodríguez, J.Y.; Mwacalimba, K.K.; Sundstrom K.D., et al. Optimizing heartworm diagnosis in dogs using multiple test combinations. *Parasites Vectors*. 2021; 14:224-231.
- Lang, R.M.; Badano, L.P.; Victor, M.; Afilalo, J.; Armstrong, A.; Ernande, L.; et al. Recommendations for cardiac chamber quantification by echocardiography in adults: An update from the American Society of Echocardiography and the European Association of Cardiovascular Imaging. *J Echocardiogr*. 2015; 28:1-39.
- Lee, S.G.; Moon, H.S.; Hyun, C. Percutaneous heartworm removal from dogs with severe heart worm (*Dirofilaria immitis*) infestation *J Vet Sci*. 2008; 9:197-202.
- Lee, Y.; Kim, H.; Yoon, K.; Park, J.; Oh, Y.; Oh, M.; et al. Clinical application of a newly developed basket device for interventional heartworm extraction in three dogs. *J Vet Clin*. 2022; 39:177-184.
- Levy, J.K.; Burling, A.N.; Crandall, M.M.; Tucker, S.J.; Wood, E.G.; Foster, J.D. Seroprevalence of heartworm infection, risk factors for seropositivity, and frequency of prescribing heartworm preventives for cats in the United States and Canada. *J Am Vet Med Assoc*. 2017; 250:873-880.

- Liesner, J.M.; Kruecken, J.; Schaper, R.; Pachnicke, S.; Kohn, B.; Mueller, E.; et al. Vector-borne pathogens in dogs and red foxes from the federal state of Brandenburg. Germany. *Vet Parasitol.* 2016; 224:44-51.
- Locatelli, C.; Spalla, I.; Zanaboni, A.M.; Brambilla, P.G.; Bussadori, C. Assessment of right ventricular function by feature-tracking echocardiography in conscious healthy dogs. *Res J Vet Sci.* 2016; 105:103-110.
- Lyssens, A.; Lekane, M.; Gommeren, K.; Merveille, A.C. Focused Cardiac Ultrasound to Detect Pre-capillary Pulmonary Hypertension. *Front Vet Sci.* 2022; 9: 83-91.
- Maerz, I. Clinical and diagnostic imaging findings in 37 rescued dogs with heartworm disease in Germany. *Vet Parasitol.* 2020; 283:523-530.
- Maia, C.; Coimbra, M.; Ramos, C.; Cristovao, J.M.; Cardoso, L.; Campino, L. Serological investigation of *Leishmania infantum*, *Dirofilaria immitis* and *Angiostrongylus vasorum* in dogs from southern Portugal. *Parasites Vectors.* 2015; 8:152-155.
- Mandour, A.S.; Samir, H.; Yoshida, T.; Matsuura, K.; Abdelmageed, H.A., Elbadawy, M.; et al. Assessment of the Cardiac Functions Using Full Conventional Echocardiography with Tissue Doppler Imaging before and after Xylazine Sedation in Male Shiba Goats. *Animals.* 2020; 10:232-250.
- Manoj, R.R.S.; Latrofa, M.S.; Epis, S.; Otranto, D. Wolbachia: endosymbiont of onchocercid nematodes and their vectors. *Parasit Vectors.* 2021; 14:245-269.
- McCall, J.W.; Genchi, C.; Kramer, L.H.; Guerrero, J.; Venco, L. Heartworm disease in animals and humans. *Adv Parasitol.* 2008; 66:193-285.
- Merveille, A.C.; Bolen, G.; Krafft, E.; Roles, E.; Gomart, S.; Etienne, A.L.; Clercx C.; Entee, K.M. Pulmonary Vein-to-Pulmonary Artery Ratio is an Echocardiographic Index of Congestive Heart Failure in Dogs with Degenerative Mitral Valve Disease. *J Vet Intern Med.* 2015; 29:1502-1509.
- Montoya-Alonso J.A.; Carretón, E.; Morchón, R.; Silveira-Viera, L.; Falcón, Y.; Simón, F. The impact of the climate on the epidemiology of *Dirofilaria immitis* in the pet population of the Canary Islands. *Vet parasitol.* 2016; 216:66-71.
- Montoya-Alonso, J. A.; Morchón, R.; Costa-Rodríguez, N.; Matos, J.I.; Falcón-Cordón, Y.; Carretón, E. Current Distribution of Selected Vector-Borne Diseases in Dogs in Spain. *Front Vet Sci.* 2020; 7:164-175.
- Montoya-Alonso, J.A.; Carretón, E.; Simón, L.; González-Miguel, J.; García-Guasch L.; Morchón, R.; et al. Prevalence of *Dirofilaria immitis* in dogs from Barcelona: Validation of a geospatial prediction model. *Vet Parasitol.* 2015; 212: 456-459.
- Montoya-Alonso, J.A.; García-Rodríguez, S.N.; Carretón, E.; Rodríguez-Escolar I.; Costa-Rodríguez, N.; Matos, J.I.; et al. Seroprevalence of feline heartworm in Spain: completing the epidemiological puzzle of a neglected disease in the cat. *Front Vet Sci.* 2022; 9:900-909.
- Montoya-Alonso, J.A.; Morchón, R.; Falcón-Cordón, Y.; et al. Prevalence of heartworm in dogs and cats of Madrid, Spain. *Parasites Vectors.* 2017; 10:354-359.
- Montoya-Alonso, J.A.; Morchón, R.; García-Rodríguez, S.N.; Falcón-Cordón, Y.; Costa-Rodríguez, N.; Matos, J.I.; et al. Expansion of canine heartworm in Spain. *Animals.* 2022; 12:1268-1281.
- Montoya, J.A.; Carretón, E. *Dirofilariosis: pautas de manejo clínico.* Barcelona. Multiméica ediciones veterinarias. 2012. pp. 1-135.
- Morchón, R.; Carretón, E.; González-Miguel, J.; Mellado-Hernández, I. Heartworm Disease (*Dirofilaria immitis*) and Their vectors in Europe - new distribution trends. *Front Physiol.* 2012; 3:196-207.
- Morchón, R.; Montoya-Alonso, J.A.; Rodríguez-Escolar, I.; Carretón, E. What Has Happened to Heartworm Disease in Europe in the Last 10 Years? *Pathogens.* 2022; 11: 104-123.
- Morita, T.; Nakamura, K.; Osuga, T.; Morishita, K.; Sasaki, N.; Ohta, H.; et al. Right ventricular



function and dyssynchrony measured by echocardiography in dogs with precapillary pulmonary hypertension. *J Vet Cardiol.* 2019; 23:1-14.

- Morita, T.; Nakamura, K.; Osuga, T.; Takiguchi, M. Incremental predictive value of echocardiographic indices of right ventricular function in the assessment of long-term prognosis in dogs with myxomatous mitral valve disease. *J Vet Cardiol.* 2022, 39: 51-62.
- Morita, T.; Nakamura, K.; Osuga, T.; Yokoyama, N.; Khoirun, N.; Morishita, K.; Sasaki, N. The repeatability and characteristics of right ventricular longitudinal strain imaging by speckle-tracking echocardiography in healthy dogs. *J Vet Cardiol.* 2017, 19: 351-362.
- Nagueh, S.F.; Appleton, C.P.; Gillebert, T.C.; Marino, P.N.; Oh, J.K.; Smiseth, O.A.; et al. Recommendations for the evaluation of left ventricular diastolic function by echocardiography. *Eur J Echocardiogr.* 2009; 10:165-193.
- Nijhawan, D.; Chawla, R.; Saxena, M.; Dixi, S.; Sharma, V. To Assess the Clinical Value of the RPAD Index in Dogs with Varying Degrees of Pulmonary Hypertension. *Asian J Med Res.* 2019; 8:4-10.
- Pajas, A.M.G.; Acorda J.A. Echocardiographic, electrocardiographic and thoracic radiographic findings in dogs with dirofilariasis. *Philipp J Vet Med.* 2018; 55:71-84.
- Paradies, P.; Spagnolo, P.P.; Amato, M.E.; Pulpito, D.; Sasanelli, M. Doppler echocardiographic evidence of pulmonary hypertension in dogs: a retrospective clinical investigation. *Vet Res Commun.* 2014; 38:63-71.
- Pariaut, R.; Jung, S.W.; Vila, J.; Newhard, D.K. Resolution of caval syndrome during initial hemodynamic stabilization in dogs with heartworm disease. *J Vet Emerg Crit Care.* 2020; 30:1-7.
- Patata, V.; Caivano, D.; Porciello, F.; Rishniw, M.; Domenech, O.; Marchesotti, F.; Giorgi, M.E.; Guglielmini, C.; Poser, H.; Spina, F.; Biretoni, F. Pulmonary vein to pulmonary artery ratio in healthy and cardiomyopathic cats. *J Vet Cardiol.* 2019; 27:23-33.
- Payne, J.R.; Borgeat, K.; Connolly, D.J.; Boswood, A.; Dennis, S.; Wagner, T.; et al. Prognostic indicators in cats with hypertrophic cardiomyopathy. *J Vet Intern Med.* 2013; 27:1427-1436.
- Pérez-Pérez, P.; Rodríguez-Escolar, I.; Carretón, E.; Sánchez-Agudo, J.A.; Lorenzo-Morales, J.; Montoya-Alonso J.A.; et al. Serological Survey of Canine Vector-Borne Infections in North-Center Spain. *Front Vet Sci.* 2021; 8:184-195.
- Piantedosi, D.; Neola, B.; D'Alessio, N.; Di Prisco, F.; Santoro, M.; Pacifico, L.; et al. Seroprevalence and risk factors associated with *Ehrlichia canis*, *Anaplasma* spp., *Borrelia burgdorferi sensu lato*, and *D. immitis* in hunting dogs from southern Italy. *Parasitol Res.* 2017; 116: 2651-2660.
- Reef, V.B.; Bain, F.T.; Spencer, P.A. Severe mitral regurgitation in horses: clinical, echocardiographic and pathological findings. *Equine Vet J.* 1998; 30:18-27.
- Reef, V.B.; Bonagura, J.; Buhl, R.; McGurrin, M.K.; Schwarzwald, C.C.; Van-Loon, G.; et al. Recommendations for management of equine athletes with cardiovascular abnormalities. *J Vet Intern Med.* 2014; 28:749-761.
- Reiner, C.; Visser, L.C.; Kellihan, H.B.; Masseau, I.; Rozanski, E.; Clercx, C.; et al. ACVIM consensus statement guidelines for the diagnosis, classification, treatment, and monitoring of pulmonary hypertension in dogs. *Vet Intern Med.* 2020; 34: 549-573.
- Rodríguez-Bendas, A.J.; Alberigi, B.; Galardo, S.; Labarthe, N.; Mendes-De-Almeida, F. Clinical and blood count findings in dogs naturally infected with *Dirofilaria immitis*. *Rev Bras Med Vet.* 2022; 44:324-335.
- Roels, E.; Fastrès, A.; Merveille, A.C.; Bolen, G.; Teske, E.; Clercx, C.; et al. The prevalence of pulmonary hypertension assessed using the pulmonary vein-to-right pulmonary artery ratio and its association with survival in West Highland white terriers with canine idiopathic pulmonary fibrosis. *BMC Vet Res.* 2021; 17:171-178.

- Roldán-Alzate, A.; Frydrychowicz, A.; Johnson, K.M.; Kelliham, H.; Chesler, N.C.; Wieben, O.; et al. Non-invasive assessment of cardiac function and pulmonary vascular resistance in an canine model of acute thromboembolic pulmonary hypertension using 4D flow cardiovascular magnetic resonance. *J Cardiovasc Magn Reson.* 2014; 16:23-32.
- Roles, E.; Merveille, A.C.; Moyses, E.; Gomart, S.; Clercx, C.; Entee, K.M. Diagnostic value of the pulmonary vein-to-right pulmonary artery ratio in dogs with pulmonary hypertension of precapillary origin. *J Vet Cardiol.* 2019; 24:85-94.
- Romano, A.E.; Saunders, A.B.; Gordon, S.G.; Wesselowsky, S. Intracardiac heartworms in dogs: Clinical and echocardiographic characteristics in 72 cases. *J Vet Intern Med.* 2021; 35:88-97.
- Sampedrano, C.C.; Chetboul, V.; Gouni, V.; Nicolle, A.P.; Pouchelon, J.L.; Tissier, R. Systolic and diastolic myocardial dysfunction in cats with hypertrophic cardiomyopathy or systemic hypertension. *J Vet Intern Med.* 2006; 20:1106-1115.
- Santhakumari, R.R.; Latrofa, M.S.; Epis, S.; Otranto, D. Wolbachia: endosymbiont of onchocercid nematodes and their vectors. *Parasites Vectors.* 2021; 14:245-251.
- Sasai, H.; Kato, K.; Sasaki, T.; Koyama, S.; Kotani, T.; Fukata, T. Echocardiographic diagnosis of dirofilariasis in a ferret. *J Small Anim Pract.* 2000; 41:172-174.
- Schafer, M.; Berry, C.R. Cardiac and pulmonary artery mensuration in feline heartworm disease. *J Vet Radiol Ultrasound.* 1995; 36: 499-505.
- Schober, K.E.; Baade, H. Doppler echocardiographic prediction of pulmonary hypertension in West Highland white terriers with chronic pulmonary disease. *J Vet Intern Med.* 2006; 20: 912-920.
- Serrano-Parreño, B.; Carretón, E.; Caro-Vadillo, A.; Falcón-Cordón, Y.; Falcón-Cordón, S.; Montoya-Alonso, J.A. Evaluation of pulmonary hypertension and clinical status in dogs with heartworm by Right Pulmonary Artery Distensibility Index and other echocardiographic parameters. *Parasites Vectors.* 2017; 10:106-111.
- Serrano-Parreño, B.; Carretón, E.; Caro-Vadillo, A.; Falcón-Cordón, S.; Falcón-Cordón, Y.; Montoya-Alonso, J.A. Pulmonary hypertension in dogs with heartworm before and after the adulticide protocol recommended by the American Heartworm Society. *Vet Parasitol.* 2017; 236:34-37.
- Serres, F.; Chetboul, V.; Gouni, V.; Tissier, R.; Sampedrano, C.C.; Pouchelon, J.L. Diagnostic value of echo-Doppler and Tissue Doppler Imaging in dogs with pulmonary arterial hypertension. *J Vet Intern Med.* 2007; 21:1280-1289.
- Silva, M.S.G.; Leles, D.; Sudré, A.P.; Millar, P.R.; Uchôa, F.; Brener, B. Prevalence and Molecular Characterization of *Dirofilaria immitis* (Filarioidea: Onchocercidae) in Dogs from Endemic Areas of Rio De Janeiro State. Brazil *J Parasitol.* 2019; 105: 387-390.
- Silva, V.B.C.; Wolf, M.; Lucina, S.B.; Sarraff-Lopes, A.P.; Sousa, M.G. Assessment of right ventricular systolic function by tissue motion annular displacement in healthy dogs. *J Vet Cardiol.* 2020; 32: 40-48.
- Simón, F.; López-Belmonte, J.; Marcos-Atxutegi, C.; Morchón, R.; Martín-Pacho, J. R. What is happening outside North America regarding human dirofilariasis? *Vet parasitol.* 2005; 133: 181-189.
- Simón, F.; Morchón, R.; González-Miguel, J.; Marcos-Atxutegi, C.; Siles-Lucas, M. What is new about animal and human dirofilariasis? *Trends Parasitol.* 2009; 25:404-409.
- Simón, F.; Siles-Lucas, M.; Morchón, R.; González-Miguel, J.; Mellado, I.; Carretón E.; et al. Human and Animal Dirofilariasis: the Emergence of a Zoonotic Mosaic. *J Clin Microbiol.* 2012; 25:507-544.
- Small, M.T.; Atkins, C.E.; Gordon, S.G.; Birkeheuer, A.J.; Booth-Sayer, M.A.; Keene, B.W.; et al. Use of a nitinol gooseneck snare catheter for removal of adult *Dirofilaria immitis* in two cats. *J Am Vet Med Assoc.* 2008; 233:1441-1445.

- Small, M.T.; Atkins, C.E.; Gordon, S.G.; Birkeheuer, A.J.; Booth-Sayer, M.A.; Keene, B.W.; et al. Use of a nitinol gooseneck snare catheter for removal of adult *Dirofilaria immitis* in two cats. *J Am Vet Med Assoc.* 2008; 233: 1441-1445.
- Smith, R.; Murillo, D.F.B.; Chenoweth, K.; Barua, S.; Kelly, P.J.; Starkey, L.; Blagburn, B.; Wood, T.; Wang C. Nationwide molecular survey of *Dirofilaria immitis* and *Dirofilaria repens* in companion dogs and cats, United States of America. *Parasites Vectors.* 2022; 15:367-376.
- Spasojevic-Kosic, L.; Lalosevic, V. Dog heartworm disease is here to stay: the most important aspects of clinical relevance. *Vet Glas.* 2020; 74:125-143.
- Strickland, K.N. Canine and feline caval syndrome. *Clin Tech Small Anim Pract.* 1998; 13: 88-95.
- Supakorndej, P.; Lewis, R.E.; McCall, J.W.; Dzimianski, M.T.; Holmes, R.A. Radiographic and angiographic evaluations of ferrets experimentally infected with *Dirofilaria*. *Vet Radiol Ultrasound.* 1995; 36: 23-29.
- Sutherland-Smith, J.; Hankin, E.J.; Cunningham, S.M., Sato, A.F.; Barton, B.A. Comparison of a computed tomographic pulmonary trunk to aorta diameter ratio with echocardiographic indices of pulmonary hypertension in dogs. *Vet Radiol Ultrasound.* 2018; 59:18-26.
- Tae-Rim, L.; Sun-Hwee, H.; Kyoung, S.; Kun, S. Evaluation of serum NT-proBNP and cardiac troponin I concentrations in dogs with heartworm disease. *J Vet Clin.* 2020; 37: 311-316.
- Teshima, K.; Asano, K.; Iwanaga, K.; Koie, H.; Uechi, M.; Kato, Y.; et al. Evaluation of right ventricular Tei Index (Index of Myocardial Performance) in healthy dogs and dogs with tricuspid regurgitation. *Intern Med J.* 2006; 68:1307-1313.
- Tidholm, A.; Ljungvall, I.; Höglund, K.; Westling, A.B.; Häggström, J. Tissue Doppler and strain imaging in dogs with myxomatous mitral valve disease in different stages of congestive heart failure. *J Vet Intern Med.* 2009; 23:1197-1207.
- Tjostheim, S.S.; Kellihan, H.B.; Grint, K.A.; Stepien, R.L. Effect of sildenafil and pimobendan on intracardiac heartworm infections in four dogs. *J Vet Cardiol.* 2019; 23: 96-103.
- Toaldo, M.; Poser, H.; Menciotti, G.; Battaia, S.; Contiero, B.; Cipone, M.; et al. Utility of Tissue Doppler Imaging in the Echocardiographic Evaluation of Left and Right Ventricular Function in Dogs with Myxomatous Mitral Valve Disease with or without Pulmonary Hypertension. *J Vet Intern Med.* 2016; 30:697-705.
- Tudor, N.; Ionita, L.; Tapaloaga, D.; Tudor, P.; Ionita, C.; Vlagioiu, C. Radiographic cardiopulmonary changes in dogs with heartworm disease. *Rom Biotechnol Lett.* 2014; 19:6-11.
- Tuleski, G.L.R.; Wolf, M.; Garcia-Ribeiro, M.J.; Dos Santos, J.P.; Sousa, M.G. Tissue motion annular displacement to assess the left ventricular systolic function in healthy cats. *Vet Res Commun.* 2022; 46:823-836.
- Venco, L.; Genchi, C.; Vigevani, C.P.; Kramer, L. Relative utility of echocardiography, radiography, serologic testing and microfilariae counts to predict adult worm burden in dogs naturally infected with heartworms. *Recent Advances in Heartworm Disease. Symposium'01.* Batavia, IL: American Heartworm Society. 2004; 24-111.
- Venco, L.; Mihaylova, L.; Boon, J.A. Right Pulmonary Artery Distensibility Index (RPAD Index). A field study of an echocardiographic method to detect early development of pulmonary hypertension and its severity even in the absence of regurgitant jets for Doppler evaluation in heartworm-infected dogs. *Vet Parasitol.* 2014; 206:60-66.
- Vezzosi, T.; Domenech, O.; Costa, G.; Marchesotti, F.; Venco, L.; Zini, E.; et al. Echocardiographic evaluation of the right ventricular dimension and systolic function in dogs with pulmonary hypertension. *J Vet Intern Med.* 2018a; 32: 1541-1548.
- Vezzosi, T.; Domenech, O.; Iacona, M.; Marchesotti, F.; Zini, E.; Venco, L.; Tognetti R. Echocardiographic evaluation of the Right Atrial Area index in dogs with pulmonary hypertension. *J Vet Intern Med.* 2018b; 32:42-47.

- Villanueva-Saz, S.; Giner, J.; Verde, M.; Yzuel, A.; González, A.; Lacasta, D.; et al. Prevalence of microfilariae, antigen and antibodies of feline dirofilariosis infection (*Dirofilaria immitis*) in the Zaragoza metropolitan area, Spain. *Vet Parasitol Reg Stud Rep*. 2021; 23:105-110.
- Villanueva-Saz, S.; Giner, J.; Verde, M.; Yzuel, A.; Lacasta, D.; Ruíz, H.; Basurco, A.; González, A.; Marteles, D.; Fernández, A. First serological study of *Dirofilaria immitis* antibodies in household domestic ferrets (*Mustela putorius furo*) in southern Spain - Short communication. *Acta Vet Hung*. 2022; 70: 282-286.
- Visser, L.C.; Im, M.K.; Johnson, L.R.; Stern, J.A. Diagnostic value of right pulmonary artery distensibility index in dogs with pulmonary hypertension: comparison with Doppler echocardiographic estimates of pulmonary arterial pressure. *J Vet Intern Med*. 2016; 30:543-552.
- Visser, L.C.; Scansen, B.A.; Brown, N.V.; Schober, K.E.; Bonagura, J.D. Echocardiographic assessment of right ventricular systolic function in conscious healthy dogs following a single dose of pimobendan versus atenolol. *J Vet Cardiol*. 2015b; 17:161-172.
- Visser, L.C.; Scansen, B.A.; Schober, K.E.; Bonagura, J.D. Echocardiographic assessment of right ventricular systolic function in conscious healthy dogs: Repeatability and reference intervals. *J Vet Cardiol*. 2015a; 17: 83-96.
- Visser, L.C.; Sintov, D.J.; Oldach, M.S. Evaluation of tricuspid annular plane systolic excursion measured by two dimensional echocardiography in healthy dogs: repeatability, reference intervals, and comparison with M-mode assessment. *J Vet Cardiol*. 2018; 20:165-174.
- Visser, L.C.; Wood, J.E.; Johnson, L.J. Survival characteristics and prognostic importance of echocardiographic measurements of right heart size and function in dogs with pulmonary hypertension. *J Vet Intern Med*. 2020; 34:1379-1388.
- Wang, J.; Kelly, P.; Zhang, J.; Shi, Z.; Song, C.; Zheng, X.; Zhang, Y.; Hao, Y.; Dong, H.; ElMahallawy, H.S.; Xiong, W.; Wang, H.; Li, J.; Zhang, X.; Wang, C. Detection of *Dirofilaria immitis* antigen and antibodies against *Anaplasma phagocytophilum*, *Borrelia burgdorferi* and *Ehrlichia canis* in dogs from ten provinces of China. *Acta Parasitol*. 2018; 63: 412-415.
- Wang, S.; Zhang, N.; Zhang, Z.; Wang, D.; Yao, Z.; Zhang, H.; et al. Prevalence of *Dirofilaria immitis* infection in dogs in Henan province, central China. *Parasite*. 2016; 23: 43-47.
- Wess, G.; Domenech, O.; Dukes-McEwan, J.; Häggström, J.; Gordon, S. European Society of Veterinary Cardiology screening guidelines for dilated cardiomyopathy in Doberman Pinschers. *J Vet Cardiol*. 2017; 19: 405-415.
- Wolf, M.; Lucina, S.B.; Bruler, B.S.; Tuleski, G.L.R.; Silva, V.B.C.; Sousa, M.G. Assessment of longitudinal systolic function using tissue motion annular displacement in healthy dogs. *J Vet Cardiol*. 2018, 20, 175-185.
- Wolf, M.; Lucina, S.B.; Silva, V.; Tuleski, G.; Sarraff, A.P.; Komatsu, E.Y.; et al. Assessment of longitudinal systolic function using tissue motion annular displacement in dogs with degenerative mitral valve disease. *J Vet Cardiol*. 2021; 38: 44-58.
- Yoon, W.K.; Choi, R.; Lee, S.G.; Hyun, C. Comparison of 2 retrieval devices for heartworm removal in 52 dogs with heavy worm burden. *J Vet Intern Med*. 2013; 27: 469-473.
- Yoon, W.K.; Han, D.; Hyun, C. Catheter-guided percutaneous heartworm removal using a nitinol basket in dogs with caval syndrome. *J Vet Sci*. 2011; 12:199-201.



The background features a light beige, textured surface. It is decorated with several wavy, overlapping lines in shades of green and grey, creating a sense of movement and depth. Three solid, olive-green circles are scattered across the page: one large one on the left, one smaller one in the upper right, and another large one at the bottom center.

# 9. SCIENTIFIC CONTRIBUTIONS

**Relevant scientific contributions linked to the  
research developed during the doctoral period**



## 9.1. Participation in national and international congress

1. Carretón, E.; Falcón-Cordón, Y.; Falcón-Cordón, S.; Morchón, R.; Matos, J.I.; Montoya-Alonso, J.A. Evaluation of different dosages of doxycycline during the adulticide treatment of *Dirofilaria immitis* in dogs. 2019 American Heartworm Society Triennial Symposium. September 8-11, 2019, New Orleans, USA.
2. Carretón, E.; Falcón-Cordón, Y.; Rodón, J.; Matos, J.I.; Morchón, R.; Montoya-Alonso, J.A. Early detection of renal damage in heartworm-infected dogs. 2019 American Heartworm Society Triennial Symposium. September 8-11, 2019, New Orleans, USA.
3. Melián-Henríquez, A.; Matos-Rivero, J.I.; Montoya-Alonso, J.A.; García-Rodríguez, S.N.; Costa-Rodríguez, N.; Carretón, E. Echocardiographic evaluation of pulmonary hypertension in dogs with heartworm disease using the pulmonary vein to pulmonary artery ratio. XXXI Congresso SolPa & 2021 ESDA Event. June 16-19, 2021, Teramo, Italy.
4. Falcón-Cordón, Y.; Montoya-Alonso, J.A.; Costa-Rodríguez, N.; Caro-Vadillo, A.; García-Rodríguez, S.N.; Matos-Rivero, J.I.; Carretón, E. Serum acute phase proteins in dogs with heartworm disease (*Dirofilaria immitis*) before and after adulticide treatment. XXXI Congresso SolPa & 2021 ESDA Event. June 16-19, 2021, Teramo, Italy.
5. Falcón-Cordón, Y.; Carretón-Gómez, E.; Martínez, S.; Tvarijonaviciute, A.; Franco, L.; Costa-Rodríguez, N.; García-Rodríguez, S.N.; Matos-Rivero, J.I.; Montoya-Alonso, J.A. Evaluation of serum Endothelin-1 in dogs with heartworm disease (*Dirofilaria immitis*) before and after adulticide treatment. XXVIII International Conference of the World Association for the Advancement of Veterinary Parasitology. July 19-22, 2021, Dublin, Ireland.
6. Falcón-Cordón, S.; Carretón, E.; Matos-Rivero, J.I.; Costa-Rodríguez, N.; García-Rodríguez, S.N.; Montoya-Alonso, J.A. Utility of thoracic radiology as clinical indicator of pulmonary hypertension in dogs with heartworm disease (*Dirofilaria immitis*). XXVIII International Conference of the World Association for the Advancement of Veterinary Parasitology. July 19-22, 2021, Dublin, Ireland.
7. Matos-Rivero, J.I.; Falcón-Cordón, Y.; García-Rodríguez, S.N.; Costa-Rodríguez, N.; Carretón, E.; Montoya-Alonso, J.A. Evaluation of pulmonary hypertension in dogs with heartworm disease using the pulmonary trunk to descending aorta diameter ratio. World Small Animal Veterinary Association Congress (WSAVA 2021). November 13-15, 2021, Dublin, Ireland.
8. Matos-Rivero, J.I.; García-Rodríguez, S.N.; Costa-Rodríguez, N.; Carretón, E.; Falcón-Cordón, Y.; Montoya-Alonso, J.A. Evaluación de la hipertensión pulmonar en perros con dirofilariosis cardiopulmonar mediante el uso del ratio broncoarterial. XVI Andalusian Congress of Veterinarians Specialists in small Animals. November 12-13, 2021, Almería, Spain.
9. Costa-Rodríguez, N.; García Rodríguez, S.N.; Matos-Rivero, J.I.; Morchón, R.; Montoya-Alonso, J.A.; Carretón, E. Evaluación laboratorial de la hipercoagulabilidad en perros con *Dirofilaria immitis*. Andalusian Congress of Veterinarians Specialists in small Animals. November 12-13, 2021, Almería, Spain.
10. Matos-Rivero, J.I.; Falcón-Cordón, Y.; García-Rodríguez, S.N.; Costa-Rodríguez, N.; Carretón, E.; Montoya-Alonso, J.A. Assessment of pulmonary hypertension in dogs with heartworm by using the ratio between the right and left ventricle. 32nd ECVIM-CA Congress. September 1-3, 2022, Gothenburg, Sweden.
11. Matos-Rivero, J.I.; Pérez-Menchén D.; García-Rodríguez, S.N.; Costa-Rodríguez, N.; Carretón, E.; Montoya-Alonso, J.A. Usefulness of tissue doppler imaging in the evaluation of pulmonary hypertension in dogs with heartworm. 32nd ECVIM-CA Congress. September 1-3, 2022, Gothenburg, Sweden.



12. Matos-Rivero, J.I.; Falcón-Cordón, Y.; García-Rodríguez, S.N.; Costa-Rodríguez, N.; Carretón, E.; Montoya-Alonso, J.A. Usefulness of computed tomography pulmonary vein to pulmonary artery ratio in the assessment of pulmonary hypertension in dogs with heartworm disease. 15th International Congress of Parasitology (ICOPA 2022). August 21-26, 2022, Copenhagen, Denmark.
13. Costa-Rodríguez, N.; Hernández-Jiménez L.; Falcón-Cordón, Y.; García-Rodríguez, S.N.; Matos-Rivero, J.I.; Carretón, E.; Montoya-Alonso, J.A. Elevations in serum cortisol in dogs with heartworm disease as a biomarker of stress. 32nd ECVIM-CA Congress. September 1-3, 2022, Gothenburg, Sweden.
14. Matos-Rivero, J.I.; García-Rodríguez, S.N.; Costa-Rodríguez, N.; Falcón-Cordón, Y.; Carretón, E.; Montoya-Alonso, J.A. Importance of anamnesis and physical examination in canine heartworm disease. 7th ESDA Congress (ESDA 2022). September 22-24, 2022, Madrid, Spain.
15. Matos-Rivero, J.I.; García-Rodríguez, S.N.; Costa-Rodríguez, N.; Falcón-Cordón, Y.; Carretón, E.; Montoya-Alonso, J.A. Two-dimensional echocardiographic measurements for diagnosis and staging of heartworm disease. 7th ESDA Congress (ESDA 2022). September 22-24, 2022, Madrid, Spain.
16. Matos-Rivero, J.I.; García-Rodríguez, S.N.; Costa-Rodríguez, N.; Falcón-Cordón, Y.; Carretón, E.; Montoya-Alonso, J.A. Tricuspid Regurgitation Velocity/Pulmonary Artery Flow Velocity Time Integral Measured By Echocardiography In Canine Heartworm Disease. 7th ESDA Congress (ESDA 2022). September 22-24, 2022, Madrid, Spain.
17. Martínez-Bencomo A.; Falcón-Cordón Y.; Falcón-Cordón S.; Matos-Rivero, J.I.; Montoya-Alonso, J.A.; Carretón, E. Usefulness of Thoracic Radiological Signs for the Diagnosis and Staging of Severity in Dogs with Heartworm. 7th ESDA Congress (ESDA 2022). September 22-24, 2022, Madrid, Spain.
18. Matos-Rivero, J.I.; García-Rodríguez, S.N.; Costa-Rodríguez, N.; Falcón-Cordón, Y.; Carretón, E.; Montoya-Alonso, J.A. Evaluation of thoracic computed tomography findings in dogs naturally infected by *Dirofilaria immitis*. 7th ESDA Congress (ESDA 2022). September 22-24, 2022, Madrid, Spain.
19. Costa-Rodríguez, N.; Matos-Rivero, J.I.; Falcón-Cordón, Y.; Morchón R.; García-Rodríguez, S.N.; Montoya-Alonso, J.A.; Carretón, E. Measurement of cortisol in dogs infected by *dirofilaria immitis*. 7th ESDA Congress (ESDA 2022). September 22-24, 2022, Madrid, Spain.
20. Costa-Rodríguez, N.; García-Rodríguez, S.N.; Matos-Rivero, J.I.; Montoya-Alonso, J.A.; Morchón R.; Carretón, E. Usefulness of NT-proBNP in dogs with heartworm: Could this biomarker be useful to evaluate pulmonary hypertension? 2022 American Heartworm Society Triennial Symposium. September 8-11, 2022, New Orleans, USA.
21. Matos-Rivero, J.I.; García-Rodríguez, S.N.; García-Guasch L.; Costa-Rodríguez, N.; Falcón-Cordón, Y.; Carretón, E.; Montoya-Alonso, J.A. Análisis comparativo de la determinación del RPADi en la dirofilariosis cardiopulmonar canina. XXII Congress of Veterinary Specialties of AVEPA. April 21-22, 2023, Bilbao, Spain.
22. Matos-Rivero, J.I.; Abecassis, R.; García-Rodríguez, S.N.; Santana J.A.; Saavedra, D.; Costa-Rodríguez, N.; Carretón, E.; Montoya-Alonso, J.A. Clinical and echocardiographic findings in dogs with heartworm caval syndrome. 33rd ECVIM Congress. September 21-23, 2023, Barcelona, Spain.
23. Chang, W.I.; García-Guash, I.; Chan, I.P.; Montoya-Alonso, J.A.; Matos-Rivero J.I., Lo, P.I.; Lam, M.C.; Lin, C.H. The pulmonary hypertension remodeling/hemodynamic-induced manifestations on echocardiography (PRIME) score for predicting the severity of canine pulmonary hypertension. 33rd ECVIM Congress. September 21-23, 2023, Barcelona, Spain.

24. Costa-Rodríguez, N.; Falcón-Cordón, Y.; García-Rodríguez, S.N.; Falcón-Cordón, S.; Matos, J.I.; Montoya-Alonso, J.A.; Carretón, E. Correlation of serum N-Terminal pro B-type natriuretic peptide with pulmonary hypertension in heartworm infected dogs during adulticide treatment. 33rd ECVIM Congress. September 21-23, 2023, Barcelona, Spain.
25. Matos-Rivero, J.I.; García-Rodríguez, S.N.; García-Guasch L.; Falcón-Cordón, Y.; Costa-Rodríguez, N.; Carretón, E.; Montoya-Alonso, J.A. Utilidad de la determinación de la resistencia vascular pulmonar estimada por ecocardiografía en la dirofilariosis canina. AVEPA National Congress - Southern European Veterinary Conference 2023 (AVEPA-SEVC 2023). November 9-11, 2023, Barcelona, Spain.

## 9.2. Q1 Scientific publications

1. Carretón, E.; Falcón-Cordón, Y.; Falcón-Cordón, S.; Morchón, R.; Matos, J.I.; Montoya-Alonso, J.A. Variation of the adulticide protocol for the treatment of canine heartworm infection: Can it be shorter? *Vet Parasitol.* 2019; 271:54–56.
2. Falcón-Cordón, Y.; Montoya-Alonso, J.A.; Caro-Vadillo, A.; Matos-Rivero, J.I.; Carretón, E. Persistence of pulmonary endarteritis in canine heartworm infection 10 months after the eradication of adult parasites of *Dirofilaria immitis*. *Vet Parasitol.* 2019; 273: 1-4.
3. Carretón, E.; Morchón, R.; Falcón-Cordón, Y.; Falcón-Cordón, S.; Matos, J.I.; Montoya-Alonso, J.A. Evaluation of different dosages of doxycycline during the adulticide treatment of heartworm (*Dirofilaria immitis*) in dogs. *Vet Parasitol.* 2020; 283 :1-4.
4. Carretón, E.; Falcón-Cordón, Y.; Rodon, J.; Matos, J.I.; Morchón, R.; Montoya-Alonso, J.A. Evaluation of serum biomarkers and proteinuria for the early detection of renal damage in dogs with heartworm (*Dirofilaria immitis*). *Vet Parasitol.* 2020; 283 :1-4.
5. Carretón, E.; Morchón, R.; Falcón-Cordón, Y.; Matos, J.I.; Costa-Rodríguez, N.; Montoya-Alonso, J.A. First epidemiological survey of *Angiostrongylus vasorum* in domestic dogs from Spain. *Parasite Vectors.* 2020; 13 :306-311.
6. Montoya-Alonso, J.A.; Morchón, R.; Costa-Rodríguez, N.; Matos, J.I.; Falcón-Cordón, Y.; Carretón, E. Current distribution of selected Vector-Borne Diseases in dogs in Spain. *Front Vet Sci.* 2020; 22: 564429.
7. Montoya-Alonso, J.A.; Morchón R.; Matos, J.I.; Falcón-Cordón, Y.; Costa-Rodríguez, N.; Carretón, E. *Dirofilaria immitis* Could Be a Risk Factor for the Development of Allergic Diseases in Humans. *Animals.* 2020; 10:1847.
8. Montoya-Alonso, J.A.; Morchón R.; García-Rodríguez, S.N, Falcón-Cordón, Y.; Costa-Rodríguez, N.; Matos, J.I.; Escolar, I.R.; Carretón, E. Expansion of Canine Heartworm in Spain. *Animals.* 2022; 12:1268.
9. Montoya-Alonso, J.A.; García Rodríguez, S.N.; Carretón, E.; Escolar, I.; Costa-Rodríguez, N.; Matos, J.I.; Morchón, R. Seroprevalence of Feline Heartworm in Spain: Completing the Epidemiological Puzzle of a Neglected Disease in the Cat. *Front Vet Sci.* 2022; 9:900371.
10. Carretón, E.; Morchón, R.; García-Rodríguez, S.N.; Escolar, I.; Matos, J.I.; Costa-Rodríguez, N.; Montoya-Alonso, J.A. Comprehensive map of canine angiostrongylosis in dogs in Spain. *Animals.* 2022; 12:2217.
11. García-Rodríguez, S.N.; Costa-Rodríguez, N.; Matos, J.I.; Falcón-Cordón, Y.; Morchon, R.; Carretón, E.; Montoya-Alonso J.A. Feline heartworm disease and environmental allergens hypersensitivity: is there a link? *Parasite Vectors.* 2023; 16:192.

12. Matos, J.I.; Falcón-Cordón, Y.; García-Rodríguez, S.N.; Costa-Rodríguez, N.; Montoya-Alonso, J.A.; Carretón, E. Evaluation of Pulmonary Hypertension in Dogs with Heartworm Disease Using the Computed Tomographic Pulmonary Trunk to Aorta Diameter Ratio. *Animals*. 2022; 12:2421-2431.
13. Matos, J.I.; Caro-Vadillo, A.; Falcón-Cordón, Y.; García-Rodríguez, S.N.; Costa-Rodríguez, N.; Carretón, E.; Montoya-Alonso J.A. Echocardiographic Assessment of the Pulmonary Vein to Pulmonary Artery Ratio in Canine Heartworm Disease. *Animals*. 2023, 13:703-713.
14. Costa-Rodríguez, N.; García-Rodríguez, S.N.; Matos, J.I.; Falcón-Cordón, Y.; Morchon-García, R.; Montoya-Alonso, J.A.; Carretón, E. Usefulness of NT-proBNP in dogs with heartworm: could this biomarker be useful to evaluate pulmonary hypertension? *Parasite Vectors*. 2023; 16:192-199.
15. Matos, J.I.; García-Rodríguez, S.N.; Costa-Rodríguez, N.; Caro-Vadillo, A.; Carretón, E.; Montoya-Alonso J.A. Montoya-Alonso. Right ventricle strain assessed by 2-dimensional speckle tracking echocardiography (2D-STE) to evaluate pulmonary hypertension in dogs with *Dirofilaria immitis*. *Animals*. 2023; 14: 26-37.
16. Matos, J.I.; García-Rodríguez, S.N.; Costa-Rodríguez, N.; Caro-Vadillo, A.; Carretón, E.; Montoya-Alonso J.A. Usefulness of Tissue Doppler Imaging for the Evaluation of Pulmonary Hypertension in Canine Heartworm Disease. *Animals*. 2023; 13:3647-3658.

### 9.3. Final project degrees

1. Echocardiographic evaluation of pulmonary hypertension in dogs with heartworm disease using the pulmonary vein to pulmonary artery ratio. Presented by student Adrian Melian Henríquez. University of Las Palmas de Gran Canaria. Degree in Veterinary Medicine. Academic year 2020-2021.
2. Usefulness of tissue doppler imaging for the evaluation of pulmonary hypertension in canine heartworm disease. Presented by the student David Pérez Menchen. University of Las Palmas de Gran Canaria. Degree in Veterinary Medicine. Academic year 2021-2022.
3. Usefulness of thoracic radiological signs for the diagnosis and staging of severity in dogs with heartworm (*Dirofilaria immitis*). Presented by the student Ana Martínez Bencomo. University of Las Palmas de Gran Canaria. Degree in Veterinary Medicine. Academic year 2021-2022.
4. Clinical and echocardiographic findings in dogs with heartworm caval syndrome. Presented by the student Raquel Abecassis Rodríguez. University of Las Palmas de Gran Canaria. Degree in Veterinary Medicine. Academic year 2022-2023.
5. First successful transvenous heartworm extraction in a natural infected ferret (*Mustela putorius furo*) with caval syndrome. Presented by the student Marta María Deniz Santana. University of Las Palmas de Gran Canaria. Degree in Veterinary Medicine. Academic year 2022-2023.



Hipócrates de Cos, prestigioso médico de la Antigua Grecia, formuló: "Declara el pasado, diagnostica el presente y pronostica el futuro. Practica estos actos". Los severos signos clínicos y el alto porcentaje de pacientes caninos afectados por hipertensión pulmonar en la dirofilariosis cardiopulmonar canina han motivado a encontrar mejoras en el diagnóstico ecocardiográfico de este complejo trastorno cardiovascular. La investigación realizada pretende ofrecer nuevas herramientas que permitan conocer los mecanismos relacionados con la fisiopatología de la enfermedad y establecer criterios contundentes para conseguir avances en los protocolos de tratamientos empleados. Asimismo, los autores esperan que los resultados obtenidos sean compartidos y ampliados con futuras contribuciones, con el fin último de mejorar las condiciones de vida de nuestros pacientes.